THE INFLUENCE OF SODIUM DODECYL SULPHATE ON THE DISSOLUTION OF HYDROPHOBIC DRUGS

by

SUKMINDER MALL

B.Pharm., M.R. Pharm.S.

The School of Pharmacy,

University of London.

March, 1996.

Thesis submitted for the degree of Doctor of Philosophy in the University of London.

ProQuest Number: 10104845

All rights reserved

INFORMATION TO ALL USERS
The quality of this reproduction is dependent upon the quality of the copy submitted.

In the unlikely event that the author did not send a complete manuscript
and there are missing pages, these will be noted. Also, if material had to be removed,
a note will indicate the deletion.

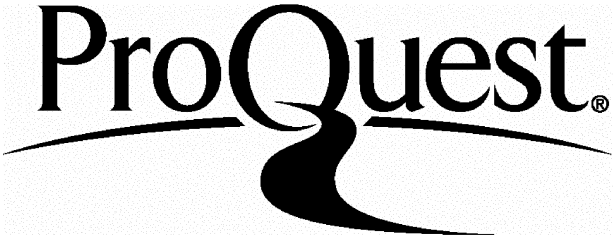

ProQuest 10104845

Published by ProQuest LLC(2016). Copyright of the Dissertation is held by the Author.

All rights reserved.
This work is protected against unauthorized copying under Title 17, United States Code.
Microform Edition © ProQuest LLC.

ProQuest LLC
789 East Eisenhower Parkway
P.O. Box 1346
Ann Arbor, MI 48106-1346

ABSTRACT.

The purpose of this study was to investigate the influence of the anionic surfactant, sodium dodecyl sulphate, on the dissolution of hydrophobic drugs.

The surface energy of each drug studied was considered in terms of a Lifshitz-van der Waals contribution and a polar contribution which was divided into electron donor and electron acceptor parameters. These data were obtained from contact angle experiments, using an automated Wilhelmy plate technique. The surface energy data for the solids were used along with surface energy terms for the head groups and the hydrophobic tails of the micelle to give a free energy of adhesion to each region of the micelle for each of the drugs.

The solubilities of these drugs were considered in both water and aqueous micellar sodium dodecyl sulphate solutions, as a function of temperature, and also by considering parallel experiments in which the pH was buffered at the pK_a of the drug.

A Taylor-Aris diffusion technique was also used to provide a direct measurement of partition between a buffered aqueous phase and the micelles, again as a function of temperature. The thermodynamics of transfer were calculated for each experimental procedure by use of the van't Hoff isochore.

The initial rotating disk dissolution rate of drug compacts was measured in water and water with SDS micelles at a range of temperatures. The thermodynamic parameters of activation were calculated from the rate data.

Correlations were obtained between the measured solubilities, partitioning and dissolution data and the free energy of adhesion obtained from surface energy data. These properties were found to be strongly influenced by a polar repulsion energy between the monopolar surfactant head group.

This work provides an insight into a possible mechanism of solubilisation, using the Lewis acid-base approach and the prospect of understanding different partitioning behaviour.

ACKNOWLEDGEMENTS.

Thanks must go firstly to my supervisor, Graham Buckton for his constant advice and encouragement during this work and whose enthusiasm for the subject was always very motivating.

Many people in the School of Pharmacy have helped me during this work to whom I am very grateful, particularly the technical staff in the pharmaceutics department. Special thanks must go to Brian Bissenden for his continual guidance in constructing and maintaining much of the equipment used for this work.

Thanks are also due to my industrial supervisors, initially David Storey and then David Rawlins for their advice and interest over this period of research. Financial support from the School of Pharmacy and M.S.D. is greatly appreciated.

I also wish to thank my friends at the School of Pharmacy for making the past three years very enjoyable, especially David Carthew for his help with computers and also his valued friendship. Thanks must also go to my family for their interest in this work.

Finally, I would like to thank Keith for his encouragement, support and patience throughout my Ph D.

To my parents

TABLE OF CONTENTS

Page

Page

Page

List of Figures

Page

Page

Page

List of Tables

Page

Page

Page

Page

List of Symbols

a	constant
A	collision number
A_s	surface area of a powder, or another material
b	constant
c	concentration of solute in solution
c_{oct}	concentration of drug in octan-1-ol
c_s	concentration dissolved at saturated solubility
c_{water}	concentration of drug in water
CMC	critical micelle concentration
CMT	critical micelle temperature
D	diffusion coefficient
d_h	diffusion layer thickness
D_m	diffusion coefficient of the micelle in aqueous solution
D_w	solute diffusion in aqueous solution
E	activation energy
f	fraction of solute in the micellar phase
F	force
F_d	detachment force
F_e	equilibrium force
$F_{z.d.o.i.}$	force at the zero depth of immersion
g	acceleration due to gravity
IPDR	initial powder dissolution rate
k	dissolution rate constant
K	solubility of an infinitely large particle
m	mass
M_v	molecular volume
p	perimeter of a plate
pK_a	dissociation constant
pK_u	3 units above the dissociation constant value

P	partition coefficient
P_o	polarity
r	radius
R	gas constant
RDIDR	rotating disk initial dissolution rate
t	time
T	absolute temperature
W_a	work of adhesion
W_i	work of immersion
W_s	work of spreading

Greek symbols

γ_{LV}	surface tension of a liquid
γ_{SL}	solid/liquid interfacial energy
γ_{SV}	surface energy of the solid
γ_c	critical surface tension
γ^d	dispersive contribution to surface energy
γ^p	polar contribution to surface energy
γ^{TOT}	the total surface energy
γ^{AB}	Lewis acid-Lewis base contribution to surface tension (or surface energy)
γ^{LW}	Lifshitz-van der Waal's contribution to surface tension (or surface energy)
γ^-	electron donator component of the surface free energy
γ^+	electron acceptor component of the surface free energy
Δ	difference in or change in, *eg* change in enthalpy ΔH
ΔG	Gibbs free energy change
$\Delta G^{\ddagger}$	free energy of activation change
ΔG_{head}	free energy of adhesion to the head groups of the surfactant
ΔG_{tail}	free energy of adhesion to the tail groups of the surfactant

$\Delta G_{head + tail}$	free energy of adhesion to the head and tail groups of the surfactant
ΔG_{1w2}	adhesion between solid 1 and 2, in presence of water
ΔH	enthalpy change
$\Delta H^{\ddagger}$	enthalpy of activation change
ΔH_{vap}	enthalpy of vaporisation
ΔH°	standard state enthalpy change
ΔS	entropy change
$\Delta S^{\ddagger}$	entropy of activation change
δ_A	overall polar component of solubility parameter
δ_d	dispersive component of solubility parameter
δ_h	hydrogen bonding component of solubility parameter
δ_p	polar component of solubility parameter
δ_s	solubility parameter
θ	contact angle
θ_a	advancing contact angle
θ_e	equilibrium contact angle
θ_r	receding contact angle
λ_{max}	maximum absorbance
ν	kinematic viscosity
σ	the variance of the dispersion curve
ϕ	rotational speed

CHAPTER 1

INTRODUCTION

1.1. INTRODUCTION

The physical characterisation of pharmaceutical powders is important when considering the formulation of dosage forms (*eg* Parsons *et al.*, 1992b and York, 1983). Bulk material properties often bear little relationship to surface properties, thus this work involves investigation of the *surface properties* of pharmaceutical powders. This is because contact between materials occurs at interfaces and a knowledge of surface properties is necessary if the behaviour of materials, in terms of interactions with other phases, is to be understood (or predicted). Such information has proved useful in the past for the prediction of the performance of solid dosage forms and suspensions *eg* Rowe (1989), Parsons *et al.*, (1992b) and Pinto *et al.*,(1995). Therefore it was decided to estimate surface properties of materials by investigating their behaviour when in interfacial contact with a number of well characterised different materials. The aim being to relate the estimated interactions of a pharmaceutical powder with the various measured interactions a solid dosage form encounters on oral delivery, such as solubility, dissolution and partitioning.

1.1.1. Interfacial phenomena.

Consideration of the interaction between the phases is fundamental to the understanding of the nature and behaviour of surfaces. When considering pharmaceutical systems, the following interfaces are relevant;

vapour/liquid	liquid/liquid	solid/solid
vapour/solid	liquid/solid	

Since this work is concerned with the surface properties of powders, the assessment of the solid/vapour and the solid/liquid interfaces is of most interest.

1.1.2. Surface tension of a liquid (γ_{LV}).

In a liquid, the molecules at the surface are not completely surrounded by other like molecules, unlike those in the bulk of the liquid. At the surface, each liquid molecule is surrounded by other liquid molecules to the sides and below, whilst above the molecule, there are gas molecules in the vapour.

The intermolecular forces between the liquid and vapour molecules are much weaker than those between the liquid molecules. Molecules at the surface are pulled inward by molecules below the surface of the liquid. The liquid attempts to contract to give minimum surface area *ie* to attain the minimum surface energy, which for a free drop would result in the formation of a sphere (which is a tendency for the surface to contract). The contraction of the liquid/vapour surface is spontaneous. The liquid surface exists in a state of tension and the phenomenom is termed *surface tension* (γ_{LV}).

1.1.3. Surface free energy of a solid.

The value of the work required per unit area to move molecules to the surface of a liquid is termed the *surface free energy*. For a liquid/vapour interface, the surface tension ($mN.m^{-1}$) and the surface free energy ($mJ.m^{-2}$) are numerically equal. The surface free energy of a solid is similar to the surface tension of a liquid, since it results from the same phenomena. The solid surface, however, differs from the liquid surface as the

intermolecular forces are far greater and therefore, the molecules are unable to move freely.

1.1.4. Solid/ liquid interfacial energy (γ_{SL}).

This also occurs due to an imbalance of forces at the interface. It will depend on the surface free energy and surface tension of the solid and liquid involved.

1.1.5. Wettability of powders.

The wettability of a powder represents the extent of its interaction with a liquid. Indirect methods are used to measure wettability. When a drop of liquid is placed at the surface of a solid, an angle is produced between the powder and the liquid. This angle is known as the *contact angle,* θ, and represents an equilibrium of three energies, γ_{SV} - surface energy of the solid, γ_{LV} - surface tension of the liquid and γ_{SL} - solid/liquid interfacial energy. See Figure 1.1.1.

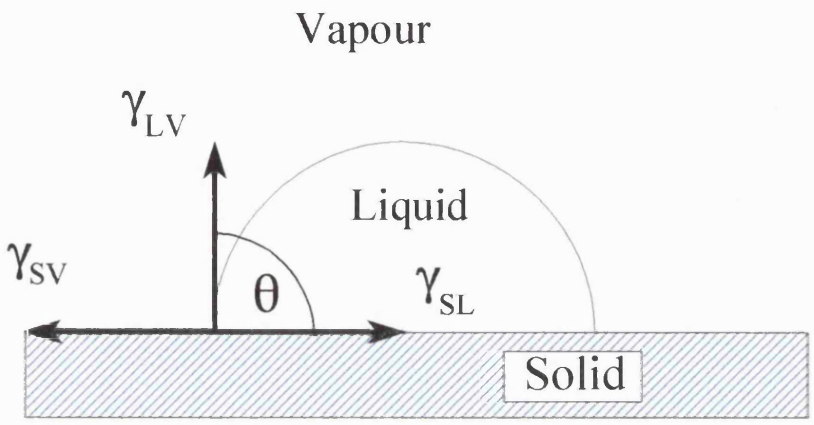

Figure 1.1.1. Diagram to illustrate the equilibrium of forces acting on a drop of liquid on a solid.

These forces can be described by Young's equation (Young, 1805).

$$\gamma_{SV} = \gamma_{SL} + \gamma_{LV} (\cos \theta) \qquad (1.1.1.)$$

The smaller the value of θ, the greater the wettablity. Thus, θ provides a means of evaluating the wettability of powders as a measurable quantity.

1.1.5.1. The thermodynamics of wetting.

A useful model describing the three stages in the wetting process has been given by Parfitt (1973). This is shown in Figure 1.1.2.

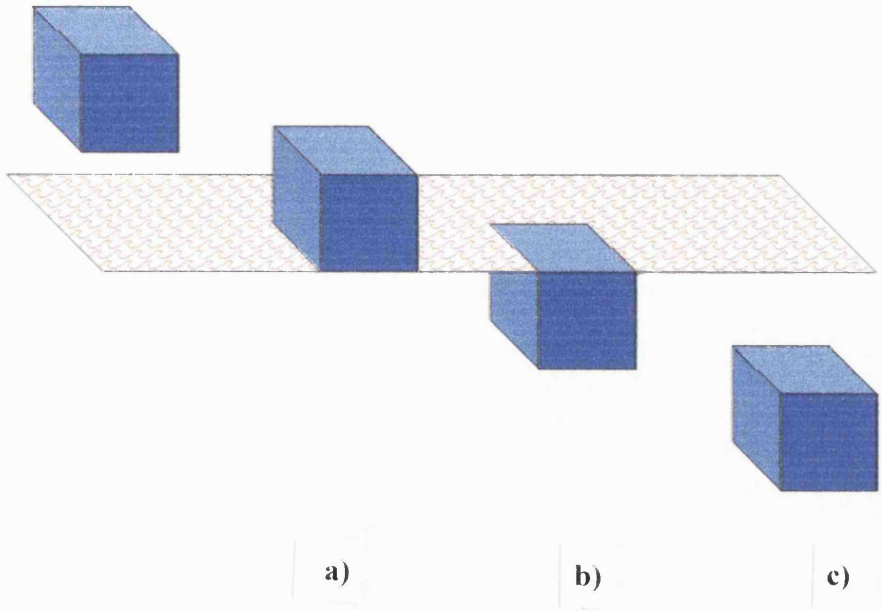

Figure 1.1.2. The three stages in the wetting process;

a) Adhesional wetting

b) Immersional wetting

c) Spreading wetting

1.1.5.2. Adhesional wetting.

In adhesional wetting, the solid is brought into contact with the liquid surface which adheres to it, resulting in the loss of a liquid/vapour interface. The driving force for this process is known as the work of adhesion, W_a, which is described in Equation 1.1.3.

$$W_a = \gamma_{SL} - (\gamma_{SV} + \gamma_{LV}) \qquad (1.1.3.)$$

In combination with Young's equation (Eq. 1.1.1.), this gives the Young-Dupré equation;

$$W_a = -\gamma_{LV} (\cos \theta + 1) \qquad (1.1.4.)$$

1.1.5.3. Immersional wetting.

Immersional wetting is the process whereby a unit area of surface is completely immersed in the liquid. It involves the replacement of the solid/vapour interface with a solid/liquid interface. The work involved, W_i, per unit area of surface, is called the work of immersion and is given by;

$$W_i = 4\gamma_{SL} - 4\gamma_{SV} \qquad (1.1.5.)$$

which, combined with Young's equation (Eq. 1.1.1.) to remove the solid related surface energy terms yields:

$$W_i = -4\gamma_{LV}(\cos\theta) \qquad (1.1.6.)$$

1.1.5.4. Spreading wetting.

In spreading wetting, the liquid spreads over the solid surface replacing solid surface area in equal amounts by liquid surface and solid/liquid interface. Hence the work of spreading wetting, W_s is given by;

$$W_s = \gamma_{SV} - \gamma_{SL} + \gamma_{LV} \qquad (1.1.7.)$$

which in combination with Eq. 1.1.1. gives;

$$W_s = -\gamma_{LV}(\cos\theta - 1) \qquad (1.1.8.)$$

1.1.5.5. Conditions for spontaneous wetting.

For spontaneous wetting to occur, the work of adhesion, immersion and spreading must be positive. The following conditions must be met;

a) Adhesional - $\gamma_{LV}(1 + \cos\theta) \geq 0$

b) Immersional - $\gamma_{LV} \cos\theta \geq 0$

c) Spreading - $\gamma_{LV}(\cos\theta - 1) \geq 0$

Since the surface tension, γ_{LV}, is always positive, the value of cos θ determines whether each condition is satisfied, as shown below;

a) $\cos\theta \leq -1$ *ie* $\theta \leq 180°$

b) $\cos\theta \geq 0$ *ie* $\theta \leq 90°$

c) $\cos\theta \geq 1$ *ie* $\theta \leq 0°$

1.2. SURFACTANTS.

Surface active agents or surfactants, are molecules which are characterised by having two regions in their chemical structure, one hydrophobic (water-hating) and the other hydrophilic (water-liking). The hydrophobic region would consist of a hydrocarbon chain, and the hydrophilic region can be an ionisable, polar or water soluble group. Surfactants are often referred to as amphiphilic molecules as they have an attraction in both aqueous and oil phases.

It is energetically favourable for surfactants, when dissolved, to adsorb at interfaces, orientating themselves in such a manner that the regions are associated with the appropriate solvent. Because of the accumulation of surfactant molecules at surfaces and interfaces, there will be an expansion which will reduce surface and interfacial tensions. Surfactants will lower surface tension to different degrees.

1.2.1. Classification of surfactants.

Surfactants are characterised by the possession of both polar and non-polar regions on the same molecule (Florence and Attwood, 1988). The polar or hydrophilic region of the molecule may carry a positive or negative charge, giving rise to cationic or anionic surfactants respectively, or may be composed of a polyoxyethylene chain, as in many of the non-ionic surfactants. The non-polar or hydrophobic portion of the molecule is most commonly one or more hydrocarbon chains.

Surfactants can be classified into four groups:

1.2.1.1. Anionic.

These are surfactants in which the hydrophilic portion of the molecule carries a negative charge. A common example is sodium lauryl sulphate (also known as sodium dodecyl sulphate), which is:

$$CH_3 (CH_2)_{11} - SO_4^-.Na^+$$

Other examples have the general structure R - COO^- or R - SO_3^- (where R represents the hydrocarbon based chain).

1.2.1.2. Cationic.

In this case, the cation of the compound is the surface active species *eg* hexadecyltrimethylammonium bromide:

$$CH_3 (CH_2)_{15} N^+ (CH_3)_3 Br^-$$

1.2.1.3. Ampholytic.

This type of surfactant can behave as either an anionic, non-ionic or cationic species, depending on the pH of the solution (*ie* the extent of ionisation of the various functional groups). An example would be N-dodecyl-N, N-dimethyl betaine, shown in its zwitterion form;

$$C_{12}H_{25}N^+ (CH_3)_2 CH_2COO^-$$

1.2.1.4. Non-ionic.

These are surfactants which have a water soluble hydrophilic region, which is not ionic. The water soluble moiety of this type can contain hydroxyl groups or a polyoxyethylene chain *eg* polyoxyethylene monohexadecyl ether;

$$CH_3\,(CH_2)_{15}\,(OCH_2CH_2)_{21}OH$$

1.2.2. General properties of some surfactants used pharmaceutically.

1.2.2.1. Anionic surfactants.

This group includes a) soaps, b) alkyl sulphates and c) alkyl sulphonates.

a) Soaps

The most commonly used soaps are the alkali- metal soaps, RCOOX where X is sodium, potassium or ammonium. The chain length, R, of the fatty acid is generally between C_{10} and C_{20}. A pharmaceutically important soap is sodium stearate, used as an emulsifying agent, a cleaning agent and in glycerin suppositories.

b) Alkyl sulphates

These are prepared from fixed oils, such as coconut oil, whereby the oil is converted to a mixture of alcohols ranging in chain length from about 12 to 20 carbons. Sodium dodecyl sulphate is an example used pharmaceutically as a pre-operative skin cleanser (having bacteriostatic action against gram-positive bacteria), in medicated shampoos and is a poor tablet lubricant.

c) Alkyl sulphonates

The best known pharmaceutical example in this group is Dioctyl sodium sulphosuccinate or Docusate sodium. Its surface active properties account for its use as a faecal softener.

1.2.2.2. Cationic surfactants.

This category includes the quaternary ammonium salts. They are water soluble, non-caustic, stable and incompatible with anionic agents. These are important pharmaceutically because of their bactericidal activity against a wide range of gram-positive and some gram-negative organisms. Two common examples are a) cetrimide and b) benzalkonium chloride.

a) Cetrimide

Solutions containing 0.1 to 1% cetrimide are used for cleansing the skin, wounds and burns, for cleaning contaminated vessels and for storage of sterilised surgical instruments. Solutions of cetrimide are also used in shampoos for seborrhoea.

b) Benzalkonium chloride

This is used as a preservative for eyedrops. It is also in preparations used as anti-infectives in mouthwashes and for application to burns and wounds.

1.2.2.3. Non-ionic surfactants.

The advantage of non-ionic surfactants over ionic surfactants is that they are compatible with all other types of surfactant and their properties are little affected by pH. Common examples include cetomacrogol, which is used in many cream formulations, as well as the Span, Tween and Brij series of surfactants (Buckton,1995).

1.2.3. Micellization.

1.2.3.1. Critical micelle concentration.

Surfactants form monolayers at the surface or interface of a two phase system; the polar portion of the molecule protruding into the aqueous phase while the nonpolar portion extends into the oily or non aqueous phase (Kayes, 1988). When the concentration of surfactant is such that the interface contains more surfactant than that required to form a monolayer, the excess forms aggregates or *micelles*, in which the lipophilic hydrocarbon chains are orientated towards the interior of the micelle, leaving the hydrophilic groups in contact with the aqueous medium (this can invert in non-polar solvents). The concentration of a surfactant at which micelles form is termed *critical micelle concentration* (CMC) for the surfactant.

1.2.3.2. Micellar structure.

At the point where micelles begin to form, the concentration of monomers will have reached a maximum in the solution. Surfactants exist in a number of different states as the concentration is changed. These have been reviewed by Buckton (1995).

As concentration is increased, the solution first passes the CMC to form spherical micelles. Further increases may then lead to the formation of cylindrical micelles which may subsequently be forced to join into hexagonal bundles of rods (see Figure 1.2.1.). These bundles of rods are termed the "middle phase". Alternatively, the system may form lamellar structures, which are known as the "neat phase".

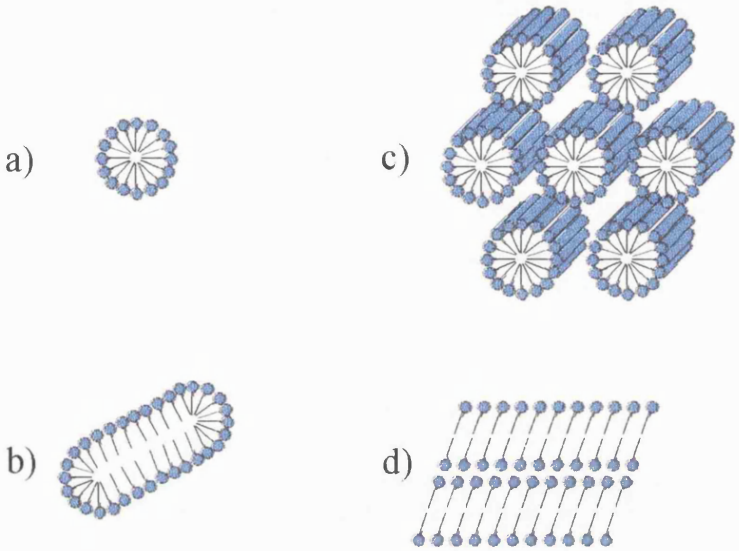

Figure 1.2.1. Structures formed at high concentrations of surfactant (above that which produces spherical micelles; a) Spherical micelles b) Cylindrical micelles, c) Middle phase (hexagonal rods) and d) Neat phase (lamalae).

1.2.3.3. The Krafft phenomenon.

Micelle forming surfactants exhibit an unusual phenomenon in that their solubilities show a rapid increase above a certain temperature. This temperature is known as the "Krafft point" and is characteristic for any particular surface active agent (Shaw, 1966). This is explained by the fact that unassociated surfactant has a limited solubility, whereas the micelles are highly soluble. Below the Krafft temperature, the solubility of the surfactant is insufficient for micellization. As the temperature is raised, the solubility slowly increases until at the Krafft point, the CMC is reached. This temperature is often called the 'critical micelle temperature' or CMT. A relatively large amount of surfactant can now

be dispersed in the form of micelles so that a large increase in solubility is observed.

1.2.3.4. Solubilisation.

As mentioned earlier, the interior core of a micelle can be considered to have the properties of a liquid hydrocarbon and is thus capable of dissolving materials that are soluble in such liquids. Thus *solubilisation* may be defined as the formation of a greater solubility of a solute in a solvent, by the production of a thermodynamically stable isotropic solution, following the introduction of one or more amphiphilic components at or above their critical micelle concentration (Attwood and Florence, 1983).

The extent to which solubility can be increased by solubilisation will depend upon the amount and type of surfactant present and the nature of the solute. Also the effect of temperature and of added electrolytes are important issues in the solubilisation process (Elworthy *et al.*, 1968).

1.2.3.5. Pharmaceutical aspects of solubilisation.

The literature on pharmaceutical applications of micellar solubilisation is extensive. Water insoluble bactericides, vitamins, steroids, essential oils and antibiotics have been formulated in micellar systems, thus facilitating their use in medicine (Elworthy *et al.*, 1968).

Whilst solubilisation is an excellent means of producing an aqueous solution of a water-insoluble drug, it should be realised that it may well have effects on the drug's activity and

absorption characteristics.

Examples of solubilisation include improving the solubility of phenolic compounds such as cresol and chloroxylenol by solubilisation with soaps. Glycerol has also been used with polysorbate 80 to improve the solubility of vitamin A (Coles and Thomas, 1952). This complex topic has been reviewed by Elworthy *et al.*, (1968). However recent examples include Sjöström *et al.*, (1993) who looked at the suspension of small particles of poorly water-soluble drugs under the influence of emulsification and surfactant concentration. Warren *et al.*, (1995) investigated using micellar solubilisation to enhance the solubility of salbutamol and triamcinolone acetonide in chlorofluorocarbon solvents, with the aim of formulating solution metered dose inhaler products of these drugs.

Many surface active molecules also occur naturally in the body. Bile salts are surfactants which are synthesised in the liver and which are present in the gastrointestinal tract (GIT). One of the main functions of bile salts is to solubilise fat in the gastrointestinal tract and to facilitate its absorption. It is probable that bile salts are involved in the process of absorption of certain hydrophilic drugs from the GIT, both as a wetting agent to aid dissolution and as an absorption enhancer.

1.3. SURFACE TENSION & CONTACT ANGLES.

1.3.1. Surface tension measurement.

There are many methods available for measuring the surface tension of liquids, such as capillary rise, drop volume and drop weight methods, Du Noüy ring tensiometer method and the Wilhelmy plate method. These techniques have been discussed in detail by Fell, (1988) and Sheridan *et al.*, (1994a). We will only be concerned with one of these, which is the Wilhelmy plate method.

1.3.1.1. The Wilhelmy plate method.

The three versions of this method are: equilibrium, detachment and dynamic. A thin rectangular plate of glass, platinum or filter paper is suspended vertically from a torsion balance above a clean beaker containing the test liquid, which is placed on a mechanical stage. The equilibrium method involves the stage being raised slowly until the plate makes contact with the liquid (see Figure 1.3.1.), the force, F_e is noted and the surface tension may be calculated using Equation 1.3.1.

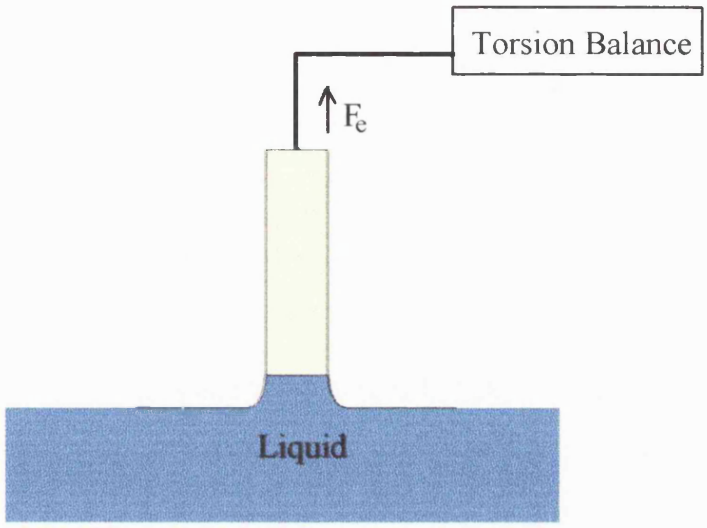

Figure 1.3.1. Diagram illustrating the Wilhelmy plate method with the plate at equilibrium.

$$\gamma_{LV} = F_e \, g \, / \, p \qquad (1.3.1.)$$

where;

p = perimeter of the plate

g = acceleration due to gravity

For the detachment method, the stage is raised until the plate just dips into the liquid. The stage is then lowered slowly until the plate is just at the point of detachment. The force F_d is read from the torsion balance and the surface tension may be calculated using Equation 1.3.1. replacing F_e with F_d.

The dynamic method involves use of the automated equipment, Cahn Dynamic Contact Angle analyser, which allows easier and more accurate measurement of surface tension.

With this technique, the test liquid is placed on a motorised platform and the glass slide or filter paper is attached to one arm of a microbalance. Both the microbalance and the motorised platform are linked to a personal computer. The platform is then raised, at a constant pre-set speed until the plate is immersed 5-10 mm into the liquid. The platform is then lowered to its initial position. The force and relative position of the platform is obtained by the computer at one second intervals.

A graph of the force is plotted as a function of the stage position. The buoyancy slope can be extrapolated back to the stage position which corresponds to the point where the plate initially makes contact with the liquid. As shown in Figure 1.3.2. the force at the zero depth of immersion, $F_{z.d.o.i.}$ can be determined, which is the point at which the only force acting on the plate is due to a function of the surface tension of the liquid and its contact angle with the plate.

Using Equation 1.3.1. the surface tension may then be calculated by replacing F_e with $F_{z.d.o.i.}$. This method of extrapolating the buoyancy slope to determine F is much more accurate than the single point determination used for the equilibrium methods, therefore the dynamic Wilhelmy plate technique is more widely used.

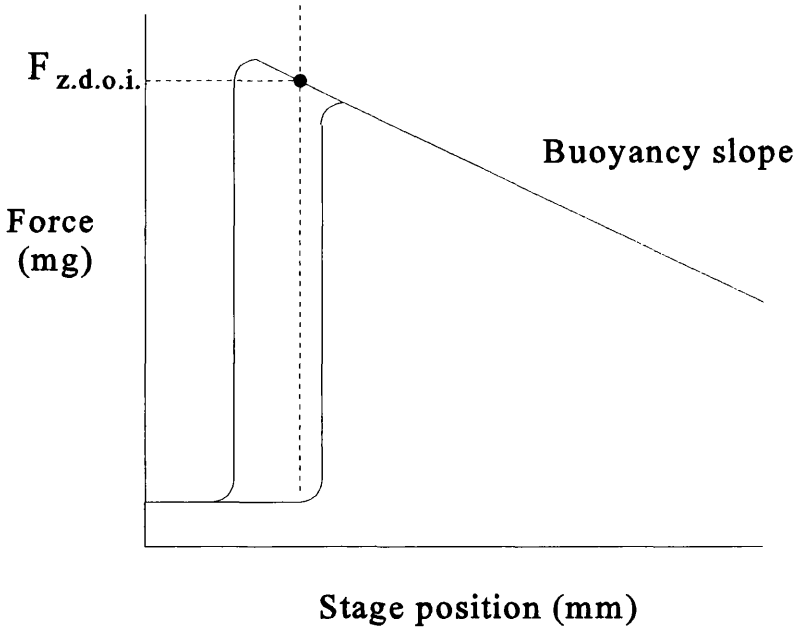

Figure 1.3.2. Determination of $F_{z.d.o.i.}$

1.3.2. Contact angle measurement.

Again, as with surface tension measurements, there are several methods available to measure contact angles such as liquid penetration, tilting plate method, sessile drop method and the Wilhelmy plate technique. These methods of measuring contact angles for pharmaceutical powders can be split into two broad groups:

a) liquid penetration techniques

b) compressed powder plate methods.

There have been several publications reviewing contact angle measurement methods (*eg* Neumann and Good, 1979 and Buckton, 1990b). However the technique which will be discussed here is the Wilhelmy plate method.

1.3.2.1. The Wilhelmy plate technique.

As described in section 1.3.1. this method has been used to measure surface tension. For contact angle measurement, a compressed powder plate is employed instead of a glass slide. Equation 1.3.2. is used instead of Equation 1.3.1. as cos θ is no longer unity.

$$\cos \theta = F\, g / p\, \gamma_{LV} \qquad (1.3.2.)$$

where F = force and

g = acceleration due to gravity

The powder compact is suspended from a microbalance above the test liquid. The motorised platform is raised until the plate makes contact with the liquid. Figure 1.3.4. shows a typical chart recorder output.

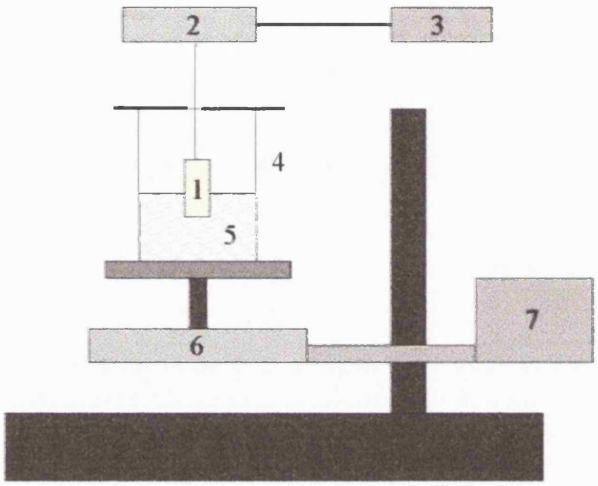

Figure 1.3.3. A schematic diagram of the Wilhelmy plate method. 1. Wilhelmy plate, 2. microbalance, 3. chart recorder, 4. clean beaker, 5. test liquid, 6. moving platform, 7. motor.

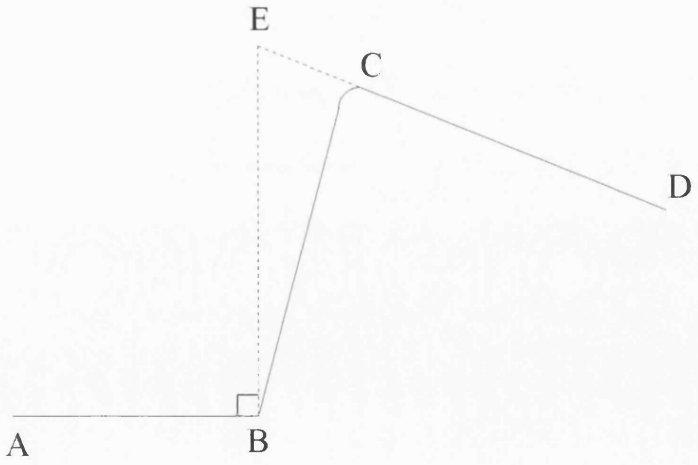

Figure 1.3.4. A typical chart recorder trace.

A-B is the region prior to contact between the plate and the liquid. As soon as contact is made, a deflection is observed (C) and continued immersion of the plate causes the line CD to be formed. Extrapolation of the line CD back to the perpendicular to AB, at B gives the true measured force, BE. This force is then used in Equation 1.3.2. to calculate $\cos \theta$.

In previous reviews, the advantages and disadvantages of methods of measuring contact angles have been discussed *eg* Heertjes *et al.*, (1967). This Wilhelmy plate technique has several advantages over the other available methods.

1. It is an automated method and therefore is not as operator dependent as the other methods *eg* sesseile drop.
2. Contact angle hysteresis can be studied as advancing and receding data can be obtained easily.
3. It is not necessary to pre-saturate the compact prior to measurement.
4. Any deformation of the plate occurring during measurement, will do so below the liquid surface. Although if this occurs, it is not possible to obtain receding data.

The main disadvantage of this method, as for all techniques employing compressed powder plates, is that the compaction process may alter the outer surface of the plate (Buckton and Newton, 1986) by plastic deformation. Chawla *et al.*, (1994) found a further problem with surface roughness, which is unique to the Wilhelmy plate approach to contact angle measurement. It was observed that if the perceived perimeter (the outer dimensions measured by micrometer) was significantly different from the effective

perimeter, due to surface roughness or plate porosity, then the calculated angle would be in error.

1.3.2.2. Contact angle hysteresis.

Contact angle hysteresis is defined as the difference between the advancing, θ_a and the receding angle θ_r. This can be illustrated with a drop of liquid on a tilted plate as shown in Figure 1.3.5.

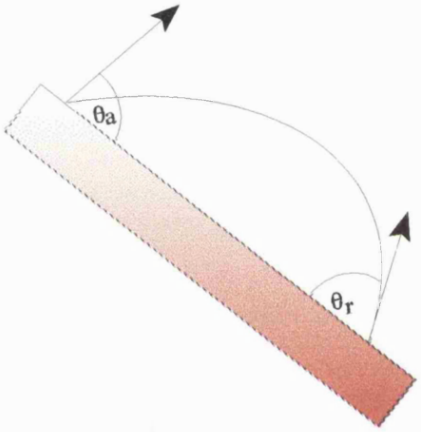

Figure 1.3.5. Contact angle hysteresis on a tilted surface.

Much work has been carried out on this phenomena (Dettre and Johnson, 1965), where both θ_a and θ_r are found to be different to the equilibrium angle θ_e. Possible reasons for contact hysteresis are:

a) surface contamination

b) surface heterogeneity

c) surface roughness

1.4. CALCULATION OF SURFACE ENERGIES FROM CONTACT ANGLES.

1.4.1. Critical surface tension, γ_c.

The critical surface tension, γ_c of a solid represents a measure of the wettability of the solid. It may be defined as the value of the surface tension of a wetting liquid, above which spontaneous wetting (*ie* adhesion, immersion and spreading) does not occur for that solid.

Fox and Zisman (1950) developed γ_c, which represents the value of γ_{LV} when cos θ is extrapolated back to equal 1 as shown in Figure 1.4.1.

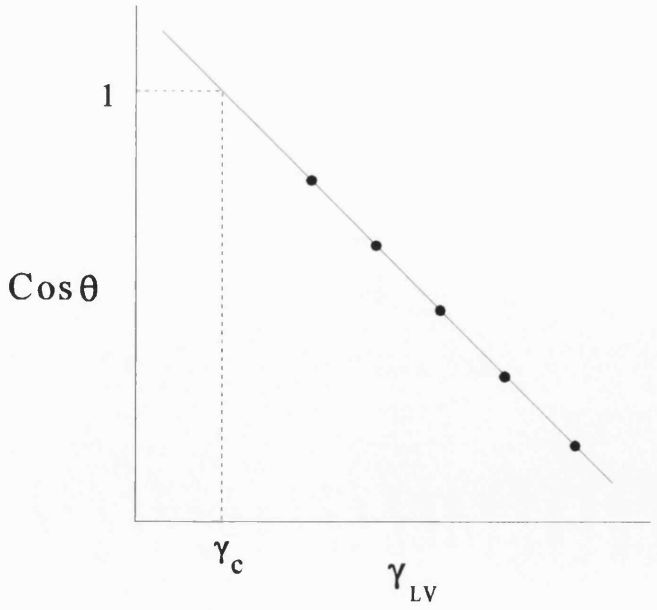

Figure 1.4.1. Graph of cos θ vs. γ_{LV} used to determine the critical surface tension, γ_c.

A considerable amount of work has been undertaken on critical surface tension determination. It was noted that a homologous series of pure liquids would usually give higher values for γ_c than liquid mixtures (Good,1977). Furthermore, a plot of cos θ as a function of $\gamma_{LV}^{0.5}$ was found to be a more appropriate approach to the accurate determination of the critical surface tension (Good, 1977).

1.4.2. Polar and dispersion components of surface energy.

Fowkes (1964) proposed that surface energy be considered as additive contributions representing polar (p) and dispersion (d) forces, where γ^{TOT} is the total surface energy.

$$\gamma^{TOT} = \gamma^{p} + \gamma^{d} \qquad (1.4.1.)$$

It was important to consider the nature of different forces which could act across interfaces. It is usual to consider physical forces as polar interactions, which can be electrostatic interactions (also called Coulombic) and a group of forces which are collectively termed van der Waals interactions. Coulombic interactions existing between charged molecules and being of high energy, are not of great concern to interfacial phenomena.

Van der Waals interactions consist of three types of forces: dipole, induced dipole and dispersion forces. These low energy interactions between materials are of more relevance to this line of work. Thus the interfacial force was considered to be composed of dispersion forces and a polar term which is the sum of the other two types of forces.

1.4.2.1. Calculation of polar and dispersion forces.

Fowkes (1964) derived a relationship which allows the calculation of the dispersion component of the surface energy of a solid, from a contact angle measured using a liquid which has a surface tension, which is entirely non-polar.

$$\gamma_L (1 + \cos \theta) = 2 (\gamma_1^d . \gamma_2^d)^{0.5} \qquad (1.4.2.)$$

where γ_1^d = the dispersive component of the surface tension of a liquid

γ_2^d = the dispersive component of the surface energy of a solid

γ_L = the surface tension of a liquid

This equation was represented by Zografi and Tam (1976) in a form which can be solved iteratively by use of simple computer programmes to find the polar and dispersion components of the surface energy of any solid if a contact angle is measured on the solid, using two different liquids, each of known surface tension and polarity. Polarity being the polar component of surface tension divided by the total surface tension.

The theory of polar and dispersion forces to characterise interfacial phenomena has been used by many for over 20 years. However, more recently *eg* Fowkes *et al.*, (1990) found that this theory may be incorrect, as interfacial tensions between squalene and many other liquids were considered and observed behaviour was found not to correlate with predictions that were based on polar and dispersive interactions. Such interactions were accurately modelled by considering the polar term as being either acidic and/or basic in nature.

1.4.3. Theory of non-additive surface energy components.

Van Oss *et al.*, (1987) described difficulties in considering polar interactions as all being of a similar type and pointed out that there were materials which could be described as polar which were dipolar, hydrogen-bonding, Lewis acids or Lewis bases. Dipolar materials have a permanent dipole. Hydrogen bonding materials could be of three distinct classes *ie* those which are proton donors and proton acceptors (*eg* water), those which are predominantly proton donors (*eg* chloroform) and those which are predominantly proton acceptors (*eg* ketones).

Similarly a subdivision is possible with the Lewis acid-Lewis base materials, which can be considered as either bipolar or monopolar in either the electron donor or the electron acceptor sense (van Oss *et al.*, 1987). Two polar materials of the same sign can repel each other. Monopolar repulsion energies are significantly stronger than apolar interactions and will have a dominant influence on interfacial behaviour. It has been shown that many materials are monopolar.

Van Oss *et al.*, (1987) suggested treating dispersion forces as a non-polar term which is an additive contribution of all dispersion and induced-dipole-induced dipole forces, which is defined as the Lifshitz-van der Waals term (γ^{LW}). A surface energy term can then be defined in terms of γ^{TOT} and its constituent parts, γ^{LW} and its acid-base contribution, γ^{AB}, the acid-base parameter being further divided into an electron-donor (γ^-) and an electron acceptor (γ^+) contribution (Wu *et al.*, 1995).

1.4.3.1. Calculation of acid-base surface energy parameters.

The first stage is to accept that no interaction can occur between the LW and the AB forces, thus;

$$\gamma^{TOT} = \gamma^{LW} + \gamma^{AB} \qquad (1.4.3.)$$

For a liquid, once the total surface tension is known, the γ^{LW} component of the surface tension can be found by contact angle (θ) measurement on a completely apolar surface, such as Teflon, by using Eq. 1.4.4.

$$\gamma_L (1 + \cos \theta) = 2 (\sqrt{\gamma_S^{LW} . \gamma_L^{LW}}) \qquad (1.4.4.)$$

The γ^{LW} component of the surface tension of solids can similarly be determined by contact angle measurement, with apolar liquids for which $\gamma_L = \gamma^{LW}$ using the following equation;

$$1 + \cos \theta = 2 (\sqrt{\gamma_S^{LW}/\gamma_L}) \qquad (1.4.5.)$$

According to the Dupré equation, the apolar interaction energy (ΔG_{132}^{LW}) between materials 1 and 2 immersed in a liquid 3 is

$$\Delta G_{132}^{LW} = \gamma_{12}^{LW} - \gamma_{13}^{LW} - \gamma_{23}^{LW} \qquad (1.4.6.)$$

where

$$\gamma_{12}^{LW} = (\sqrt{\gamma_1^{LW}} - \sqrt{\gamma_2^{LW}})^2 \qquad (1.4.7.)$$

In addition to apolar interactions, polar interaction of, for example the hydrogen-bonding type can occur. The polar component of the free energy of interaction between two

materials 1 and 2 can be expressed as

$$\Delta G^{AB} = \gamma_{12}^{AB} - \gamma_1^{AB} - \gamma_2^{AB} \qquad (1.4.8.)$$

where

$$\gamma_{12}^{AB} = 2\left(\sqrt{\gamma_1^+\gamma_1^-} + \sqrt{\gamma_2^+\gamma_2^-} - \sqrt{\gamma_1^+\gamma_2^-} - \sqrt{\gamma_1^-\gamma_2^+}\right) \qquad (1.4.9.)$$

and

$$\gamma_1^{AB} = 2\sqrt{\gamma_1^+\gamma_1^-} \qquad (1.4.10.)$$

Expressing the Young-Dupré equation as

$$(1 + \cos\theta)\,\gamma_L = -\Delta G^{TOT} \qquad (1.4.11.)$$

and considering that

$$\Delta G^{TOT} = \Delta G^{LW} + \Delta G^{AB} \qquad (1.4.12.)$$

we obtain

$$(1 + \cos\theta)\,\gamma_L = -\Delta G^{LW} - \Delta G^{AB} \qquad (1.4.13.)$$

which becomes

$$(1 + \cos\theta)\,\gamma_L = 2\left(\sqrt{\gamma_S^{LW}\gamma_L^{LW}} + \sqrt{\gamma_S^+\gamma_L^-} + \sqrt{\gamma_S^-\gamma_L^+}\right) \qquad (1.4.14.)$$

Thus by contact angle (θ) measurement with three different liquids (of which two must be polar) with known γ_L^{LW}, γ_L^+ and γ_L^- values using Equation 1.4.14. three times, the γ_S^{LW}, γ_S^+ and γ_S^- of any solid can be determined. Similarly by contact angle measurement of a liquid on various solids (of which two must be polar) the γ_L^{LW}, γ_L^+ and γ_L^- can be

determined.

Once all the parameters are determined for two different materials 1 and 2, their interfacial tension, γ_{12} is

$$\gamma_{12} = (\sqrt{\gamma_1^{LW}} - \sqrt{\gamma_2^{LW}})^2 + 2 (\sqrt{\gamma_1^{+}\gamma_1^{-}} + \sqrt{\gamma_2^{+}\gamma_2^{-}} - \sqrt{\gamma_1^{+}\gamma_2^{-}} - \sqrt{\gamma_1^{-}\gamma_2^{+}}) \qquad (1.4.15.)$$

According to the Dupré equation for interactions between particles or molecules 1 and 2 in a liquid 3

$$\Delta G_{132}^{TOT} = \gamma_{12} - \gamma_{13} - \gamma_{23} \qquad (1.4.16.)$$

For the specific case of an interaction between phase 1 and 2 in the presence of water (w) the full term for the free energy of adhesion would be;

$$\Delta G_{1w2} = (\sqrt{\gamma_1^{LW}} - \sqrt{\gamma_2^{LW}})^2 - (\sqrt{\gamma_1^{LW}} - \sqrt{\gamma_w^{LW}})^2 - (\sqrt{\gamma_2^{LW}} - \sqrt{\gamma_w^{LW}})^2 + 2 [\sqrt{\gamma_w^{+}} (\sqrt{\gamma_1^{-}} + \sqrt{\gamma_2^{-}} - \sqrt{\gamma_w^{-}}) + \sqrt{\gamma_w^{-}} (\sqrt{\gamma_1^{+}} + \sqrt{\gamma_2^{+}} - \sqrt{\gamma_w^{+}}) - \sqrt{(\gamma_1^{+}\gamma_2^{-})} - \sqrt{(\gamma_1^{-}\gamma_2^{+})}]$$

(1.4.17.)

A negative value for the free energy of interaction will result in a net attraction between substance 1 and 2 immersed in water.

1.5. SOLUBILITY.

The solution produced when equilibrium is established between undissolved and dissolved solute in a dissolution process is termed a "saturated solution". The amount of substance that passes into solution in order to establish the equilibrium at constant temperature and pressure and so produce a saturated solution is known as the *solubility* of the substance. An understanding of the process of solution and the factors governing the solubility of drugs is important in pharmaceutics for several reasons.

1.5.1. The process of solution.

A simple way to consider solubility is by use of the cavity model. See Figure 1.5.1. where it can be seen that, for a solid to dissolve, it is necessary for a molecule to be detached from the solid, to form a cavity in the liquid, and finally for the detached solute molecule to be incorporated into the liquid.

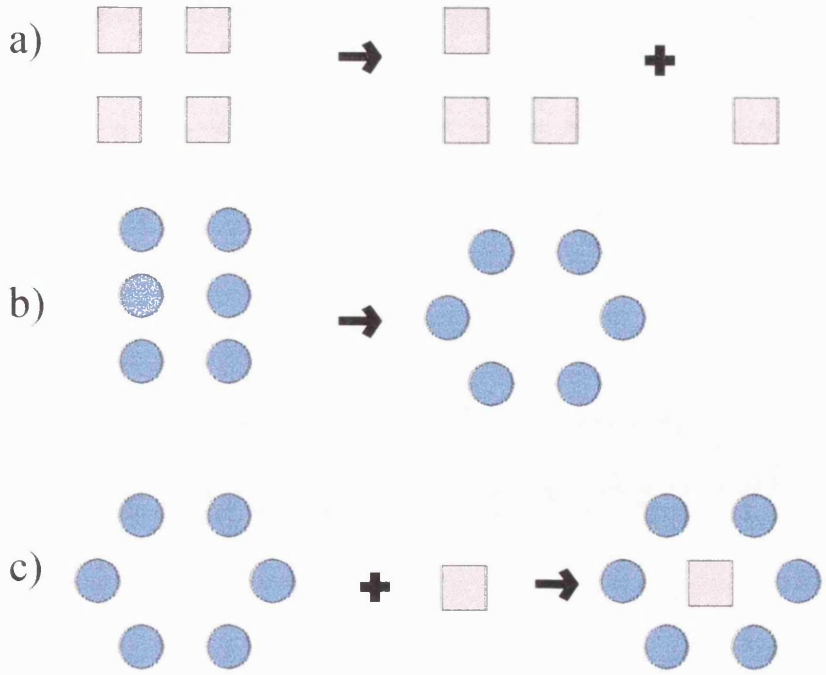

Figure 1.5.1. Cavity model to show the process of solution;

a) the detachment of a molecule from the solid

b) the formation of a cavity in the liquid

c) incorporation of the solute molecule into the solvent cavity.

1.5.2. Aspects of structure relating to solubility.

Both the nature of the solute and solvent are important considerations when dealing with solubility. The first aspect is the lattice energy of the solute, which determines how easily a solute molecule is detached. Yalkowsky *et al.*, (1972) and Forster *et al.*, (1991) have shown solubility to be correlated with solid melting point due to the last point made. The formation of the cavity in the solvent will be linked to the solvent boiling point.

When considering the third aspect of incorporating the solute into the liquid cavity, the nature of the solute, in terms of size, shape and hydrophilic/ hydrophobic balance will all be important. The size and shape determine the volume of the cavity that is needed. "Like dissolves like", therefore the hydrophilic nature is important, thus polar molecules will be more readily accommodated in polar liquids and vice versa (Buckton, 1995). The hydrophobic nature of the material or the lattice energy (which are both related to molecular structure), may be possible factors which limit solubility.

The effect of structure on solubility is discussed in more detail by Florence and Attwood, (1988) who review the influence of molecular surface area and the effect of substituents on solubility.

1.5.3. Wettability and solubility relationships.

Solubility parameters describe the solvent power of a liquid and thus relate to solubility. However they can also be used to estimate surface energy values for materials. Solubility parameter was originally used to define the nature of non-polar solvents, for which it was a measure of the intermolecular forces that existed within the system. The nature of the solvent was taken as being related to the energy required to vaporise the liquid. The solubility parameter (δ_s) is equal to the square root of the cohesive energy density of a material:

$$\delta_s = \{ (\Delta H_{vap} - RT) / M_v \}^{0.5} \qquad (1.5.1.)$$

where ΔH_{vap} is the enthalpy of vaporisation (determined by calorimetric experiments) and M_v is the molecular volume.

The solubility parameter can be divided up into constituent parts in an identical manner to that proposed for surface energies by Fowkes (see section 1.4.2.). In this instance, however, it is usual to consider the solubility parameter in terms of dispersion, polar and hydrogen bonding contributions (represented by subscripts d, p and h respectively):

$$\delta_s = (\delta_d^2 + \delta_p^2 + \delta_h^2)^{0.5} \qquad (1.5.2.)$$

As with the surface energy theory, the hydrogen bonding and polar terms can be combined to give an overall polar solubility parameter (δ_A):

$$\delta_A = (\delta_p^2 + \delta_h^2)^{0.5} \qquad (1.5.3.)$$

In many cases, surface energy estimated from solubility parameter, correlates well with the measured surface energy but this is not always the case. Forster *et al.*, (1991) and Sheridan *et al.*, (1994b) both investigated the wettability of the alkyl-p-hydroxybenzoates and Forster *et al.*,(1991) compared them to solubility data.

Variation of aqueous and non-aqueous solubility with alkyl chain length for the alkyl-p-hydroxybenzoates correlate although there is an idiosyncratic response for the methyl derivative (Forster *et al.*, 1991). However the trends seen in aqueous and non-aqueous solubility are not correlated with wettability data reported by Sheridan *et al.*, (1994b).

It follows that the wettability is related to structure and that the solubility is related to the structure, but the wettability is not directly related to the solubility. Buckton (1990a) described similar findings for a series of barbiturates, by use of compensation analysis to compare thermodynamic parameters for wettability and solubility.

1.6. DISSOLUTION.

The process by which a drug dissolves from a product is termed *dissolution.* The dissolution of a solid in a liquid may be regarded as being composed of two consecutive stages, rather than consisting of one process. The first stage being an interfacial reaction, which results in the liberation of solute molecules from the solid phase. This is followed by the second stage which is the transport of these molecules away from the interface into the bulk of the liquid phase, under the influence of diffusion or convection.

In the absence of a chemical reaction between solute and solvent, the slowest stage is usually the diffusion of dissolved solute across the static boundary layer of liquid that exists at a solid/liquid interface.

1.6.1. The Noyes-Whitney equation.

Under the conditions detailed above, the rate of dissolution of a solid in a liquid may be described quantitatively by the Noyes-Whitney equation;

$$dm / dt = (A. D / d_h). (C_s - C) \qquad (1.6.1.)$$

where;

m = mass of the solute that has passed into solution

t = time

dm/dt = rate of dissolution

A_s = surface area of the undissolved solid in contact with the solvent

D = diffusion coefficient

d_h = thickness of the unstirred layer through which dissolved drug must diffuse

C_s = concentration of solute required to saturate the solvent *ie* saturated solubility

C = amount of drug dissolved at time, t

If $C \ll C_s$ then the dissolution rate will be directly proportional to the saturated concentration (*ie* solubility) and the term may be simplified to;

$$dm / dt = k.A_s.C_s \qquad (1.6.2.)$$

where k is the dissolution rate constant.

These circumstances are normally called "sink conditions" and occur when the concentration of solute does not exceed 10% of the amount needed for equilibrium saturation. This situation is possible when the solute is removed from the medium at a faster rate than it passes into solution, or when the volume of the medium is very large. Sink conditions may arise in vivo when a drug is absorbed from its solution in the gastrointestinal fluids faster than it dissolves in those fluids.

1.6.2. Dissolution of solid drugs.

Figure 1.6.1. shows a schematic diagram of dissolution from a solid surface. This model is based on the Noyes-Whitney equation which can be used to predict the effect of parameters *eg* solvent change on the dissolution rate of solid drugs.

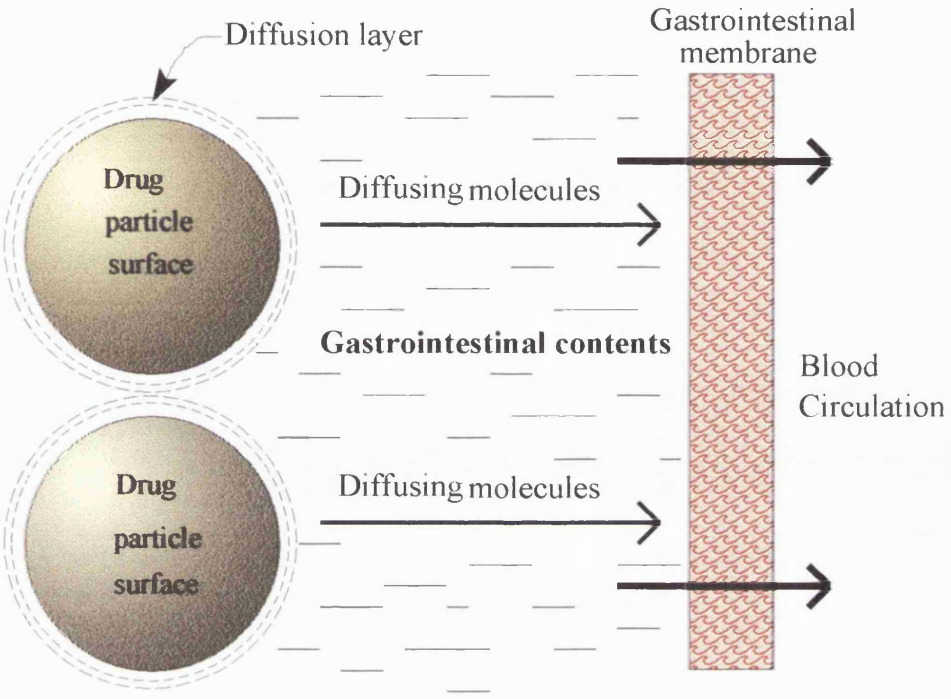

Figure 1.6.1. Schematic diagram of dissolution for a solid surface.

1.6.3. Factors affecting dissolution rate.

There are many factors which affect the in vitro dissolution rates of solids in liquids and are based on the various terms in the Noyes-Whitney equation. These factors are;

a) A_s - surface area of the undissolved solid

b) C_s - solubility of solid in dissolution medium

c) C - concentration of solute in solution at time, t

d) d_h - thickness of boundary layer

e) D - diffusion coefficient of solute in the dissolution medium

a) A_s - surface area of the undissolved solid

This will depend on the size of the solid particles, dispersibility of powdered solid in dissolution medium and the porosity of solid particles. Particle size will change during the dissolution process because large particles will become smaller and small particles will eventually disappear. Mosharraf *et al.*, (1995) found that both particle shape and size were related to dissolution rates of sparingly soluble micro-particles. Also the surface area available for dissolution is reduced if particles tend to form coherent masses in the disssolution medium. This may be overcome by the addition of a wetting agent (Efentakis *et al.*, 1991).

b) Solubility of solid in dissolution medium

This may be affected by temperature, the nature of the dissolution medium and presence of other compounds. The temperature effect on dissolution behaviour was investigated by Otsuka *et al.*, (1992), who looked at the nitrofurantoin anhydrate and monohydrate. Basically, the dissolution rates increased with an elevation of temperature for the two modifications of nitrofurantoin. Ozturk *et al.*, (1988) found the dissolution rate of ionisable drugs (weak acids or bases) to be dependent on the pK_a and solubility and the medium properties of buffered and unbuffered solutions.

The presence of other compounds such as solubilising agents can affect solubility *eg* de Smidt *et al.*, (1994) discussed the dissolution kinetics of griseofulvin in mixed micellar solutions. It was shown that the solubilisation of this poorly soluble drug by mixed micelles affected its dissolution rate depending on the concentration of the solution.

c) The concentration of solute in solution at time, t.

This is affected by the volume of dissolution medium and also any process that removes dissolved solute from the dissolution medium. For example, adsorption onto an insoluble adsorbent or by continuous replacement of solution by fresh dissolution medium.

d) Thickness of the boundary layer.

This is affected by the degree of agitation, which depends on speed of stirring or shaking, shape, size and position of stirrer, volume of dissolution medium, shape and size of container and viscosity of dissolution medium.

e) The diffusion coefficient of solute in the dissolution medium.

This is affected by the viscosity of dissolution medium and the size of diffusing molecules.

1.6.4. Measurement of dissolution rates.

Many methods have been described in the literature, particularly relating to the determination of the rate of release of drugs into solution from tablet and capsule formation (Jashnani *et al.*, 1993, Otsuka *et al.*, 1992, Efentakis *et al.*, 1991 and Burns *et al.*, 1995).

The methods for determining dissolution rates have been reviewed by Leeson and Carstensen (1974). Classifications have been made based mainly on whether or not the mixing processes that take place in the various methods occur by natural convection arising from density gradients produced in the dissolution medium or by forced convection

brought about by stirring or shaking the system.

Briefly the various methods used are;

a) flask-stirrer method

b) rotating basket method

c) paddle method

d) rotating disk method.

Descriptions of all these methods may be found in Aulton (1988) and Florence and Attwood (1988).

1.7. PARTITIONING.

With the partitioning phenomena, if two immiscible phases are placed in contact, one containing a solute soluble in both phases, the solute will distribute itself so that when equilibrium is obtained, no further transfer of solute takes place (Florence and Attwood, 1988).

Both the solubility and partitioning of drugs are the most important factors influencing the biological performance after oral administration (Yalkowsky, 1980).

1.7.1. Partition coefficients.

The partition of a drug from being in solution entirely in water to being in equilibrium between water and a second immiscible phase is defined by an equilibrium constant called the *partition coefficient*, P. This is normally expressed as log P and has been shown to correlate very well with biological response (Hansch *et al.*, 1968).

One may expect the partition of a molecule between an aqueous and a non-aqueous liquid to relate to both the wettability (*ie* surface energy) and to the solubility of the material. Cammarata *et al.*, (1980) has shown solubility parameters to correlate with partitioning behaviour.

Partition coefficients of drugs influence the transport and absorption processes. Leo and Hansch (1971) have collected vast amounts of experimental data on partition coefficients of drugs, using the octanol/water partitioning system. There is little evidence to suggest that the surface energies of drugs correlate with their log P values and this will be discussed further in Chapter 6.

1.7.2. Water dragging effect.

Tsai *et al.*, (1993) reported on the average number of water molecules that are 'dragged' into a non-aqueous phase during partitioning. This was shown to be due primarily to the hydrogen bond donating capacity of the solutes. See Figure 1.7.1. for a simplified version to demonstrate this water-dragging effect.

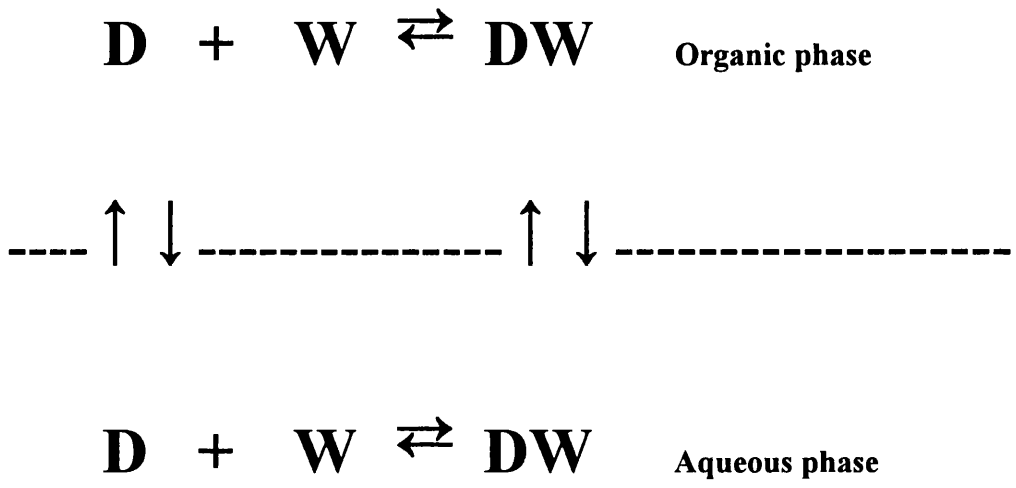

Figure 1.7.1. Diagrammatic representation of solute partitioning between water and another liquid, either alone or associated with water.

The solute will associate with water both in the aqueous and non-aqueous phases. If the solute associates with water in the non-aqueous phase, there will be a measurable excess of water in that phase. This excess of water has been measured for many different materials (Tsai *et al.*, 1993). The extent of association between the solute and water both in the aqueous and non-aqueous phase will affect the amount of material which partitions

(Buckton, 1995). A correlation existed between the water dragging effects and the electron donor/electron receptor characteristics of the solute, thus the acid-base parameters of surface energy would be expected to correlate with partition.

1.7.3. Choice of solvent.

Partition coefficients correlate with biological response as they roughly predict the tendency for a drug to move from an aqueous environment into a membrane (Tomlinson *et al.*, 1983). Octan-1-ol has been used extensively as the non-aqueous solvent and this has been questioned by Beezer *et al.*, (1987) in terms of the biological relevance of this solvent. Octan-1-ol consists of a lipophilic chain and a polar head, thus molecules will align in a manner similar to that of a membrane structure.

The Collander equation relates the water/solvent partitioning behaviour of a solute in one system (P_1) to the value obtained for the same solute partitioning from water to a different solvent (P_2):

$$\log P_1 = a + b \log P_2 \qquad (1.7.1.)$$

It has been suggested by Leo and Hansch (1971) that the value of 'a' reflects the solvent lipophilicity and the water content of the solvent at saturation. The values of 'b' reflect the similarity of the solvent environment with respect to the solute (Katz and Diamond, 1974 a,b).

Yamagami *et al.*, (1993), investigated the relationships between the partition coefficients obtained for substituted diazines in a range of partitioning solvents. They found that the difference between the partition into the various solvents was due to the number of hydrogen bonding sites in the substituent. This meant that the electron donor and electron receptor roles of the solute and the solvent will determine partitioning.

1.8. ABSORPTION.

Drug absorption requires the passage of the drug in a molecular form across the barrier membrane. Most drugs are delivered to the body as solid or semisolid dosage forms, which must first release their drug content. The drug must then dissolve, followed by passage from a region of high concentration to a region of low concentration across the membrane surrounding the site of absorption into the blood. Figure 1.8.1. illustrates the sequence of events in drug absorption from formulations.

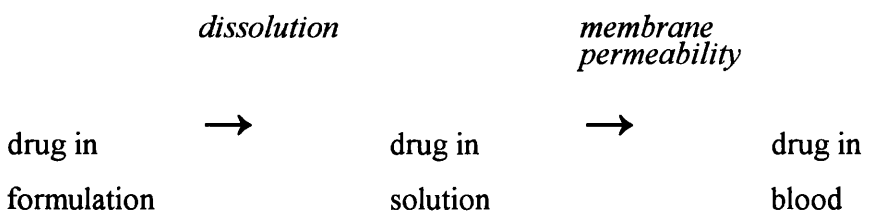

Figure 1.8.1. Drug absorption from a formulation.

1.8.1. Absorption across biological membranes.

Absorption across different biological membranes can change the rate of absorption, the bioavailability and thus the therapeutic benefit of drugs. However all the routes involve passage across a lipid membrane.

The role of surfactants in promoting absorption of drug from dosage forms is one area of interest. The gastrointestinal tract contains bile salts which help with the digestion and absorption of food. The role of bile salts in the absorption of drugs has been reviewed by Poelma *et al.*, (1990). Bile salts do not exist in high enough concentrations to cause

damage to the mucosal membrane. Bile salts increase absorption by the solubilisation of poorly water soluble drugs.

Anderberg *et al.*, (1992) studied the effects of bile salts and surfactant excipients on the permeability of cell cultured models of intestinal epithelia (Caco-2 cells). The surfactants demonstrated concentration-dependent effects on the permeability of the cell culture. Different hydrophilic marker molecules passed through the epithelial monolayers through different pathways at different concentrations of the surfactants. Sodium dodecyl sulphate was found to alter membrane permeability at concentrations which are used in current pharmaceutical products.

Anderberg and Artusson (1993) showed that the absorption enhancement was due to membrane damage, which is reversible with time, providing the surfactant is not present for prolonged periods.

Burton *et al.*, (1992) also used Caco-2 cells to demonstrate how the structure of orally bioavailable peptides and peptide-like substances influences absorption across the intestinal mucosa.

Uchegbu *et al.*, (1995) investigated the encapsulation of doxorubicin in niosomes (prepared from the surfactant Span 60) as a route to tumour targeting in the mouse.

1.9. AIMS AND OBJECTIVES.

The purpose of this work was to assess the surface properties of a group of poorly soluble pharmaceutical powders, with the aim of providing information on the interactions of these drugs with a surfactant. This was with a view to gaining an improved understanding of the role of SDS in aiding drug absorption from solid dosage forms.

The following methods will be explored:

1. Contact angle measurement, using the Wilhelmy plate technique and subsequent calculation of surface energies (using the acid/base theory described in section 1.4.3.2.).

2. Interactions between the drugs and the head and tail groups of the surfactant in water will be predicted using the van Oss and Costanzo equation (1992).

3. The relationship between these predicted interactions and solubility, dissolution and partitioning will be described.

CHAPTER 2

MATERIALS

2.1. LIQUIDS.

All liquids shown in Table 2.1.1. are the probe liquids which were used for contact angle measurements.

Table 2.1.1. Liquids used for contact angle measurements.
These were used as received and the surface tension values of these are shown on page 103.

Liquid	Supplier
Ethylene glycol	BDH
Formamide	Sigma
Bromonaphthalene	Fisons
Di-iodomethane	Aldrich

2.1.1. Buffer

Universal buffer was used for solubility and partitioning studies (Svehla, 1979). This buffer consisted of citric acid, potassium dihydrogen orthophosphate and boric acid, all of which were AnalaR quality. Table 2.1.2. shows the quantities of these constituents needed to make a 1 litre solution of universal buffer.

Table 2.1.2. Constituents of universal buffer for a 1 litre solution.

Material	Weight (g)
Citric acid	6.008
Potassium dihydrogen orthophosphate	3.893
Boric acid	1.769

2.1.2. Sodium hydroxide

The pH of the universal buffer was adjusted to equal the pK_a (Moffat, 1986) of each of the model drugs, using a 0.2M solution of sodium hydroxide (NaOH). The sodium hydroxide was obtained from BDH and had a batch number of LOT 050594H22S.

2.2. MODEL POWDERS.

A series of drugs was chosen as our model powders. In addition, one distinctly different material was selected for the studies. One surfactant powder was used throughout this work. Another material studied, Anthracene, was used as a control in the partitioning work.

1. The sulphonamides - a series of poorly soluble drugs with the same core structure but with different substituents attached to the sulphur group.
2. Sodium dodecyl sulphate - an anionic surfactant.
3. Anthracene - used as a marker solute in the Taylor-Aris diffusion technique (see section 6.2.3.2.).

2.2.1. Sulphonamides.

The sulphonamides are used in medicine as antibacterials, particularly in the treatment of urinary tract infections. Four compounds were used in this study (see Table 2.2.1.).

Table 2.2.1. The four sulphonamides and their batch numbers.

Material	Batch no.
Sulfanilamide	LOT 101H0137
Sulfadiazine	LOT 19F0627
Sulfamerazine	LOT 98F0733
Sulfamethazine	LOT 12H0642

This series of materials was chosen as it is a series of poorly soluble drugs which is commercially available. A series of low solubility was selected so that the effects of solubilisation with surfactant could be explored. Previous work has been carried out on the sulphonamides, investigating dissolution behaviour (Macheras *et al.*, 1987), absorption studies (Chow *et al.*, 1994 and Reddy *et al.*, 1976) and also partitioning work into cerebrospinal fluid (Holder *et al.*, 1965). Dissociation constant (pK_a) and partition coefficient (log P) into octanol data for the sulphonamides were obtained from Moffat (1986). This data are shown below in Table 2.2.2.

Table 2.2.2. Dissociation constants and partition coefficients for the sulphonamides.

Material	Dissociation constant (pK_a)	Partition coefficient (log P in octanol)
Sulfanilamide	10.4	-0.9
Sulfadiazine	6.5	-1.3
Sulfamerazine	7.1	-0.1
Sulfamethazine	7.4	0.3

Solubility data in water and buffer at pK_a values have been obtained for these materials and are presented in section 4.3.3.

The structures of the sulphonamides are shown in Figures 2.2.1., 2.2.2., 2.2.3. and 2.2.4.

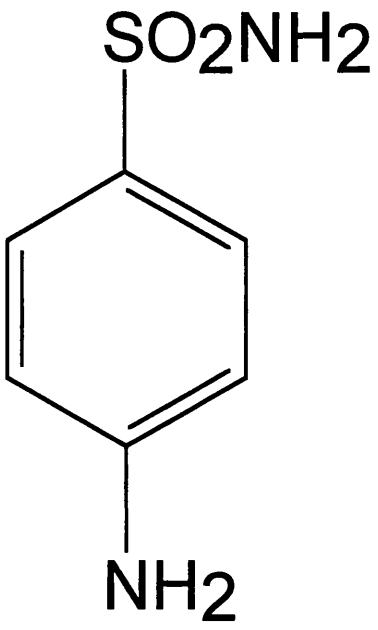

Figure 2.2.1. The structure of Sulfanilamide.

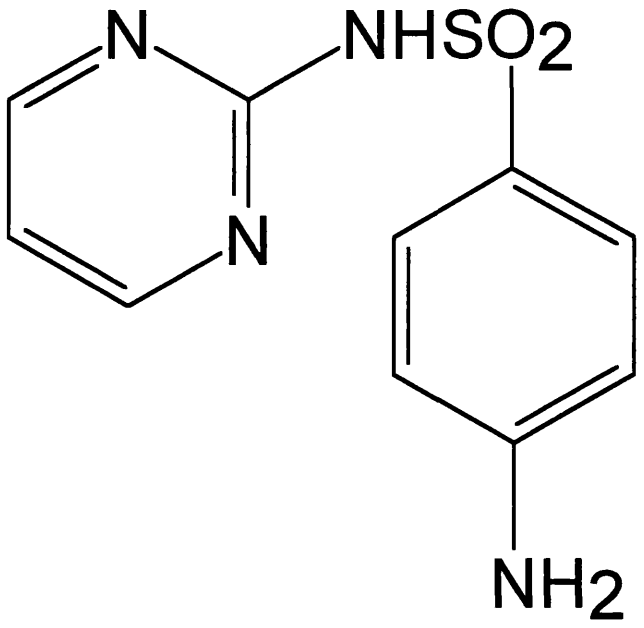

Figure 2.2.2. The structure of Sulfadiazine.

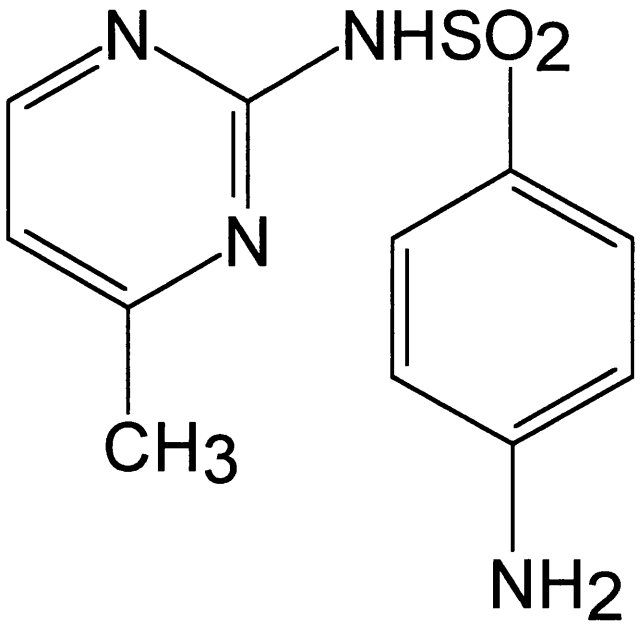

Figure 2.2.3. The structure of Sulfamerazine.

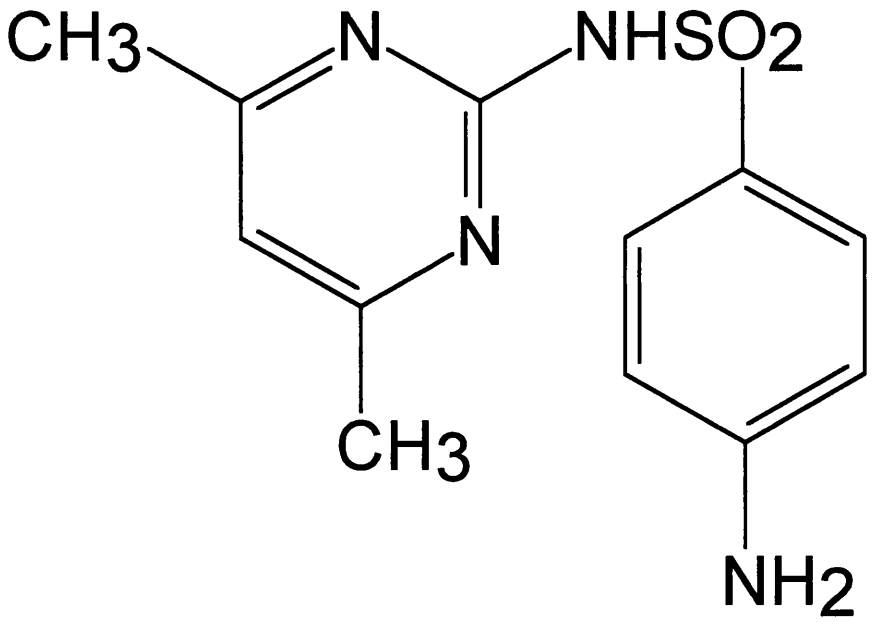

Figure 2.2.4. The structure of Sulfamethazine.

2.2.2. Sodium dodecyl sulphate

This anionic surfactant is used frequently in pharmaceutical formulations. It is commercially available and has been studied extensively in the past *eg* effect of pH on its critical micelle concentration (CMC) (Rahman *et al.*, 1983), effect of temperature and solvent on the CMC of sodium dodecyl sulphate (Onori *et al.*, 1992). It is very soluble in water, giving a clear solution. It is used pharmaceutically as a wetting agent. Sodium dodecyl sulphate, (SDS), carries a negative charge on the hydrophilic portion of the molecule. The formula for this surfactant is:

$$CH_3 (CH_2)_{11} - SO_4^-.Na^+$$

Table 2.2.3. The supplier and batch number of SDS.

Material	Supplier	Batch no.
SDS	BDH	LOT ZA1561010 442

The sample of SDS was used as received from the supplier, without further purification. This same sample was used throughout the thesis. From analysis of surface tension as a function of log concentration, it is clear that the sample (like many samples of SDS) contains a surface-active impurity. This has to be borne in mind in the interpretation of results in subsequent chapters.

2.2.3. Anthracene

This compound which is obtained from coal tar was used as the marker solute in the Taylor-Aris diffusion technique (see section 6.2.3.2.). It is insoluble in water (Merck Index, 1976) and is an important source of dyestuffs *eg* alizarin. The Anthracene used was of AnalaR grade. The structure of Anthracene is shown in Figure 2.2.5.

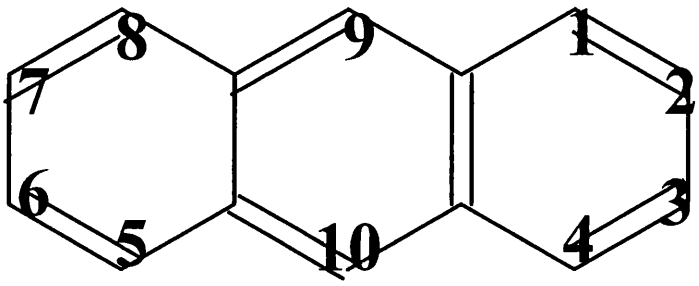

Figure 2.2.5. The structure of Anthracene.

CHAPTER 3

CONTACT ANGLE MEASUREMENT & SURFACE ENERGIES

3.1. INTRODUCTION.

A description of the Wilhelmy plate technique for measurement of contact angles is given in section 1.3.2.

The contact angle formed between a liquid and a solid medium provides useful information on the wettability of the solid. Contact angles may be obtained by direct observation of a drop of liquid on a flat surface and by measurement of the height of the drop. This method of measurement is quite simple. However, when pharmaceutical solids exist as finely divided powders, it is not possible to carry out assessment of their contact angle by direct methods. The method of contact angle selected for these studies was the Wilhelmy plate technique, which has been recently automated and is the least operator dependent of all the methods available.

Contact angle measurement is the most cited method for assessing the surface properties of pharmaceutical powders (*eg* Zografi and Tam, 1976; Lerk *et al.*, 1976; Buckton and Newton, 1986 and Parsons *et al.*, 1992b). The data obtained can be used to calculate the surface energy of the powder.

There were several reasons for obtaining contact angle data for the sulphonamides:

1. To obtain suitable contact angle data in order to calculate surface energies using the acid/base theory (*eg* van Oss *et al.*,1992).
2. To determine if there is a relationship between the surface properties of powders and

equilibrium solubilities.

3. To ascertain whether there is a relationship between the surface properties and rotating disk dissolution data.

4. To correlate with partitioning data using the Taylor-Aris diffusion technique to find any connection between the thermodynamics of transfer and the partitioning process.

By use of Wilhelmy plate technique, the surface tensions could be measured for: -

1. all the probe liquids used to calculate the surface energy values of the drug materials.

2. surfactant solutions of varying concentration, below and above their CMC values, to evaluate the CMC of the surfactant employed.

3. surfactant solutions of varying concentration at different pH values and temperature to determine how these factors effect the CMC of sodium dodecyl sulphate.

The contact angle formed by SDS solutions at varying concentrations on compacts of the different drugs was also investigated. These same concentrations are also used in the dissolution work (see Chapter 5). This was studied to determine how the wettability of the drug compacts was affected by various micellar solutions as contact angle measurement is a measure of wettability. If wetting is the rate limiting step for the dissolution of a tablet in the gut, then the concentration of surfactant used may affect the dissolution profile and therefore, drug bioavailability.

3.2. METHODS.

3.2.1. Description of the Cahn D.C.A. analyser.

A schematic diagram of the apparatus is shown in Figure 3.2.1. The apparatus is enclosed within a draught-free chamber. Both the microbalance and the motorised platform were interfaced with a personal computer. The motorised platform could be raised a maximum distance of 39mm at a constant pre-set speed between 20 and 264 $\mu msec^{-1}$. Temperature was controlled by flowing water at constant temperature from a circulator (Gallenkamp) through a jacketed vessel.

For surface tension measurement, the probe must be perfectly wetted by the test liquid. This study involved using a clean glass plate as the probe material. The microbalance was regularly calibrated using a 500mg calibration weight.

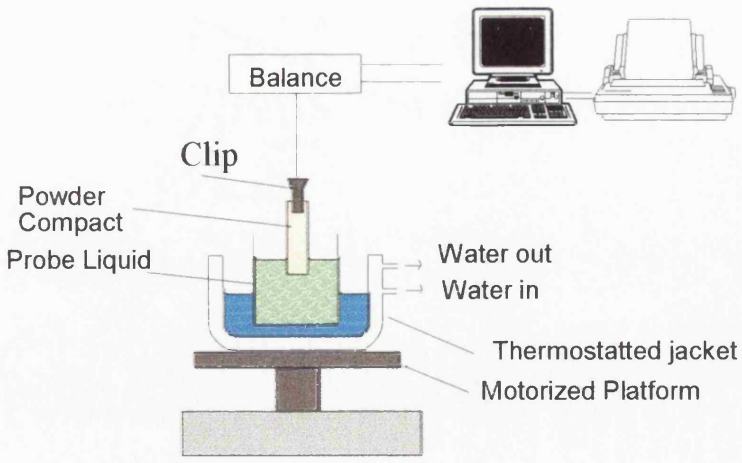

Figure 3.2.1. A diagrammatic representation of the Wilhelmy plate apparatus.

3.2.1.2. Method for cleaning glassware.

Glassware was cleaned by placing it in an ultrasonic bath containing Micro® solution (International Products Corporation, Chistlehurst, Kent) for 5 minutes at 60°C, rinsing under warm water for approximately 5 minutes and then finally rinsing using purified water before being dried in an oven.

3.2.1.3. Experimental procedure.

To perform an experiment, the beaker containing the test liquid was held in a jacketed vessel at a temperature of 25°C. The glass plate was passed through a hot flame prior to use, to burn away any organic material. The glass plate was suspended lengthways, by means of a crocodile clip, attached to the arm of the microbalance above the probe liquid. The platform was raised ~ 8mm, at a speed of 151μm sec^{-1}. Force readings were collected at one second intervals as a function of time and stage position. The $F_{z.d.o.i.}$ was determined as described in section 1.3.1.1. The surface tension was then calculated using Equation 1.3.2. (see Chapter 1). There are two unknowns in this equation, γ_{LV} and cos θ. As mentioned previously, a requirement of surface tension measurement is that the test liquid perfectly wets the probe. Therefore, cos θ = 1 and γ_{LV} can be obtained from Equation 1.3.2. shown below:

$$\gamma_{LV} = Fg / \cos\theta.p \qquad (1.3.2.)$$

where;

F = force at zero depth of immersion

g = accelaration due to gravity

p = perimeter of the glass plate

Advancing and receding data were obtained to ensure that there was no hysteresis - to ensure that the glass plates were perfectly clean.

The surface tension of the following liquids was measured:- double distilled water, ethylene glycol, formamide, di-iodomethane and bromonaphthalene. Surface tension measurements ± standard deviation are shown in Table 3.2.1. together with literature values. In each case the hysteresis was negligible (the advancing and receding readings were the same), confirming the cleanliness of glass plates.

Table 3.2.1. Surface tension values of all liquids used ($mN.m^{-1}$).

Liquid	**γ_l (mNm^{-1}) (literature value)**	**γ_l (mNm^{-1}) (measured value)**
Double distilled water[1]	72.0	72.6 ± 0.2
Ethylene glycol[1]	48.9	48.8 ± 0.5
Formamide[2]	58.0	57.9 ± 0.2
Di-iodomethane[1]	50.4	50.7 ± 0.6
Bromonaphthalene[2]	44.0	43.7 ± 0.5

1 Zografi and Tam (1976),
2 Parsons (1992b),

3.2.2. Measurement of critical micelle concentration.

This was undertaken using the Wilhelmy plate technique using the Cahn D.C.A. analyser.

3.2.2.1. Liquid preparation.

The liquids used were all solutions of sodium dodecyl sulphate (SDS), in various concentrations ranging from 3.46×10^{-4} to 3.46×10^{-2} mol.dm^{-3}. These solutions were prepared with six different batches of universal buffer, each of which had been adjusted to an individual value of pH using a 0.2M solution of sodium hydroxide. pH meter (WPA CD 300) was employed in adjusting the pH range between 3.0 and 10.4. Having prepared each solution of SDS, the pH was again checked to ensure that the addition of SDS had not altered the required pH value of any particular solution.

3.2.2.2. Experimental procedure.

For this set of experiments, the same procedure was followed as described in section 3.2.1.3. and Equation 1.3.2. was used to calculate the surface tension of the liquid.

Six replicate glass plates were used for each experiment, using SDS solutions of concentrations of 3.46×10^{-4}, 6.9×10^{-4}, 3.46×10^{-3}, 6.93×10^{-3}, 1.0×10^{-2}, 1.39×10^{-2}, 1.73×10^{-2}, 2.1×10^{-2}, 2.78×10^{-2} and 3.46×10^{-2} mol.dm^{-3}, each being buffered to a pH of 3.0, 6.5, 7.1, 7.2, 7.4 and 10.4. These surface tension experiments were again repeated employing the same solutions but this time the temperature was adjusted to 42°C. This was controlled by flowing water at constant temperature from a circulator (Gallenkamp) through a jacketed vessel.

3.2.2.3. Determination of CMC.

The critical micelle concentration was assessed by plotting log surface tension as a function of SDS concentration in mol dm^{-3} at the six different pH values as shown in Figure 3.2.2. The portion of the plot showing the onset of the plateau is extrapolated down to the intercept on the x-axis and this value is indicative of the CMC of SDS at that particular temperature and pH.

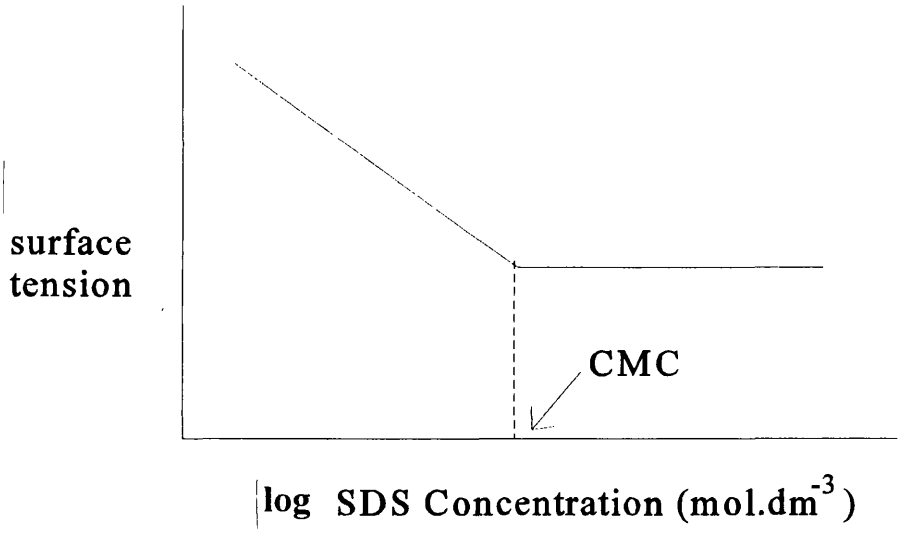

Figure 3.2.2. Showing the portion of the curve selected for determination of CMC.

3.2.3. Contact angle measurement.

This was carried out using the Wilhelmy plate technique, using the Cahn D.C.A. analyser. The two reasons for this study were:-

1. to calculate surface energies of the model powders using the acid/base theory (van Oss *et al.*, 1992).

2. to determine the contact angles formed on compacts of the different drugs by SDS solutions at varying concentrations.

3.2.3.1. Powder plate preparation.

Compressed powder plates were produced using a highly polished, stainless steel rectangular die (Figure 3.2.3.) This could be dismantled after compression, to allow easy removal of the compact. The plates were prepared using 200mg of powder, which was spread evenly in the die, in an attempt to ensure constant porosity throughout the compact. Plates were compressed using a Specac which could apply forces up to 15×10^5 kN m^{-2}. For each plate, a compaction force of 6×10^5 kNm^{-2} and a dwell time of 2 minutes was used. The plates produced were all 1.07cm x 2.00cm, but of varying thickness. The thickness of each plate was measured using a micrometer. This enabled the perimeter of the plate, p, to be calculated.

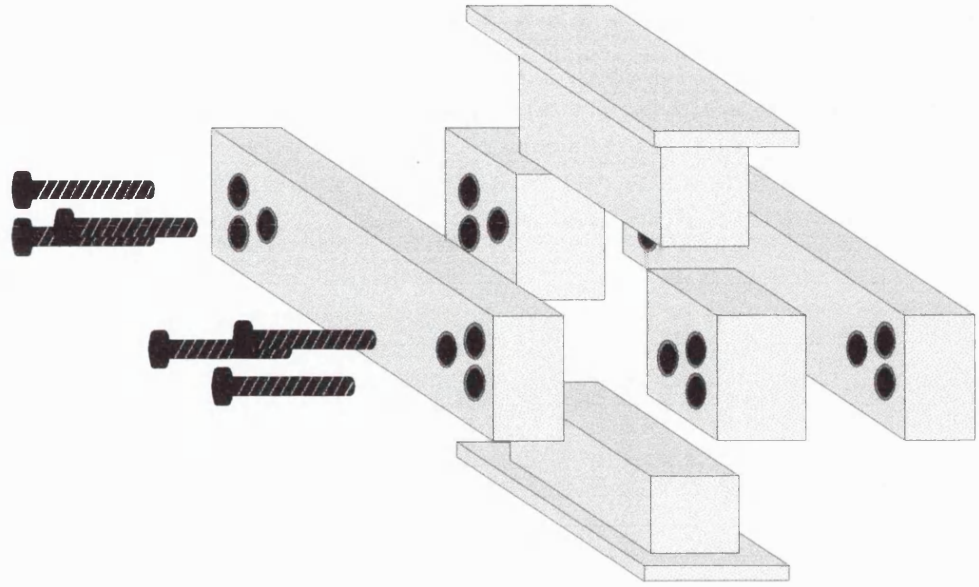

Figure 3.2.3. Schematic diagram of the punch and die used to prepare the powder plates.

3.2.3.2. Choice of liquid.

Three liquids were selected from those shown in Table 3.2.1. - two polar liquids, such as water and ethylene glycol and one non-polar liquid *ie* di-iodomethane or bromonaphthalene. In the second part of the experiment, the solutions employed were various concentrations of SDS in water *ie* 6.9×10^{-4}, 3.46×10^{-3}, 6.93×10^{-3}, 3.46×10^{-2} and 6.93×10^{-2} mol.dm^{-3}. Initially the surface tensions of these solutions were determined as described in section 3.2.1. before carrying out contact angle analysis.

3.2.3.3. Experimental procedure.

To perform an experiment, the powder plate was suspended from the arm of the microbalance. The test liquid was placed in a clean beaker and the experimental procedure described in section 3.2.1.3. was followed.

The $F_{z.d.o.i.}$ for advancing data was analysed using least squares analysis. This involved using only the straight portion of the buoyancy slope as shown in Figure 3.2.4. At least six replicate plates were used for each experiment. The data obtained using water, ethylene glycol and di-iodomethane was used to calculate the surface energies as described in section 1.4.3.2.

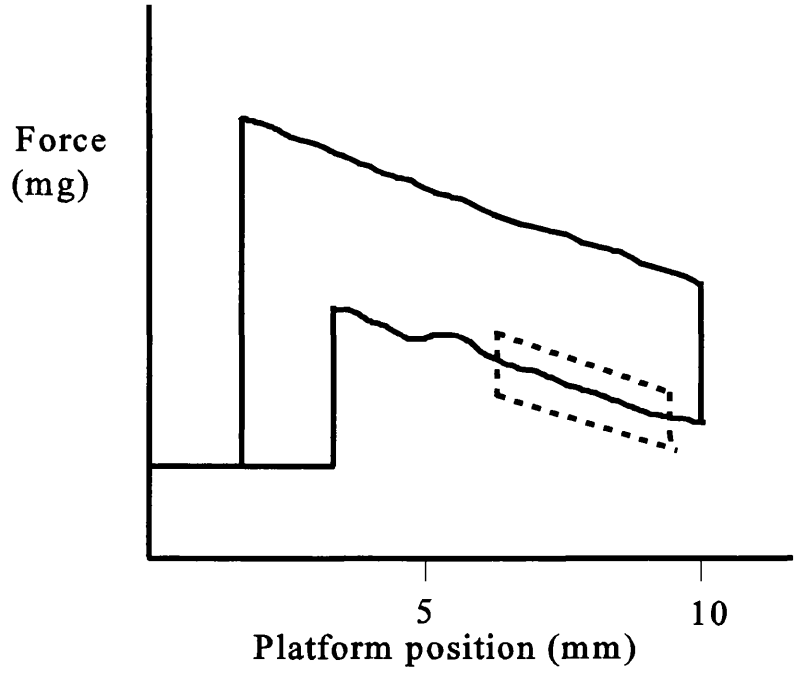

Figure 3.2.4. Showing the portion of the curve selected for analysis.

3.3. RESULTS AND DISCUSSION.

3.3.1. Surface tension data obtained for solutions of various SDS concentration.

Using the method descibed in section 3.2.2., surface tension data for solutions of different concentrations of sodium dodecyl sulphate are shown in Tables 3.3.1. and 3.3.2. The tables give data at temperatures of 25 and 42°C. Each solution was freshly prepared on the day of the experiment.

3.3.1.1. Reproducibility of the data.

Very reproducible data have been obtained for the surface tension values and this is indicated by the low standard deviation values.

3.3.1.2. Data analysis.

Data were analysed using the method described in section 3.2.2.3. A line is drawn from the onset of the plateau to the intercept on the x-axis of a plot of log surface tension as a function of SDS concentration allowing, the CMC of SDS to be determined. Table 3.3.3. shows how the CMC of SDS varies with temperature and pH. The determination of CMC is to some extent operator dependent as it is difficult to assess at exactly which point the plateau begins on the curve.

Table 3.3.1. Surface tension data ($mN.m^{-1}$) obtained for solutions of SDS of various concentrations and pH values at 25°C ± the standard deviation.

Conc. of SDS ($mol.dm^{-3}$)	pH Values					
	3	**6.5**	**7.1**	**7.2**	**7.4**	**10.4**
3.46×10^{-4}	63.95± 1.25	62.59± 0.94	63.1± 2.4	66.4± 1.34	66.31± 3.4	63.41± 2.3
6.9×10^{-4}	61.42± 2.5	60.98± 2.1	60.35± 1.36	62.84± 3.42	62.5± 1.51	60.09± 2.71
3.46×10^{-3}	50.39± 2.13	52.9± 1.14	46.1± 0.69	50.03± 2.13	49.5± 3.12	46.6± 0.43
6.93×10^{-3}	41.1± 1.01	44.1± 0.26	39.7± 1.21	42.2± 1.68	41.6± 2.58	40.8± 1.69
1.0×10^{-2}	37.3± 1.65	38.5± 0.11	35.5± 0.39	37.1± 0.14	37.7± 0.63	36.9± 0.18
1.39×10^{-2}	34.6± 0.4	36.5± 1.3	33.7± 1.06	34.8± 1.1	34.7± 1.02	34.6± 0.96
1.73×10^{-2}	32.5± 0.13	36.0± 0.25	32.4± 1.31	33.2± 0.49	33.7± 1.12	33.5± 1.41
2.1×10^{-2}	31.3± 0.31	35.7± 0.52	32.3± 1.02	33.0± 1.07	33.1± 1.2	32.7± 0.51
2.78×10^{-2}	30.8± 1.1	35.3± 1.04	32.2± 0.83	32.5± 0.64	33.0± 0.14	32.6± 1.04
3.46×10^{-2}	30.8± 0.61	35.3± 0.57	32.2± 0.78	32.2± 0.11	32.5± 0.21	32.6± 0.89

Table 3.3.2. Surface tension data ($mN.m^{-1}$) obtained for solutions of SDS of various concentrations and pH values at 42 °C ± the standard deviation.

Conc. of SDS ($mol.dm^{-3}$)	pH Values					
	3	**6.5**	**7.1**	**7.2**	**7.4**	**10.4**
3.46×10^{-4}	67.53± 1.45	62.44± 2.04	64.41± 1.89	64.91± 0.87	65.3± 0.91	61.73± 2.13
6.9×10^{-4}	65.23± 1.38	58.48± 1.12	61.16± 1.34	61.97± 0.84	61.94± 0.29	58± 0.36
3.46×10^{-3}	52.5± 1.43	47.2± 1.37	49.5± 0.98	50.83± 1.01	48.0± 0.46	47.9± 0.68
6.93×10^{-3}	44.2± 0.75	41.7± 0.61	43.3± 1.14	43.8± 1.07	40.9± 0.79	41± 1.06
1.0×10^{-2}	40.1± 1.61	37.4± 0.73	38.2± 1.04	37.5± 1.31	37.5± 0.74	36.7± 0.69
1.39×10^{-2}	36.4± 0.25	34.1± 0.54	35.1± 0.67	35.3± 1.12	34.5± 1.16	34.8± 0.94
1.73×10^{-2}	34.4± 0.37	33.2± 1.05	33.5± 1.16	34.2± 0.35	33.1± 0.86	33.4± 0.42
2.1×10^{-2}	32.4± 0.18	33.0± 0.55	33.1± 0.63	34.0± 1.08	33.0± 1.11	33.2± 0.81
2.78×10^{-2}	32.3± 1.09	32.9± 0.41	32.8± 0.74	33.8± 0.38	32.8± 1.06	32.9± 1.11
3.46×10^{-2}	32.2± 0.31	32.6± 0.48	32.6± 0.85	33.7± 1.02	32.6± 0.24	32.9± 0.16

Table 3.3.3. CMC of SDS data as a function of temperature and pH.

pH	CMC at 25°C (mol dm^{-3})	CMC at 42°C (mol dm^{-3})
3	1.82×10^{-2}	1.85×10^{-2}
6.5	1.23×10^{-2}	1.27×10^{-2}
7.1	1.48×10^{-2}	1.50×10^{-2}
7.2	1.34×10^{-2}	1.43×10^{-2}
7.4	1.47×10^{-2}	1.53×10^{-2}
10.4	1.45×10^{-2}	1.52×10^{-2}

3.3.2. Contact angle data obtained for the sulphonamides.

Table 3.3.4. shows advancing contact angle data for the sulphonamides against two polar liquids (water and ethylene glycol) and one non-polar liquid (di-iodomethane).

Table 3.3.4. Advancing contact angle data[1] obtained for the sulphonamides against water, ethylene glycol (EG) and di-iodomethane (DI) ± the standard deviation.

Powder	θ (water)	Cos θ (water)	θ (EG)	Cos θ (EG)	θ (DI)	Cos θ (DI)
Sulfamerazine	81.7 ± 2.4	0.145 ± 0.12	35.3 ± 1.4	0.816 ± 0.012	18.2 ± 1.1	0.950 ± 0.014
Sulfadiazine	75.5 ± 1.8	0.250 ± 0.031	34.2 ± 1.1	0.827 ± 0.015	17.8 ± 1.4	0.952 ± 0.015
Sulfamethazine	63.8 ± 1.9	0.441 ± 0.042	34.8 ± 0.8	0.821 ± 0.008	16.3 ± 1.0	0.960 ± 0.016
Sulfanilamide	61.6 ± 2.1	0.475 ± 0.022	38.0 ± 1.1	0.788 ± 0.024	20.1 ± 1.6	0.939 ± 0.021

[1] obtained by Therese Gregori, visiting from University of Pavia

3.3.2.1. Powder plate preparation .

To ensure that compacts had the smoothest surface possible, a high compression force was used to reduce the effect of surface roughness on contact angle measurement (see section 1.3.2.2.).

3.3.2.2. Errors in θ and cos θ values.

It is more appropriate to express the error (± standard deviation) in the cos θ value rather than the θ value (Parsons *et al.*, 1992a). This is due to the shape of the cosine curve. As θ increases (to 90°) and cos θ tends to 1, so the gradient of the cosine curve decreases.

Therefore a given change in cos θ may result in an unequal change in θ. For example, the percentage error in θ for Sulfamerazine in water and ethylene glycol are quite similar. However, the percentage errors in cos θ are very different;

Sulfamerazine in water	81.67 ± 2.4 (2.9%)	0.145 ± 0.012 (8.3%)
Sulfamerzine in ethylene glycol	35.31 ± 1.4 (3.9%)	0.816 ± 0.012 (1.4%)

Errors quoted in θ do not reflect the true accuracy of the experiment (Parsons et al., 1992a), and therefore data should be quoted as cos θ ± the standard deviation. In the past, values have been expressed as θ and hence, data is also presented here as cos θ ± the standard deviation, for comparative purposes.

Errors associated with factors affecting the Wilhelmy plate technique for powders have been investigated, (Sheridan *et al.*, 1994b). The effect of powder and plate storage conditions, the compaction force and dwell time used to prepare the plate, and the approach to defining the buoyancy slope of the Wilhelmy plate technique were all considered. It was found that effect of compaction seemed to be material dependent, and variability in measured contact angle was not associated with humidity equilibrium, or time after the plate was made for the materials studied. The major cause of variability in the contact angle seemed to be the plate roughness. This causes concern as the plate roughness does not only affect the result by normal hysteresis effects, but also because the measured perimeter (external dimensions) will underestimate the true perimeter of a rough plate. However the standard deviation for the contact angles obtained using the Wilhelmy

plate approach were smaller than for other contact angle techniques for powdered samples.

3.3.3. Contact angle data for the sulphonamides against six solutions of various SDS concentrations in water.

Firstly the surface tensions of these solutions were obtained using the method described in section 3.2.3.3. Data is shown in Table 3.3.5. From these results, it is possible to carry out contact angle analysis using compacts of drug powders against these solutions and secondly to determine the CMC of SDS in water at 25°C.

Table 3.3.5. Surface tension data ($mN.m^{-1}$) for varying concentrations of SDS solutions ($mol.dm^{-3}$) ± the standard deviation.

Conc. of SDS solution ($mol.dm^{-3}$)	Surface tension ($mN.m^{-2}$)
6.9×10^{-4}	50.35 ± 0.452
3.46×10^{-3}	39.68 ± 0.222
6.93×10^{-3}	32.43 ± 0.252
3.46×10^{-2}	35.73 ± 0.340
6.93×10^{-2}	33.5 ± 0.294
0.1	34.15 ± 0.208

3.3.3.1. CMC of SDS in water at 25°C.

The above data was then employed to determine the value for the CMC of SDS in water

at 25°C, as described by the method in section 3.2.2.3. The value obtained was 0.008 mol.dm^{-3}. The surface tension falls to a minimum before rising again to a plateau as shown in Figure 3.3.1. This effect is common for sodium dodecyl sulphate. The reason for this is due to the surfactant purity; the sodium dodecyl sulphate is often contaminated with dodecyl alcohol. The alcohol causes a further lowering of surface tension over that of the sodium dodecyl sulphate, but as the concentration is increased, the alcohol is forced out of the surface, giving the surface tension for a surface saturated with the surfactant alone. This has proved to be the case both by surface concentration measurements and by surface tension measurements on highly purified surfactant.

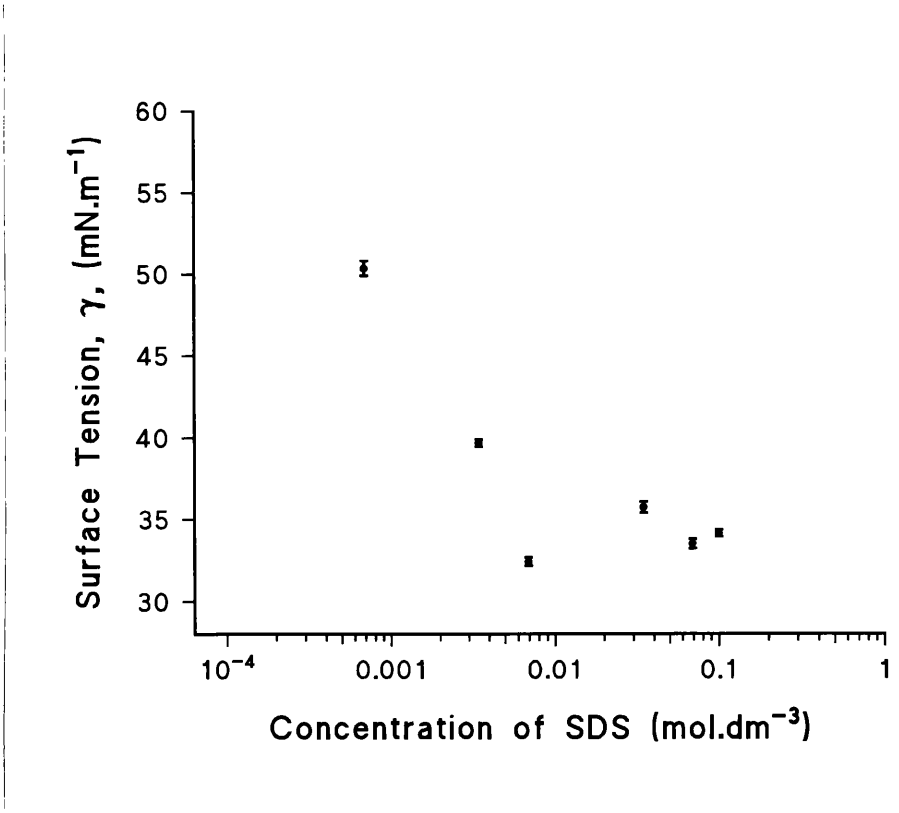

Figure 3.3.1. Surface tension concentration profile showing the surface tension fall to a minimum due to surfactant impurity.

3.3.3.2. Factors affecting the CMC.

Many factors will affect the CMC of a surfactant and are listed below:

i) structure of the hydrophobic group

ii) nature of the hydrophilic group

iii) addition of electrolytes

iv) effect of temperature

i) Regarding the hydrophobic region, an increase in the length of this chain in a homologous series results in a decrease in CMC.

ii) The hydrophilic head group of the surfactant will play different roles, depending upon whether it is ionic or neutral. In general the non-ionic surfactants have very much lower CMC values, mainly because there is less of an electrical barrier to micelle formation.

iii) The counterion associated with the charged group of ionic surfactants has a significant effect on the micellar properties. Generally, the more weakly hydrated a counterion, the larger the micelles formed by the surfactant. This is because the weakly hydrated ions can be absorbed more readily in the micellar surface and so decrease the charge repulsion between the polar groups.

iv) Addition of electrolytes to ionic surfactants decreases the CMC and increases the micellar size. The effect is explained in terms of a reduction in the magnitude of the forces of repulsion between the charged head groups in the micelle and a consequent decrease in the electrical work of micellization. Electrolyte addition has little affect on the micellar properties of non-ionic surfactants.

v) The CMC for a surfactant will change with temperature. In general the CMC will rise at high temperatures; this is due to the thermal energy preventing adhesion between surfactant monomers, but will also rise again at relatively low temperatures. However the CMC can decrease with increases in temperature, possibly because the water molecules are driven away from the surfactant monomer.

3.3.3.3. Advancing contact angle data for the sulphonamides.

This data was obtained for the sulphonamides for six solutions of various concentration of SDS in water, which were the same solutions employed in the previous section for surface tension measurement. From the data presented in Tables 3.3.6. it was possible to determine what effect the different SDS solutions had on the powder compacts.

Table 3.3.6. Advancing contact angle data obtained for the sulphonamides against solutions of various SDS concentration in water ± the standard deviation.

Conc. of SDS ($mol.dm^{-3}$)	Sulfamerazine		Sulfadiazine		Sulfamethazine		Sulfanilamide	
	θ	cos θ	θ	cos θ	θ	cos θ	θ	cos θ
6.9×10^{-4}	64.59± 0.776	0.429± 0.012	57.01± 1.14	0.544± 0.167	47.74± 0.925	0.672± 0.012	37.57± 0.608	0.793± 0.007
3.46×10^{-3}	52.39± 0.387	0.610± 0.005	49.51± 0.785	0.649± 0.010	31.84± 0.861	0.848± 0.008	28.62± 0.417	0.878± 0.004
6.93×10^{-3}	22.46± 0.524	0.924± 0.004	★	★	★	★	★	★
3.463×10^{-2}	★	★	★	★	★	★	★	★
6.925×10^{-2}	★	★	★	★	★	★	★	★
0.1	★	★	★	★	★	★	★	★

★ undefined contact angle

3.3.3.4. General discussion.

The CMC of SDS in water at 25°C was found to be 0.008 mol.dm^{-3} from the plot of log surface tension versus concentration of SDS. However, the CMC varied depending on the conditions the surfactant was subjected to. Rahman (1983) studied three different methods for the determination of CMC of SDS at various pH between 2 and 10. It was found that at low pH (below 4), the CMC decreased whereas at higher pH it remained constant. In this work, the CMC of SDS at both 25 and 42°C is higher at pH 3.0 than at other pH values, which are fairly constant. However from this data, it cannot be convincingly said that as pH is increased, the CMC of SDS tends to decrease. For each pH value used, there was an increase in the CMC at 42°C from that at 25°C. Although a comparatively small increase in temperature, this is due to the thermal energy preventing adhesion between surfactant monomers.

From the data provided by Table 3.3.6. it can be seen that solutions of 3.46 x 10^{-2} mol.dm^3 SDS and higher were all found to spread (*ie* had zero contact angle) on the drug. The contact angles appear to approach zero as the CMC is reached.

From the advancing contact angle data obtained for the sulphonamides against water, ethylene glycol and di-iodomethane, it is possible to calculate surface energies for correlation with other properties (see section 1.4.3.2.).

3.4. SURFACE ENERGIES.

The main use of contact angle measurement in formulation is to calculate the surface energies of pharmaceutical powders. The surface energy is a more useful value than a contact angle as it gives an indication of the overall surface behaviour of a powder as opposed to the extent of its interaction with a particular liquid.

3.4.1. Results and Discussion.

In the past, various theories have been applied for the calculation of surface energies. For example, Sheridan *et al* (1994a) looked at four different theories, which are listed below:-

1. Equation of state (Ward and Neumann, 1974),
2. Equation of state (Wu, 1979),
3. Geometric mean equation (Fowkes, 1964),
4. Harmonic mean equation (Wu, 1971).

As previously discussed in section 1.4.2.1. these theories are not very apprpriate. A more suitable theory is that of van Oss *et al* (1987), which is described in section 1.4.3.

3.4.1.1. Surface energies calculated using the van Oss acid/base theory.

Surface energy values obtained using this theory, using model systems, have been reported to model interfacial interactions more accurately than the theories quoted in section 3.4.1. (*eg* van Oss *et al.*, 1987). The surface energy terms shown in Table 3.4.1. have been calculated using Equation 1.4.14. in section 1.4.3.2. for the test compounds.

Values for the probe liquids and surfactant head and tail groups were taken from the literature.

Table 3.4.1. The surface energy terms for test compounds, liquids used in contact angle studies and sodium dodecyl sulphate head groups and tails.

	γ^{TOT} (mJ.m^{-2})	γ^{LW} (mJ.m^{-2})	γ^{+} (mJ.m^{-2})	γ^{-} (mJ.m^{-2})
Bromonaphthalene[a]	44.4	44.4	0	0
Ethylene glycol[a]	48.0	29.0	1.92	47.0
Water[a]	72.8	21.8	25.5	25.5
Sulfamerazine	49.3	47.7	0.5	1.4
Sulfanilamide	42.1	42.1	0	18.2
Sulfamethazine	49.3	48.1	0.02	14.6
Sulfadiazine	44.1	42.3	0.7	4.6
SDS tail group[b]	23.8	23.8	0	0
SDS head group[b]	34.6	34.6	0	46

a From van Oss *et al* (1992)
b From van Oss and Costanzo (1992).

It can be seen that , in keeping with many other materials that have been investigated to date, the powders have a tendency to be monopolar in the γ^{-} sense. The concept of monopolar materials was introduced by van Oss *et al* (1987) as a more appropriate explanation of polar interactions. The theory demonstrates that polar interaction can only be between bipolar materials or monopoles of the opposite type and that repulsion can

occur between monopoles of the same sense. In this study the SDS head group is highly polar, but the polar contribution is all of the γ^- type. This results in the clear possibility for polar repulsion interaction between the solids studied and the SDS head.

3.4.1.2. The free energy of adhesion.

Equation 1.4.17. in section 1.4.3.2. has been employed to calculate the free energy of adhesion between each of the drugs, SDS tails and SDS heads in the presence of water as shown in Table 3.4.2. The total predicted interaction between the drugs and the micelles has been taken as the sum of the free energy values for the adhesion to the heads and the tails.

Table 3.4.2. Calculated terms for free energy of adhesion between each of the drugs, SDS tails and SDS heads in the presence of water ($mJ.m^{-2}$).

Drug	ΔG_{tail}	ΔG_{head}	$\Delta G_{head + tail}$
Sulfamerazine	-84.12	-29.46	-113.6
Sulfanilamide	-59.70	6.240	-53.46
Sulfadiazine	-72.32	-19.08	-91.40
Sulfamethazine	-62.83	-1.005	-63.84

Having obtained an indication of the predicted interaction derived from measurements on the solid state, it is possible to compare the data with the measured thermodynamics of transfer. This applies to the thermodynamics of transfer from both solubility experiments and Taylor-Aris diffusion experiments (see Chapters 4 and 6) and the thermodynamics of activation from dissolution experiments (Chapter 5).

3.4.1.3. Problems associated with the van Oss acid/base theory.

It is not always possible to calculate surface energies using this theory as it is necessary to obtain contact angle data against three liquids from a list presented in a paper by van Oss *et al.*, (1992) *ie* two polar liquids and one non-polar liquid. The only non-polar liquids available are di-iodomethane, bromonaphthalene and the alkanes. The alkanes all have a lower surface tension than the other two liquids.

Surface energy values obtained using this theory, using model systems, have been reported to model interfacial interactions more accurately than the geometric and harmonic mean theories (*eg* van Oss *et al.*, 1987 and Parsons, 1992b). However, due to the necessity of requiring contact angle data against three liquids (including one non-polar liquid), this theory is unsuitable for many pharmaceutical powders. The main reason for being unable to acquire contact angle data is due to $\cos \theta = 1$.

However this approach has been used successfully for some systems, such as the determination of the most appropriate adhesive for sticking labels to glass bottles, (Buckton and Chandaria, 1993) and characterisation of the surface properties of various polymers (*eg* van Oss *et al.*, 1987). This approach appears to be useful, particularly for materials with low surface energy.

3.4.1.4. General discussion.

Surface energy, being a parameter which describes the property of the solid surface can be used to predict the properties and behaviour of pharmaceutical products. Surface free energy has been used previously to calculate the polarity of a material, P_o (*eg* Zografi and Tam, 1976). This allows some understanding of organic solid surface energetics in a relatively convenient manner. By calculation of spreading coefficients (Buckton, 1992), it is possible to quantitatively assess the interaction between two phases, *ie* to predict how easily one phase will spread over another. This approach has been used successfully on numerous occasions to predict the behaviour of various formulations. For example, binder-substrate interactions in granulation (Rowe, 1989 and Zajic and Buckton, 1990), the prediction of aggregation in suspension formulation (Young and Buckton, 1990), the physical stability in non-polar, non-aqueous suspensions (Parsons *et al*, 1992b) and some physical properties (*ie* density, crushing force, sphericity and porosity) of spheroids (Pinto *et al.*, 1995).

The relationship between the surface energy and various parameters *eg* solubility, dissolution rates and partitioning will be discussed in further chapters.

3.5. CONCLUSIONS.

1. The reproducibility of contact angle data obtained for these pharmaceutical powders is rather better than data published previously, due to the use of the automated Wilhelmy plate method.

2. The critical micelle concentration of sodium dodecyl sulphate was found to vary with pH and temperature. A rise in temperature led to an increase in the CMC of SDS. A decrease in CMC was noted at pH 3.0, however, CMC appears to be basically independent of pH between 3.0 and 11.

3. The van Oss acid/base theory has been shown to be the most appropriate theory for modelling interfacial interactions than previous theories used, which do not split the polar component into electron donor and electron receptor parameters. However, it is not always possible to use this theory as it is necessary to obtain contact angle data against three liquids: two polar and one non-polar.

CHAPTER 4

SOLUBILITY STUDIES

4.1. INTRODUCTION.

An understanding of the process of solution and the factors governing the solubility of drugs is important in pharmaceutics for several reasons. Drugs may sometimes be formulated in solution form or may be added in powder or solution form to liquids where they must be dissolved before absorption can occur across biological membranes. Therefore, the solution process frequently precedes absorption unless the drug is administered in solution form. Drugs of low aqueous solubility, such as the sulphonamides, often present problems in relation to their bioavailability.

Aqueous solvents are the most common in pharmaceutical and biological systems. Water is the most widely used solvent for use as a vehicle because of its lack of toxicity, physiological compatability and its ability to dissolve a wide range of materials. Hence this was the initial choice when investigating the solubility of the sulphonamides. It is also important to consider the process of the transport of drugs across biological and artificial membranes. This is because a primary factor in passive membrane transport is the solubility of the drug molecule in the liquid environment of the membrane interior.

In section 1.5.1. the solution process is discussed, including the individual stages involved. In spite of the great importance of aqueous solubility in pharmaceutical processes, it is still a poorly understood phenomenon. A prerequisite of a drug going into solution is that it should be first wetted by the liquid phase and then dissolved, thus the wettability of the drug becomes an important factor to consider. Work has been undertaken on the solubility and wettability of some substituted barbituric acids (Buckton and Beezer, 1989),

which investigated the possibility of structural links for these two properties. The results suggested that the solubility and perhaps the wettability have a structure/property link, but that the structural features that control solubility are not the same as those that control wettability. The implications of the finding are significant as it may be possible to alter one portion of a molecule slightly to improve either the wetting or the solution behaviour of the compound to optimise the performance.

4.1.1. Factors affecting solubility.

The solubility of a solid will depend on a number of factors. Below are listed just a few:

1) Temperature
2) pH
3) Nature of the solvent
4) Effect of electrolytes
5) Solubilising agents

4.1.2. Use of surfactant.

One of the ways in which to improve the solubility of a drug, which is normally insoluble or poorly soluble in water, is by the addition of a surface-active agent. This phenomenon of micellar solubilisation has been widely used for the formulation of solutions (Sjöström *et al.*, 1993). The amount of surfactant used for this purpose must be carefully controlled. A large excess is undesirable because of possible toxic effects and also excessive amounts may reduce the bioavailability of a drug due to its strong adsorption within the micelle.

However, an insufficient amount of surfactant may not solubilise all of the drug. The addition of surfactant to drug solution was considered in this study in an attempt to improve the solubility of the poorly soluble sulphonamides.

4.1.3. Parameters of solubility studied.

As already discussed, solubility is an important factor in drug design. Many parameters were investigated as primary steps towards improving biological performance after oral administration. For the four sulphonamides, the following areas were studied :-

1. finding the wavelength at which maximum absorbance was observed *ie* λ_{max} values.
2. constructing calibration curves for the drugs being investigated.
3. determining solubilities in aqueous, buffered and micellar solutions at various temperatures.
4. determining drug solubilities in water and various concentrations of SDS in water, above and below the CMC value at one temperature.

4.1.4. Thermodynamics of transfer.

The free energy (G) is a measure of the energy available to the system to perform work. Its value decreases during a spontaneously occurring process until an equilibrium position is reached when no more energy can be made available, *ie* $\Delta G = 0$ at equilibrium. In order for the process of solution to occur spontaneously at a constant pressure the accompanying change in free energy or Gibbs free energy (ΔG) must be negative.

This change is defined by the generally applicable thermodynamic equation:-

$$\Delta G = \Delta H - T\Delta S \qquad (4.3.1.)$$

where ΔH, which is known as the change in the enthalpy of the system, is the amount of heat absorbed or evolved as the system changes its thermodynamic state.

T = temperature in Kelvin.

ΔS is the change in the entropy, which is a measure of the degree of disorder or randomness in the system.

4.2. METHODS.

4.2.1. Determination of maximum absorbance values *ie* λ_{max}.

4.2.1.1. Experimental procedure.

A known standard solution of each of the four sulphonamides was made up in double distilled water. In each case, only a very small amount of drug was needed as all solubilities were low. The solutions were prepared and maintained at room remperature which was approximately 20°C. A sample of each solution was scanned using a Perkin Elmer 554 UV spectrophotometer between the wavelength range 900nm and 190nm. From the peaks on the scan, it was possible to tell at which point maximum absorbance occurred. Figure 4.1. shows a typical UV scan, enabling λ_{max} to be found. The same procedure was repeated with standards of drug in 0.1M SDS in water. Again λ_{max} values were found and compared with those obtained for drug in double distilled water only.

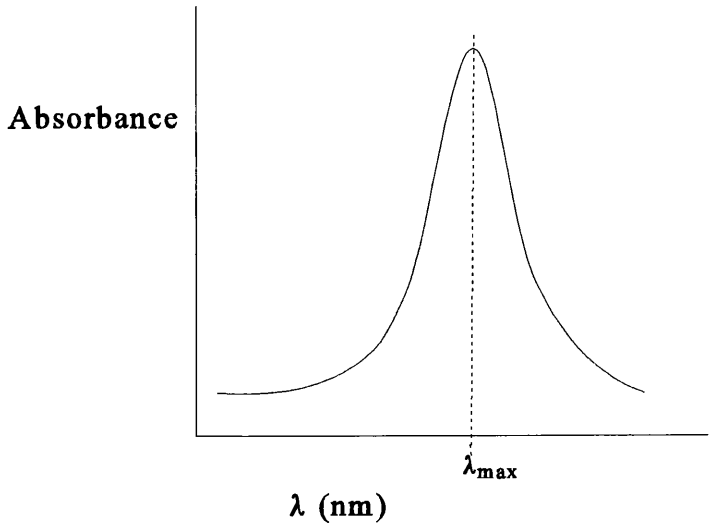

Figure 4.2.1.Typical UV scan to show the λ_{max} of a drug in solution.

4.2.2. Construction of calibration curves.

Each standard solution of drug prepared in double distilled water was used to give at least four subsequent dilutions. Using the λ_{max} value for each drug, obtained in section 4.2.1. and double distilled water as a blank, the absorbance reading of each solution was acquired. These readings were then plotted for each drug against concentration to produce a calibration curve from which an equation of best fit was found.

4.2.3. Determination of the solubility of a drug solid in a liquid.

Many points were observed when carrying out these solubility determinations:-

1. the solvent and the solute had to be pure.
2. a saturated solution had to be obtained before any solution was removed for analysis.
3. the method of separating a sample of saturated solution from undissolved solute had to be satisfactory.
4. the method of analysing the solution had to be reliable.
5. temperature had to be adequately controlled.

4.2.3.1. Experimental procedure.

An excess of each drug was put with double distilled water into a glass tube, fitted with an air-tight lid. Tubes were also prepared containing an excess of drug in 0.1M SDS in water as the solvent. All tubes were placed into four separate shaking water baths, which were maintained at temperatures of 25, 30, 37 and 42°C. At particular times, samples were withdrawn from the supernatent in each tube, using a 5ml syringe. Each sample was withdrawn after switching off the shaker in the water bath and allowing a minute

interval to enable any undissolved solute to settle. Each solution was then filtered through a 0.45μm cellulose acetate membrane filter into a glass vial, discarding the first 2mls. The capped glass vials were then maintained at their respective temperatures until an absorbance reading was ready to be taken. Readings were taken up to 24 hours, by which time equilibrium had been reached in all cases. Each experiment was repeated twice.

The process was then repeated to measure the solubilities for each drug in buffer (Svehla, 1979), at the pK_a (Moffat,1986), *ie* sulfamerazine, pK_a 7.1; sulfamethazine, $pK_a = 7.4$; sulfadiazine, $pK_a = 6.5$ and sulfanilamide, $pK_a = 10.4$. Again this was undertaken with and without SDS micelles.

4.2.4. Determination of solubilities below and above CMC of SDS.

This was carried out at one temperature to ascertain how great an effect the surfactant had on the solubility of each drug, particularly around the CMC value. This would also allow us to determine how important the wetting process is.

4.2.4.1. Experimental procedure.

Screw cap vials containing an excess of powdered drug and 25ml of the selected medium were gently agitated on an orbital mixer (Baird & Tatlock) at 37°C. The temperature was controlled by encasing the orbital mixer within a heat controlled chamber. Two ml aliquots were removed at 2, 4, 6, 8 and 24 hours, with equilibrium attained between 4 and 8 hours in all cases. Samples were filtered through 0.45μm cellulose acetate membrane

filters, discarding the first 0.5ml. Data were analysed using the UV spectrophotometer Perkin Elmer 554 as in previous sections. The media used were water, 6.9×10^{-4}, 3.46×10^{-3}, 6.93×10^{-3}, 3.46×10^{-2} and 6.93×10^{-2} mol.dm^{-3} solutions of SDS in water. Each experiment was repeated twice.

4.3. RESULTS AND DISCUSSION.

4.3.1. λ_{max} values.

From the scans of the standard solutions of each drug, Table 4.3.1. shows the λ_{max} values obtained. All further work regarding solubility and dissolution depend on these λ_{max} values, which have been obtained from several replicate scans to ensure reproducibility. The λ_{max} values for drug in water did not vary on addition of the SDS to the solution.

Table 4.3.1. Table of λ_{max} values.

Drug powder	λ_{max} value (nm)
Sulfamerazine	258
Sulfamethazine	259
Sulfadiazine	257
Sulfanilamide	256

4.3.2. Calibration curves.

From data obtained for absorbance readings of standard drug solutions and dilutions, calibration curves were constructed. Figures 4.3.1., 4.3.2., 4.3.3. and 4.3.4. show the calibration curves for the four sulphonamides, whilst Table 4.3.2. shows the equation of best fit for each calibration curve.

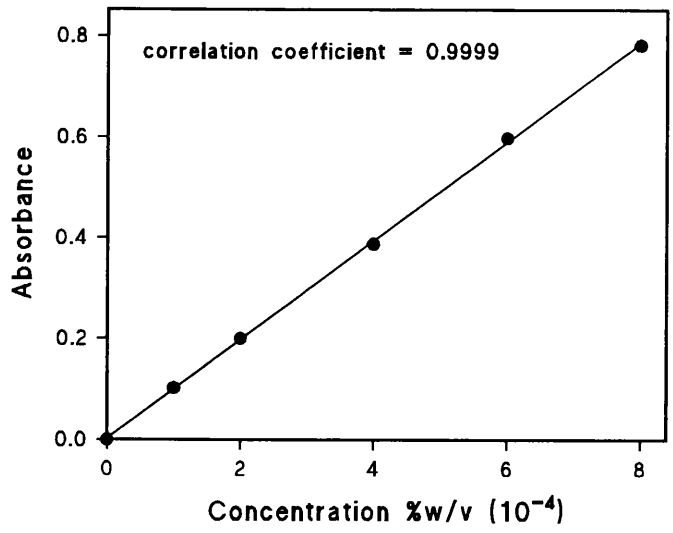

Figure 4.3.1. Calibration curve of Sulfanilamide

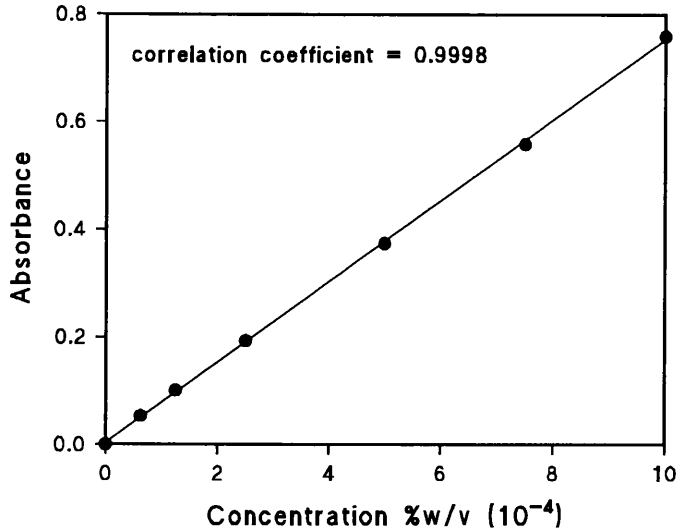

Figure 4.3.2. Calibration curve of Sulfamethazine.

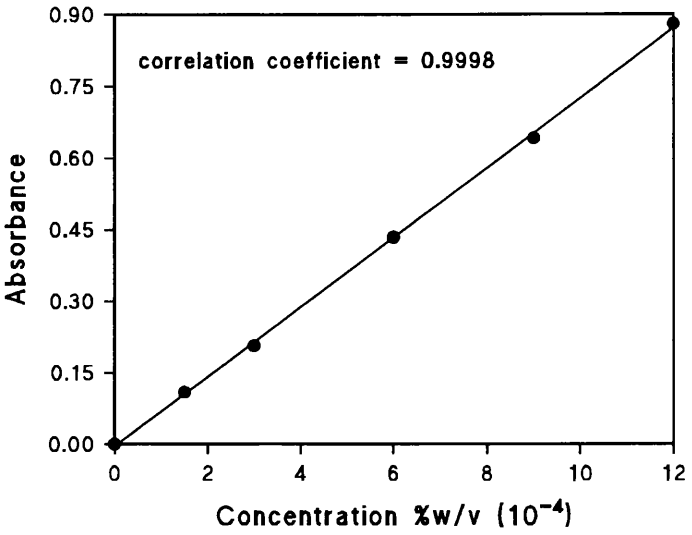

Figure 4.3.3. Calibration curve of Sulfamerazine.

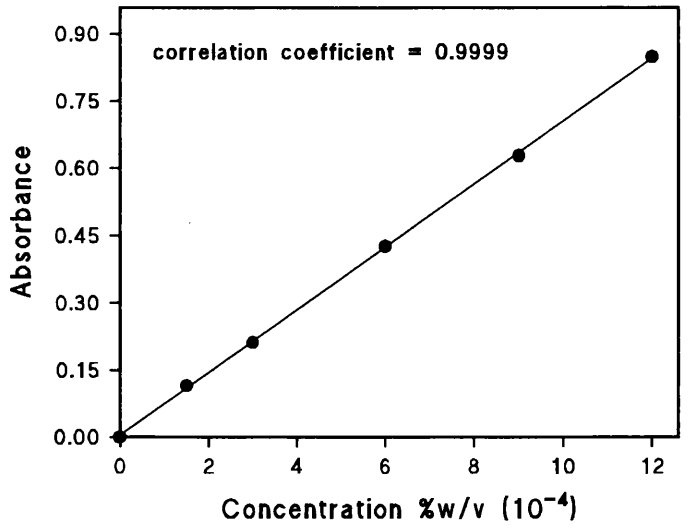

Figure 4.3.4. Calibration curve of Sulfadiazine.

Table 4.3.2. To show the equation of best fit for each calibration curve.

Drug	Equation of best fit
Sulfanilamide	y = 0.097958x + 0.002147
Sulfamethazine	y = 0.074907x + 0.003553
Sulfamerazine	y = 0.072968x + 0.004418
Sulfadiazine	y = 0.070154x + 0.003523

4.3.3. Solubility data

4.3.3.1. Data in water and 0.1M SDS.

Table 4.3.3. Solubility of the drugs in water at different temperatures with and without SDS micelles[a].

	298 K	303 K	310 K	315 K	r[b]
sulfamerazine	-7.280	-7.052	-6.799	-6.586	0.999
water	± 0.187	± 0.056	± 0.141	± 0.066	
SDS	-6.047	-5.955	-5.828	-5.711	0.998
	± 0.07	± 0.026	± 0.030	± 0.058	
sulfanilamide	-3.002	-2.850	-2.545	-2.396	0.997
water	± 0.101	± 0.017	± 0.016	± 0.078	
SDS	-2.962	-2.756	-2.524	-2.296	0.998
	± 0.042	± 0.049	± 0.032	± 0.080	
sulfamethazine	-6.544	-6.305	-6.132	-5.936	0.994
water	± 0.010	± 0.033	± 0.010	± 0.037	
SDS	-5.403	-5.295	-5.027	-4.961	0.999
	± 0.291	± 0.111	± 0.025	± 0.018	
sulfadiazine	-8.034	-7.793	-7.605	-7.437	0.993
water	± 0.053	± 0.097	± 0.010	± 0.049	
SDS	-6.982	-6.861	-6.647	-6.519	0.987
	± 0.011	± 0.084	± 0.118	± 0.064	

[a] All data presented in ln (solubility), where solubility was expressed in $mol.dm^{-3}$.
[b] r is the linear correlation coefficient for a plot of ln K as a function of 1/T.

4.3.3.2. Data in buffer and 0.1M SDS.

Table 4.3.4. Solubility of the drugs in buffer (at pH = pK_a of drug) at different temperatures with and without SDS micelles[a].

	298 K	303 K	310 K	315 K	r[b]
sulfamerazine	-6.466	-6.219	-5.967	-5.791	0.998
buffer	± 0.048	± 0.081	± 0.010	± 0.076	
SDS	-6.028	-5.908	-5.730	-5.609	0.999
	± 0.016	± 0.099	± 0.070	± 0.104	
sulfanilamide	-3.000	-2.808	-2.530	-2.363	0.999
buffer	± 0.318	± 0.010	± 0.111	± 0.126	
SDS	-2.654	-2.432	-2.240	-2.084	0.996
	± 0.057	± 0.286	± 0.092	± 0.093	
sulfamethazine	-6.121	-5.934	-5.723	-5.584	0.999
buffer	± 0.112	± 0.475	± 0.007	± 0.165	
SDS	-5.205	-5.043	-4.904	-4.772	0.994
	± 0.091	± 0.116	± 0.241	± 0.305	
sulfadiazine	-7.496	-7.228	-6.867	-6.653	0.999
buffer	± 0.174	± 0.178	± 0.333	± 0.335	
SDS	-7.264	-7.026	-6.753	-6.547	0.999
	± 0.099	± 0.096	± 0.037	± 0.048	

[a] All data presented as ln (solubility), where solubility was expressed in $mol.dm^{-3}$.
[b] r is the linear correlation coefficient for a plot of ln K as a function of 1/T.

4.3.3.3. Thermodynamics of transfer from solubility experiments.

The thermodynamic parameters were calculated from the data in Tables 4.3.3. and 4.3.4. by use of the van't Hoff isochore (see Equation 4.3.2.) and are given in Tables 4.3.5. and 4.3.6.

$$\ln K = -\Delta H / RT \qquad (4.3.2.)$$

where K = solubility,

R = gas constant,

T = temperature,

ΔH = change in enthalpy.

The difference between the enthalpy term for solubility in water and that for SDS solution is the enthalpy of transfer from water to SDS micelles.

Table 4.3.5. Calculated enthalpy parameters of solution in water and water with SDS micelles, and the thermodynamics of transfer (kJ.mol^{-1}).

Drug	ΔH_{sol}^{water}	ΔH_{sol}^{SDS}	ΔH_{trans}
sulfamerazine	31.3	15.2	-16.1
sulfanilamide	28.7	29.9	1.2
sulfamethazine	26.7	21.7	-5.0
sulfadiazine	26.5	21.6	-4.9

Table 4.3.6. Calculated free energy parameters of solution in water and water with SDS micelles, and the thermodynamics of transfer[a] ($kJ.mol^{-1}$).

Drug	ΔG_{sol}^{water}	ΔG_{sol}^{SDS}	ΔG_{trans}
sulfamerazine	18.0	14.9	-3.1
sulfanilamide	0.74	7.3	6.6
sulfamethazine	16.2	13.4	-2.8
sulfadiazine	19.9	17.3	-2.6

[a] From the data in Table 4.3.3. Free energy data calculated using 298K data.

Table 4.3.7. Calculated entropy parameters of solution in water and water with SDS micelles, and the thermodynamics of transfer[a] ($J.mol^{-1}.K^{-1}$).

Drug	ΔS_{sol}^{water}	ΔS_{sol}^{SDS}	ΔS_{trans}
sulfamerazine	44.7	1.0	-43.7
sulfanilamide	93.8	75.7	-18.1
sulfamethazine	35.2	27.9	-7.3
sulfadiazine	22.1	14.5	-7.6

[a] From the data in Table 4.3.3. Entropy data calculated using 298K data.

Table 4.3.8. Calculated enthalpy parameters of solution in buffer (at pH = pK_a of drug) and buffer with SDS micelles, and the thermodynamics of transfer ($kJ.mol^{-1}$).

Drug	ΔH_{sol}^{buffer}	ΔH_{sol}^{SDS}	ΔH_{trans}
sulfamerazine	30.6	19.3	-11.3
sulfanilamide	29.5	25.6	-3.9
sulfamethazine	24.5	19.3	-5.2
sulfadizine	39.0	32.6	-6.4

Table 4.3.9. Calculated free energy parameters of solution in buffer (at pH = pK_a of drug) and buffer with SDS micelles, and the thermodynamics of transfer[a] ($kJ.mol^{-1}$).

Drug	ΔG_{sol}^{buffer}	ΔG_{sol}^{SDS}	ΔG_{trans}
sulfamerazine	16.0	14.9	-1.1
sulfanilamide	7.4	6.6	-0.8
sulfamethazine	15.2	12.9	-2.3
sulfadiazine	18.6	18.0	-0.6

[a] From the data in Table 4.3.4. Free energy data calulated using 298K.

Table 4.3.10. Calculated entropy parameters of solution in buffer (at pH = pK_a of drug) and buffer with SDS micelles, and the thermodynamics of transfer[a] ($J.mol^{-1}.K^{-1}$).

Drug	ΔS_{sol}^{buffer}	ΔS_{sol}^{SDS}	ΔS_{trans}
sulfamerazine	49.0	14.8	-34.2
sulfanilamide	74.1	63.8	-10.3
sulfamethazine	31.2	21.3	-9.9
sulfadiazine	68.5	49.0	-19.5

[a] From the data in Table 4.3.4. Entropy data calculated using 298K.

4.3.3.4. Comparison between the free energy of adhesion and the thermodynamics of transfer.

The relationships between the total free energy of adhesion (from surface energy considerations in Chapter 3) and the enthalpy of transfer (from solubility experiments in water and buffer) are shown in Figure 4.3.5. There are reasonable correlations between the free energy of adhesion data and the enthalpy of transfer from the buffered solubility experiments (r = 0.945), but the data obtained from solubility in water show a poor correlation (r = 0.889).

As the pH of solutions of each of the drugs in water is about 3 units below the pK_a, the degree of ionization is similar for each drug in both sets of experiments (in water, almost fully ionized; at pH = pK_a, 50% ionized). It can be concluded that there is good agreement between the measured and predicted partitioning behaviour as long as the

ionization of the drug is not excessive. At low pH values, the correlation between measured and predicted behaviour starts to be lost, presumably because the ionic interactions between the drug and the SDS become a more significant influence on the solubilisation process. The fact that the pH of the experiment has little effect on the behaviour of SDS is in keeping with the fact that the critical micelle concentration of the surfactant does not change over much of the pH range that has been investigated here.

Figure 4.3.5. The relationship between the total free energy of adhesion (head and tail contribution) derived from surface energy data and the enthalpy of transfer into micelles from solubility experiments in water (•) and buffer at pH = pK_a of drug (▲).

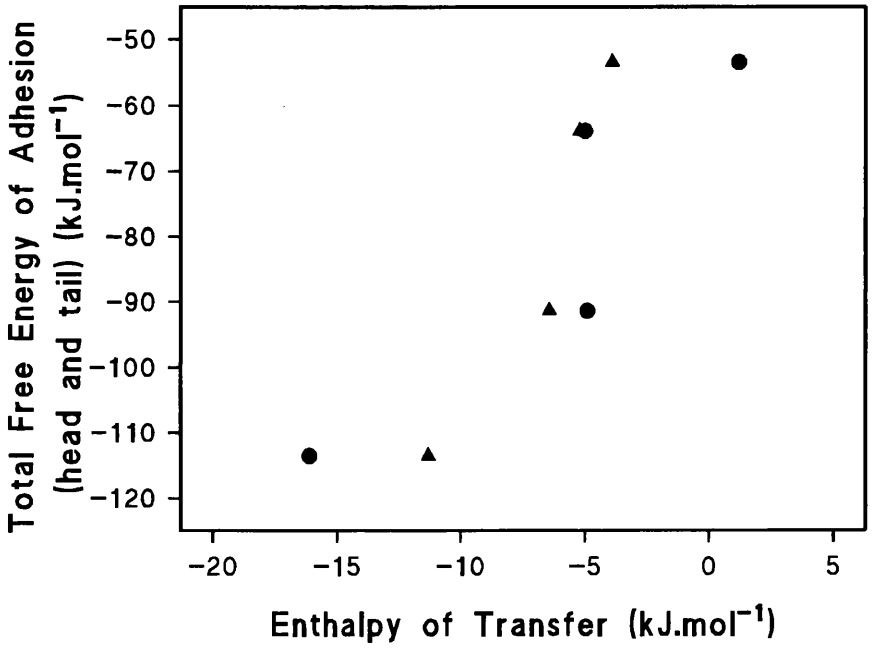

Figure 4.3.6. The relationship between the enthalpy of transfer from water solubility data and the free energy of adhesion of the drugs to SDS head groups from surface energy data.

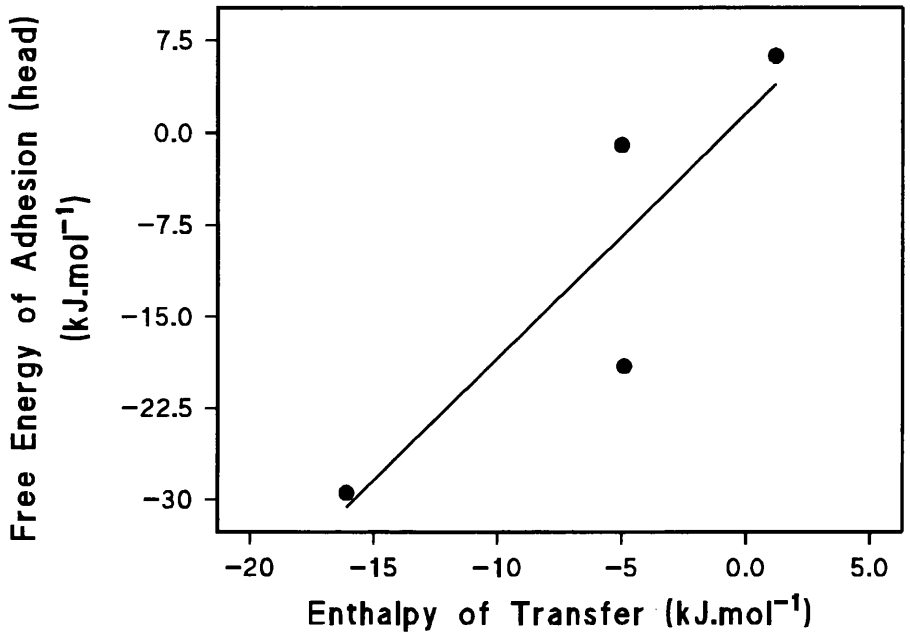

Figure 4.3.7. The relationship between the enthalpy of transfer from water solubility data and the free energy of adhesion of the drugs to SDS tail groups from surface energy data.

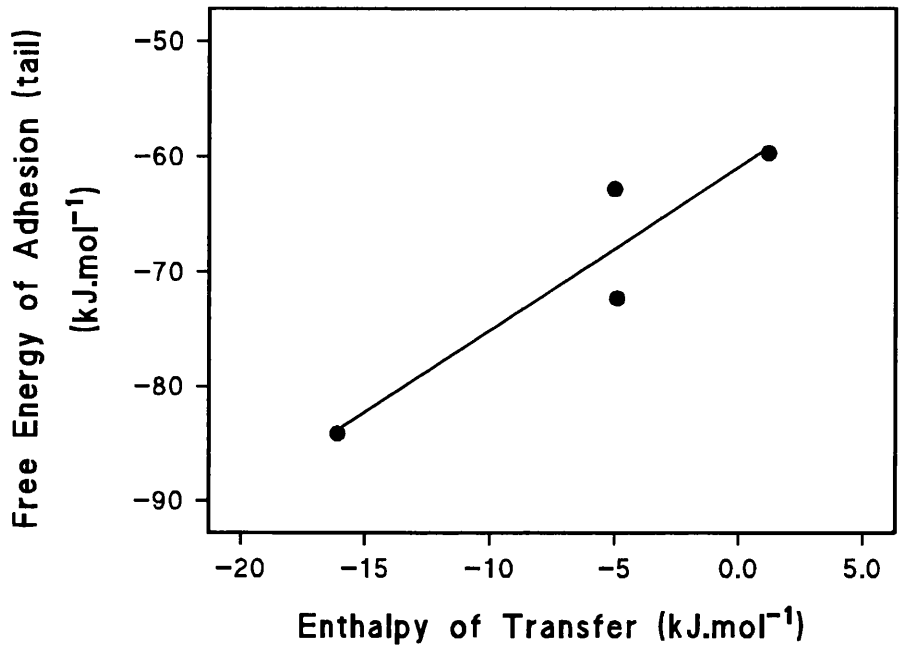

4.3.3.5. General discussion.

Regarding the solubility experiments in water, the relationship between the enthalpy of transfer and the free energy is moderately good for the head groups (Figure 4.3.6.) but much better for the tail of the SDS micelle (Figure 4.3.7.). The larger negative values for the free energy of adhesion to the tail (compared to those for adhesion to the head) indicate that these (mostly hydrophobic) molecules are more readily solubilised in the hydrophobic core, and less readily associated with the hydrophilic head groups.

With the water solubility experiments, there is no control over the ionization of the drug or the SDS head group, both of which are likely to change as a function of pH. The pH of the saturated solutions in water was measured as 3.2 for sulfadiazine, 4.0 for sulfamethazine, 5.8 for sulfanilamide, and 4.0 for sulfamerazine. At these pH values the basic group of the sulphonamides will be highly ionized.

4.3.3.6. Solubilities at pK_u values.

Preliminary solubility work was investigated for solutions at the pk_u value, 3 units above the pK_a of the drug (*ie* at a pH where the drugs may be expected to be unionised). As the pH increases, the solubility of the drugs would be expected to decrease. However, it was found that there was a marked increase in the solubility of each of the drugs, particularly for sulfanilamide which had the highest pK_u value. This can be explained by the structure of the sulphonamides. In each case the $-NHSO_2$ group is acidic, although not strongly acidic, which is why the pK_a values are high *ie* 6.5, 7.1, 7.4 and 10.4. The $-NH_2$ amine group is basic, hence this makes the drugs amphoteric, and at neutral pH, the amine seems

to control the drug. Sulfanilamide is the odd one out as it does not have the stabilising ring attached and thus it has a much higher pK_a value than the others. On adding sodium hydroxide to each buffered solution, to increase the pH, the sodium salt of the sulphonamide is formed which is stable. Therefore on increasing the pH, the solubility does not decrease, as the sodium salt of the drug is formed instead.

4.3.4. Solubilities in various SDS concentration.

Table 4.3.5. gives data for dimensionless solubilities (*ie* solubility in SDS / solubility in water) for the four sulphonamides. By normalising the solubilities, differences in particle size and surface area of the drugs are corrected for and this allows comparison of the drug solubilities.

Table 4.3.11. Dimensionless solubilities of the sulphonamides in various concentrations of SDS solutions at 37°C.

Conc. of SDS ($mol.dm^{-3}$)	Drug			
	sulfamerazine	**sulfadiazine**	**sulfamethazine**	**sulfanilamide**
6.9×10^{-4}	1.032	1.036	1.020	1.011
3.46×10^{-4}	1.113	1.205	1.056	1.001
6.93×10^{-3}	1.363	1.264	1.112	1.053
3.463×10^{-2}	2.283	2.445	2.088	1.072
6.925×10^{-2}	2.775.	3.174	3.032	1.142

4.3.4.1. Plots of dimensionless solubilities versus surfactant concentration.

Figures 4.3.8., 4.3.9., 4.3.10. and 4.3.11. show how the dimensionless solubilities of each drug vary with SDS concentration at 37°C.

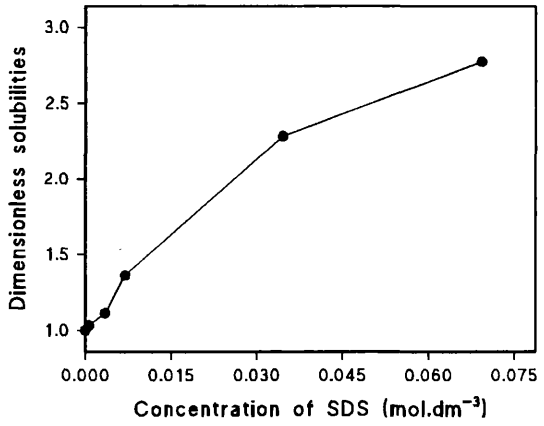

Figure 4.3.8. Dimensionless solubility of sulfamerazine in various concentrations of SDS.

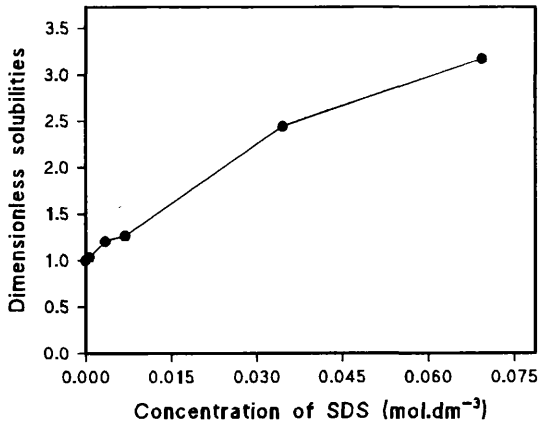

Figure 4.3.9. Dimensionless solubility of sulfadiazine in various concentrations of SDS.

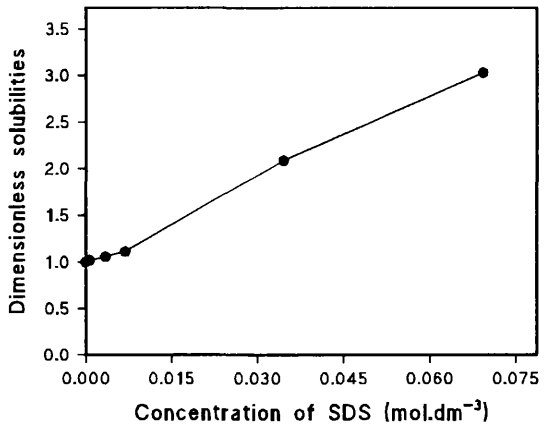

Figure 4.3.10. Dimensionless solubility of sulfamethazine in various concentrations of SDS.

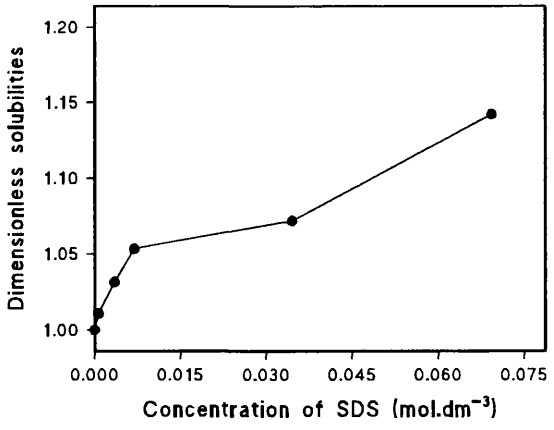

Figure 4.3.11. Dimensionless solubility of sulfanilamide in various concentrations of SDS.

4.3.4.2. General discussion.

From the Figures in section 4.3.4.1. it can be said that as the concentration of surfactant increased, so the solubility of the drug increased. In all cases except for sulfanilamide, there is a slight increase at a concentration of 3.463×10^{-2} mol.dm^{-3} of SDS. This is because at this point, the CMC of SDS has been reached and more drug is being solubilised within the hydrophobic core.

With the plot of sulfanilamide, there is more or less a straight line, with no great increase in solubility once the CMC of SDS has been reached. This suggests that with the sulfanilamide, the wetting process plays an important role, more than the solubilisation effect, occurring at and above the CMC of SDS. The dimensionless solubility will be discussed further in Chapter 7, alongside dimensionless initial powder dissolution rates which allows a comparison to be made.

4.4. CONCLUSIONS.

1. Solubility is an important factor, which governs many other processes such as dissolution and transport and influences the biological performance of a drug after oral administration. It was therefore important to establish the solubility of each of the drugs studied, under various conditions, before further processes were carried out.

2. By incorporating the surfactant, sodium dodecyl sulphate, with poorly soluble drugs such as the sulphonamides, it was found that the solubility increased both in water and in buffered solutions. However the use of buffers can also present difficulties in terms of ionic strength and the influence of different salts on the solubility.

3. For each drug, the solubility showed an improvement with increasing temperature and also with increased surfactant concentration, particularly around CMC levels. This indicates that the solubilisation process plays an important role with these drugs in order to improve their solubilities.

4. A relationship exists between the enthalpy of transfer from solubility experiments and the free energy of adhesion between head and tail groups of SDS. This is an indication that the surface energy approach discussed in Chapter 3 gives a good prediction of the interaction between drugs and micellar structures.

CHAPTER 5

DISSOLUTION RATES

5.1. INTRODUCTION.

A description of the dissolution process is given in section 1.6. and the many factors which affect it. When a drug is administered orally in solid form, one finds that the rate of absorption is controlled by the slowest step in the following sequence:

SOLID DRUG → DRUG IN SOLUTION → ABSORBED DRUG

In many instances the slowest or rate limiting step is found to be dissolution of drug in the fluids at or near the absorption site. When dissolution is the controlling step in the overall process, absorption is said to be dissolution rate limited. In such cases, any factor influencing the rate of solution must influence also the rate of absorption.

Two important parameters determining the dissolution rate of a solid in a given solvent are the solubility of the drug in the dissolution medium and the surface area of the drug exposed to the medium. In view of the Noyes-Whitney equation (described in section 1.6.1.), an increase in apparent solubility will usually result in an increase in dissolution rate. The dissolution rate of a drug, regardless of dissolution mechanism, is always directly proportional to the effective area of the drug *ie* the surface area of drug available to the dissolution fluids. The relationship between surface area, dissolution rates and gastrointestinal absorption rates have been reviewed by Fincher (1968). The relationship between wettability and dissolution rate of pharmaceutical powders have been investigated by Lippold and Ohm, 1986.

The aim of this work was to assess the dissolution rates of low solubility drugs from two forms:

i) a compressed compact and

ii) a fine powder.

Various conditions were used in assessing the dissolution rates, to determine which factors played the most important roles in the process.

The purpose of this chapter was to find any possible links between the dissolution and previous properties already discussed *ie* wettability and solubility, when developing a solid dosage form.

5.2. METHODS

In section 1.6.3. the diverse factors which effect dissolution rates are discussed. As the range is quite broad, only a few have been selected in this chapter and are discussed in greater detail. The conditions affecting dissolution rates from constant surface area disks, which were studied are:

1) varying **temperature** (constant stirring speed and medium).

2) varying **stirring speed** (constant temperature and medium).

3) varying **concentration of surfactant medium** (constant temperature and stirring speed).

Another aspect studied was:

1) **initial powder dissolution rate** from a fine powder. This was investigated using one particular temperature and stirring speed but varying concentrations of surfactant medium. These experiments were all conducted with and without the presence of SDS micelles.

5.2.1. Preparation of disk.

Disks of powder compacts were prepared by compacting 1.2g of drug, using a force of 10 kN for one minute. The disks were 1.3cm in diameter and were compacted using a Specac press. The compacted disk was then held in place by melted beeswax in a stainless steel cylinder, which was directly attached to a stirrer system, leaving a constant surface area of compact exposed (see Figure 5.2.1.).

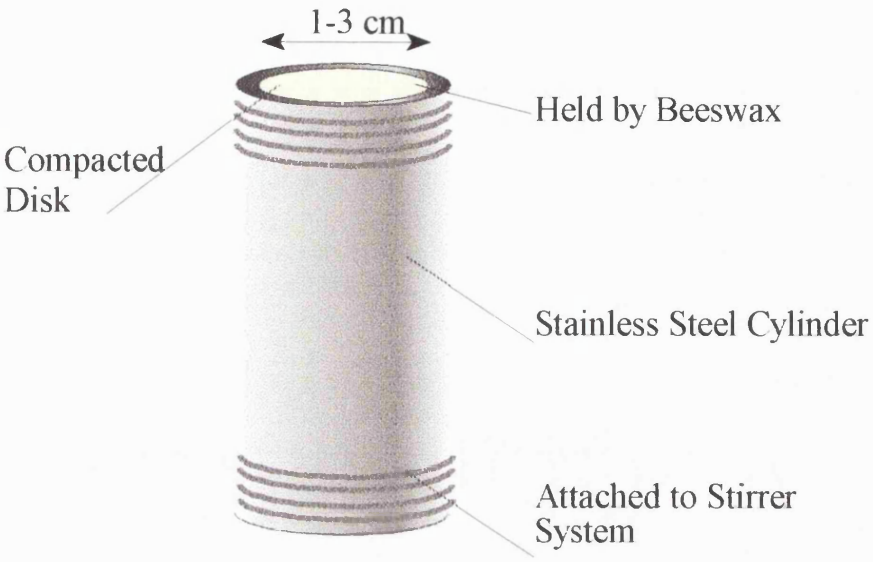

Figure 5.2.1. Disk of powder compact, held in a stainless steel cylinder.

5.2.2. Apparatus used for rotating disk dissolution.

The apparatus consisted of a flat bottomed beaker, containing 1 litre of the dissolution medium, held in a water bath, maintained at a particular temperature. The compacted disk was attached to a stirrer system consisting of a Citenco variable speed motor (type TS16) which was calibrated with a digital tachometer (Venture ATH4), (see Figure 5.2.2.). The water bath held a second beaker containing dissolution medium as replacement solvent, also kept at the same temperature. Rubber tubing attached to a syringe was inserted into both beakers to allow removal of sample and to replace with dissolution fluid. A stopclock was used to take samples at accurate time intervals.

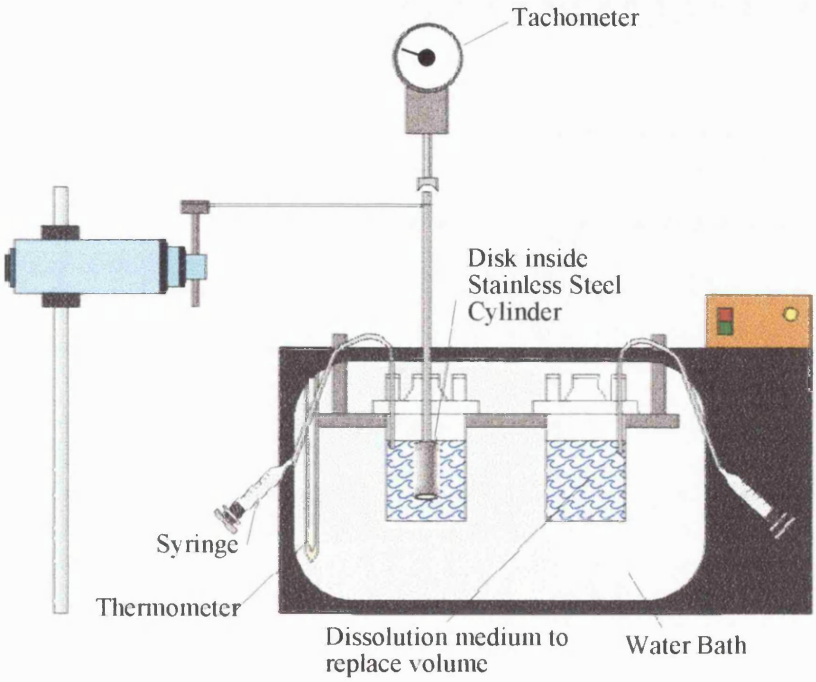

Figure 5.2.2. Rotating disk dissolution apparatus.

5.2.3. Experimental procedure for rotating disk dissolution rate studies.

Using the apparatus in Figure 5.2.2. a sample was withdrawn every ten minutes and immediately replaced with an equal volume of dissolution medium (maintained at the same temperature). The rotating velocity was checked after each reading with the digital tachometer. Samples taken were analysed using a UV spectrophotometer (Perkin Elmer 554) at the wavelength of the particular drug being studied. The sink conditions assumption was valid throughout each experiment since the concentrations measured were always below 20% of the drug's solubility in the corresponding medium.

The experimental procedure was carried out for each drug under the following conditions;

1) in 1 litre of **double distilled water**, using a stirring speed of 100rpm and at **varying temperatures** of 25, 30, 37 and 42°C.

2) in 1 litre of **0.1M SDS in water**, using a stirring speed of 100rpm and at **varying temperatures** of 25, 30 37 and 42°C.

3) in 1 litre of **double distilled water** at 37°C, at **varying stirring speeds** of 50, 100, 130 and 150 rpm.

4) in 1 litre of **0.1M SDS** in water at 37°C, at **varying stirring speeds** of 50, 100, 130 and 150 rpm.

5) at 37°C, using a stirring speed of 100rpm and in 1 litre of **varying SDS concentrations** of 0, 6.9×10^{-4}, 3.46×10^{-3}, 6.93×10^{-3}, 3.46×10^{-2} and 6.93×10^{-2} $mol.dm^{-3}$.

All experiments had three replicates for each drug.

5.2.4. Apparatus used for initial powder dissolution.

The *United States Pharmacopoeia XX and National Formulary XV* (1980) paddle method was used to determine the initial dissolution rate of drug from the powder form (IPDR). A cylindrical vessel with a spherical bottom was used and agitation was provided by a rotating paddle, (see Figure 5.2.3.). This was encased in a water bath maintained at 37°C. The paddle motor had been pre-set to stir at a speed of 100 rpm.

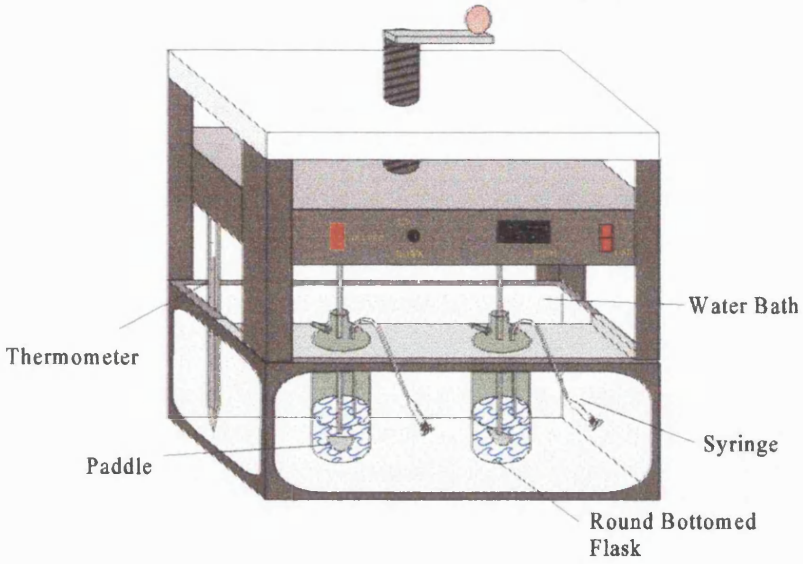

Figure 5.2.3. Initial powder dissolution apparatus.

5.2.5. Experimental procedure for initial powder dissolution studies.

Sample sizes of each drug were chosen to ensure that sink conditions were maintained throughout each experiment (*ie* 200mg of sulfamerazine, 200mg of sulfadiazine, 200mg of sulfamethazine and 3g of sulfanilamide). As sulfanilamide has a greater solubility than the others, a larger sample size of this drug was needed to obtain an initial linear plot for the rotating disk dissolution rate. The sample of drug was added to 400ml of dissolution medium at 37°C. The paddle was immediately lowered and the stirring motor started at 100 rpm together with the stopclock. Samples were withdrawn at specific time intervals, immediately replaced by an equal volume of dissolution medium, and filtered through a 0.45μm cellulose acetate membrane filter into glass vials.

Analysis of the samples was conducted by UV spectroscopy at appropriate wavelengths for each drug. The different dissolution media used were double distilled water, 6.9×10^{-4}, 3.46×10^{-3}, 6.93×10^{-3}, 3.46×10^{-2} and 6.93×10^{-2} $mol.dm^{-3}$ SDS solutions. Each experiment was performed in triplicate for each drug.

5.2.6. Data analysis.

In this work, samples were analysed using UV spectroscopy and by constructing concentration / time profiles. This method was used because it is well established and relatively simple. Also UV spectroscopy was selected to be consistent, as previous solubility work had been analysed by this method.

5.3. RESULTS AND DISCUSSION.

5.3.1. Data obtained with varying temperature.

The rotating disk dissolution rate constants (k) were determined from the initial linear portion of a plot of drug released as a function of time (see Table 5.3.1.). Arrhenius plots were constructed (In k as a function of 1/T), the gradients of which were used to determine values for the activation energy (E) of the process. This in turn was used to calculate the enthalpy of activation ($\Delta H^{\ddagger}$), as

$$\Delta H^{\ddagger} = E - RT \qquad (5.3.1.)$$

(R = gas constant)

By use of a conventional Arrhenius plot, the entropy of activation, ($\Delta S^{\ddagger}$) was calculated from the intercept (where the intercept on the y-axis is In A, with A being the collision number). The free energy of activation ($\Delta G^{\ddagger}$) was then calculated from;

$$\Delta G^{\ddagger} = \Delta H^{\ddagger} - T\Delta S^{\ddagger} \qquad (5.3.2.)$$

The difference between the enthalpy term for dissolution in water and that for SDS solution was the enthalpy of transfer from water to SDS micelles, (see Tables 5.3.3., 5.3.4. and 5.3.5.).

Table 5.3.1. Rotating disk dissolution rate data for compressed disks in water at various temperatures. All units for rate constants are % w/v.min^{-1} for disks of 132.7 mm^2. Values are means ± standard deviations.

Drug	Fluid	298K	303K	310K	315K
Sulfamerazine	**water**	3.68×10^{-6} $\pm 6.3 \times 10^{-3}$	4.09×10^{-6} $\pm 2.5 \times 10^{-3}$	5.75×10^{-6} $\pm 5.9 \times 10^{-3}$	8.51×10^{-6} $\pm 7.7 \times 10^{-3}$
	SDS	1.50×10^{-6} $\pm 5.6 \times 10^{-3}$	1.62×10^{-6} $\pm 7.1 \times 10^{-3}$	2.04×10^{-6} $\pm 9.6 \times 10^{-3}$	2.21×10^{-6} $\pm 3.9 \times 10^{-3}$
Sulfadiazine	**water**	7.4×10^{-7} $\pm 5.7 \times 10^{-4}$	1.08×10^{-6} $\pm 9.8 \times 10^{3}$	1.48×10^{-6} $\pm 6.3 \times 10^{-3}$	2.20×10^{-6} $\pm 2.7 \times 10^{-3}$
	SDS	3.26×10^{-6} $\pm 3.5 \times 10^{-3}$	4.39×10^{-6} $\pm 7.8 \times 10^{-3}$	5.17×10^{-6} $\pm 1.8 \times 10^{-2}$	7.82×10^{-6} $\pm 1.0 \times 10^{-2}$
Sulfanilamide	**water**	8.29×10^{-5} $\pm 2.9 \times 10^{-2}$	1.04×10^{-4} $\pm 9.6 \times 10^{-2}$	1.29×10^{-4} ± 0.150	1.65×10^{-4} $\pm 7.2 \times 10^{-2}$
	SDS	9.49×10^{-5} $\pm 3.0 \times 10^{-2}$	1.40×10^{-4} $\pm 6.3 \times 10^{-2}$	1.90×10^{-4} ± 0.170	2.13×10^{-4} ± 0.680
Sulfamethazine	**water**	3.73×10^{-6} $\pm 5.2 \times 10^{-3}$	4.79×10^{-6} $\pm 7.1 \times 10^{-3}$	6.78×10^{-6} $\pm 2.3 \times 10^{-3}$	9.45×10^{-6} $\pm 3.3 \times 10^{-3}$
	SDS	7.68×10^{-6} $\pm 1.5 \times 10^{-2}$	1.01×10^{-5} $\pm 5.4 \times 10^{-3}$	1.30×10^{-5} $\pm 7.2 \times 10^{-3}$	1.99×10^{-5} $\pm 1.7 \times 10^{-2}$

Table 5.3.2. Enthalpy of activation data obtained from the temperature dependence of rotating disk dissolution rate constants (thermodynamic parameters calculated from conventional Arrhenius relationship at 310 K).

Drug	$\Delta H^{\ddagger}_{SDS}$ (kJ.mol^{-1})	$\Delta H^{\ddagger}_{water}$ (kJ.mol^{-1})	$\Delta H^{\ddagger}_{trans}$ (kJ.mol^{-1})
Sulfamerazine	19.0	38.3	-19.2
Sulfadiazine	36.9	47.5	-10.6
Sulfanilamide	36.8	30.4	6.4
Sulfamethazine	41.3	42.1	-0.8

Table 5.3.3. Entropy of activation data obtained from the temperature dependence of rotating disk dissolution rate constants (thermodynamic parameters calculated from conventional Arrhenius relationship at 310 K).

Drug	$\Delta S^{\ddagger}_{SDS}$ (J.mol^{-1}.K^{-1})	$\Delta S^{\ddagger}_{water}$ (J.mol^{-1}.K^{-1})	$\Delta S^{\ddagger}_{trans}$ (J.mol^{-1}.K^{-1})
Sulfamerazine	-260.0	-188.5	-71.5
Sulfadiazine	-193.5	-170.1	-23.4
Sulfanilamide	-165.2	-188.3	23.1
Sulfamethazine	-171.8	-175.2	3.4

Table 5.3.4. Free energy of activation data obtained from the temperature dependence of rotating disk dissolution rate constants (thermodynamic parameters calculated from conventional Arrhenius relationship at 310 K).

Drug	$\Delta G^{\ddagger}_{SDS}$ (kJ.mol^{-1})	$\Delta G^{\ddagger}_{water}$ (kJ.mol^{-1})	$\Delta G^{\ddagger}_{trans}$ (kJ.mol^{-1})
Sulfamerazine	99.6	96.7	2.9
Sulfadiazine	96.9	100.2	-3.3
Sulfanilamide	88.0	88.8	-0.8
Sulfamethazine	94.5	96.4	-1.9

5.3.1.1. Relationship between dissolution data and surface energy data.

The enthalpies of transfer from dissolution data were found to correlate with predicted energies of adhesion between drug and SDS from surface energy data in Chapter 3 (see Figures 5.3.1., 5.3.2. and 5.3.3. for these relationships.

Figure 5.3.1. Relationship between the enthalpy of transfer and the free energy of adhesion to SDS head groups.

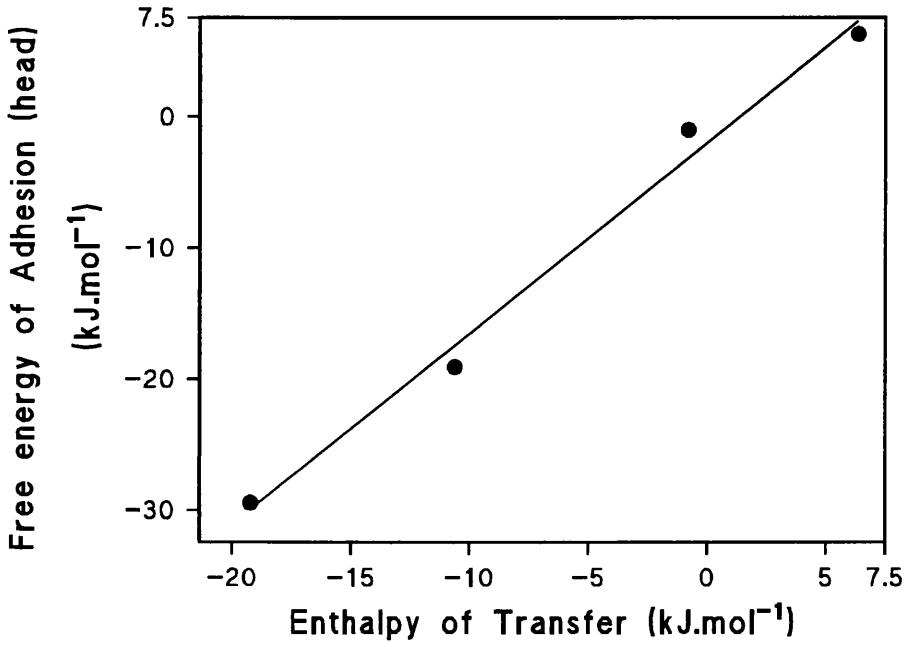

Figure 5.3.2. Relationship between the enthalpy of transfer and the free energy of adhesion to SDS tail groups.

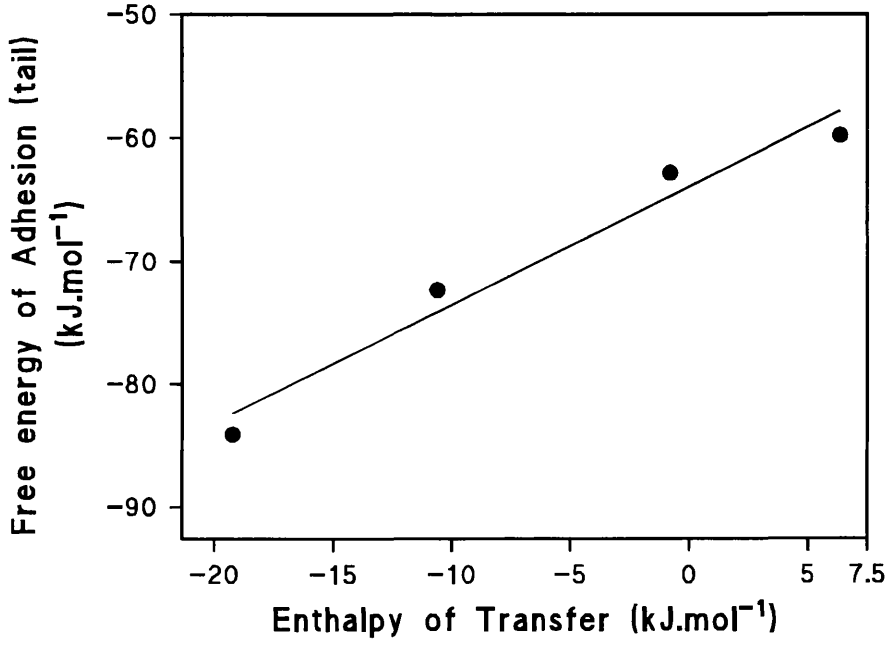

Figure 5.3.3. Relationship between the enthalpy of transfer and the total free energy of adhesion to SDS (head and tail groups).

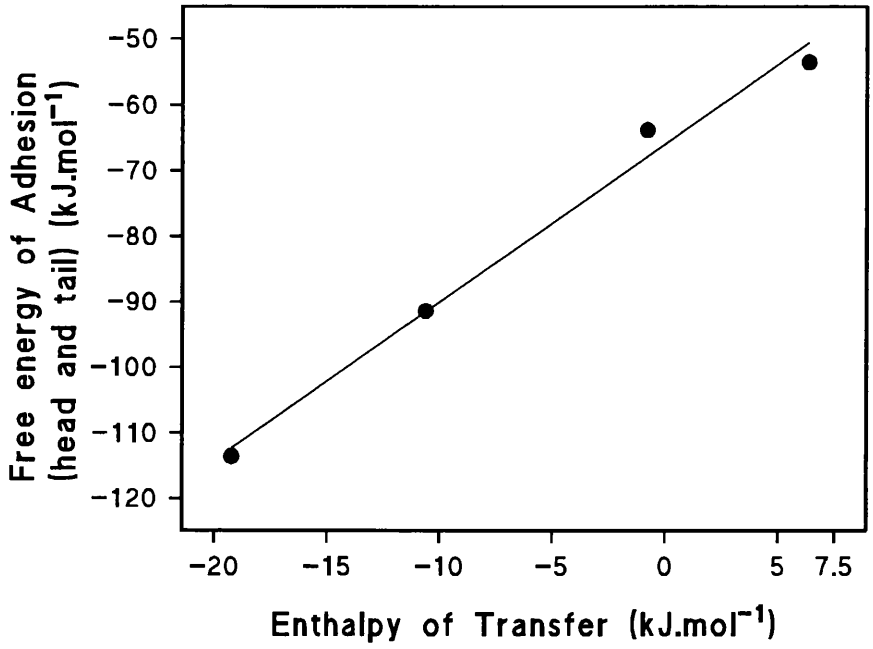

From Figures 5.3.1. and 5.3.2. it can be seen that the interaction is most favoured (*ie* largest negative value for ΔG) for the interaction between the drugs and the SDS tails, however the best correlation ($r = 0.9987$) is seen when the free energy term for partition to the head and tails are added together (Figure 5.3.3.). The enthalpy of transfer data are negative for sulfamerazine, sulfadiazine and sulfamethazine, but positive for sulfanilamide. This correlates well with the sign of the free energy of adhesion between the drugs and the SDS head groups (Figure 5.3.1.), which shows a positive value for sulfanilamide.

From van Oss *et al* (1987), the theory demonstrates that polar interaction can only be between bipolar materials or monopoles of the opposite type and that repulsion can occur between monopoles of the same type. Bipolar materials are those which have both electron donor and electron acceptor contributions to their polar nature, whilst monopolar materials are those which have either electron donor or electron receptor, but not both. In this study the SDS head group is highly polar, but the polar contribution is all of the γ^- type. Thus the positive value for the free energy of adhesion between sulfanilamide and the SDS head group is due to the repulsion between the monopolar drug and the monopolar head group (both being γ^-). It follows that the dissolution process appears to be influenced to a greater extent by this initial interaction between the micellar head groups and the drug.

5.3.2. Data obtained at various stirring rates.

Data obtained for dissolution rates at one temperature (37°C) and concentration of medium of 0.1M SDS and varying stirring rate is given in Table 5.3.6.in % w/v.min^{-1}.

Table 5.3.5. Rotating disk dissolution rate data for compressed disks in 0.1M SDS in water at 37°C, at various stirring speeds. All units for rate constants are % w/v min^{-1} for disks of 132.7mm^2. Values are means ± standard deviations.

Drug	Fluid	50 rpm	100 rpm	130 rpm	150 rpm
Sulfamerazine	**water**	2.55×10^{-6} $\pm 1.29 \times 10^{-3}$	5.75×10^{-6} $\pm 5.90 \times 10^{-3}$	1.01×10^{-5} $\pm 1.25 \times 10^{-3}$	1.27×10^{-5} $\pm 1.84 \times 10^{-3}$
	SDS	1.52×10^{-6} $\pm 2.02 \times 10^{-4}$	2.04×10^{-6} $\pm 9.59 \times 10^{-3}$	2.46×10^{-6} $\pm 9.00 \times 10^{-4}$	2.62×10^{-6} $\pm 2.79 \times 10^{-4}$
Sulfadiazine	**water**	1.07×10^{-6} $\pm 4.69 \times 10^{-4}$	1.48×10^{-6} $\pm 6.27 \times 10^{-3}$	1.75×10^{-6} $\pm 1.42 \times 10^{-3}$	1.90×10^{-6} $\pm 4.61 \times 10^{-5}$
	SDS	3.05×10^{-6} $\pm 1.21 \times 10^{-3}$	5.17×10^{-6} $\pm 1.88 \times 10^{-2}$	7.29×10^{-6} $\pm 9.22 \times 10^{-4}$	8.53×10^{-6} $\pm 1.05 \times 10^{-3}$
Sulfanilamide	**water**	1.11×10^{-4} $\pm 7.55 \times 10^{-3}$	1.29×10^{-4} ± 0.149	1.38×10^{-4} $\pm 9.88 \times 10^{-3}$	1.50×10^{-4} $\pm 9.37 \times 10^{-3}$
	SDS	1.70×10^{-4} $\pm 9.70 \times 10^{-3}$	1.90×10^{-4} ± 0.1725	2.10×10^{-4} $\pm 9.76 \times 10^{-2}$	2.22×10^{-4} 0.1844
Sulfamethazine	**water**	4.79×10^{-6} $\pm 2.15 \times 10^{-3}$	6.79×10^{-6} $\pm 2.27 \times 10^{-3}$	7.69×10^{-6} $\pm 2.12 \times 10^{-3}$	8.62×10^{-6} $\pm 2.47 \times 10^{-4}$
	SDS	5.71×10^{-6} $\pm 1.13 \times 10^{-4}$	1.30×10^{-5} $\pm 7.23 \times 10^{-3}$	1.81×10^{-5} $\pm 7.61 \times 10^{-4}$	2.07×10^{-5} $\pm 2.39 \times 10^{-3}$

Figures 5.3.4. 5.3.5., 5.3.6. and 5.3.7. show data after the rotational speed is converted from rpm to radians$^{0.5}$.

Figure 5.3.4. Initial rotating disk dissolution rate for sulfamerazine in water with and without SDS micelles as a function of stirring rate.

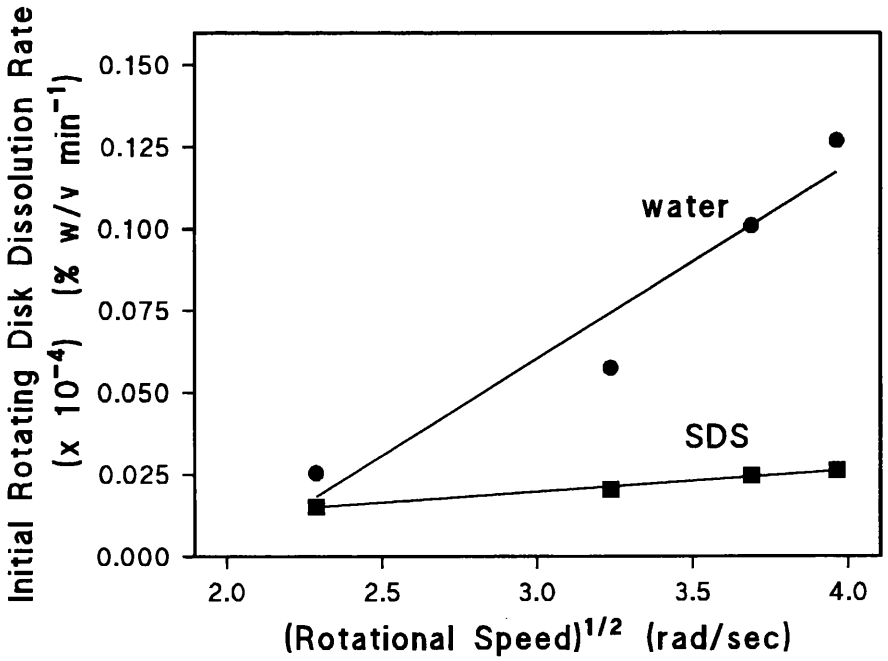

Figure 5.3.5. Initial rotating disk dissolution rate for sulfadiazine in water with and without SDS micelles as a function of stirring rate.

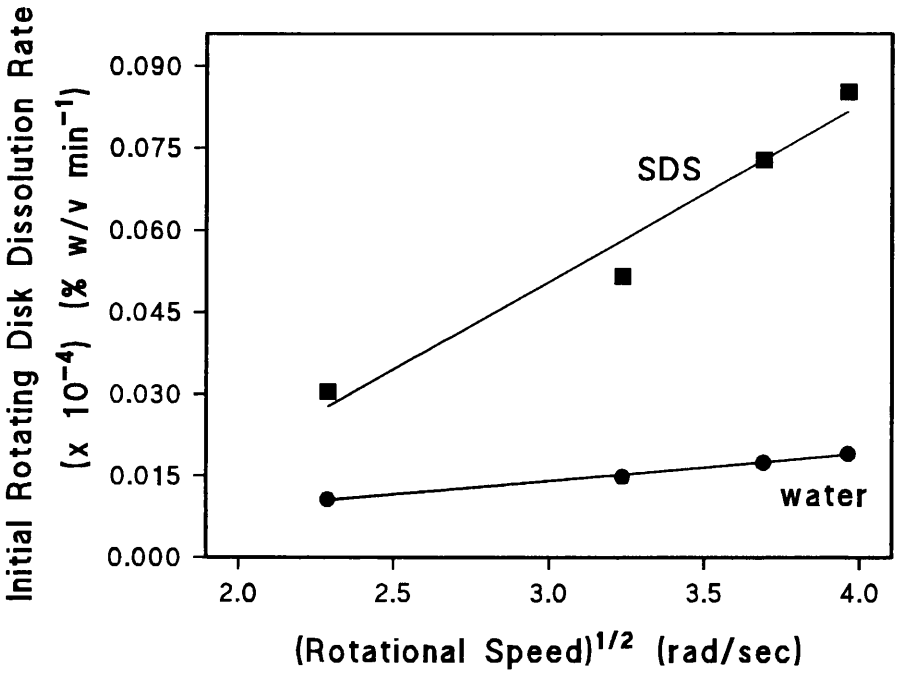

Figure 5.3.6. Initial rotating disk dissolution rate for sulfamethazine in water with and without SDS micelles as a function of stirring rate.

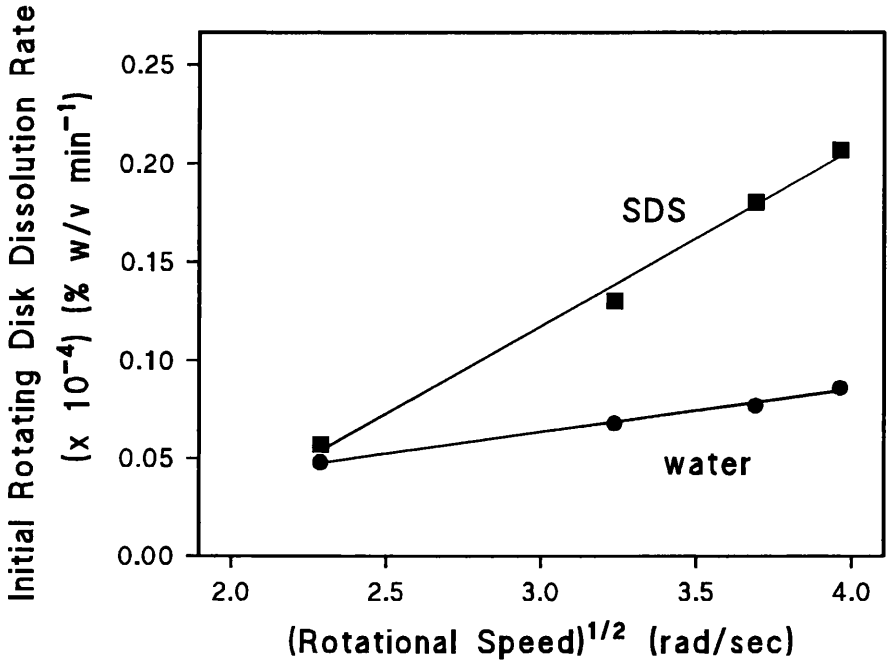

Figure 5.3.7. Initial rotating disk dissolution rate for sulfanilamide in water with and without SDS micelles as a function of stirring rate.

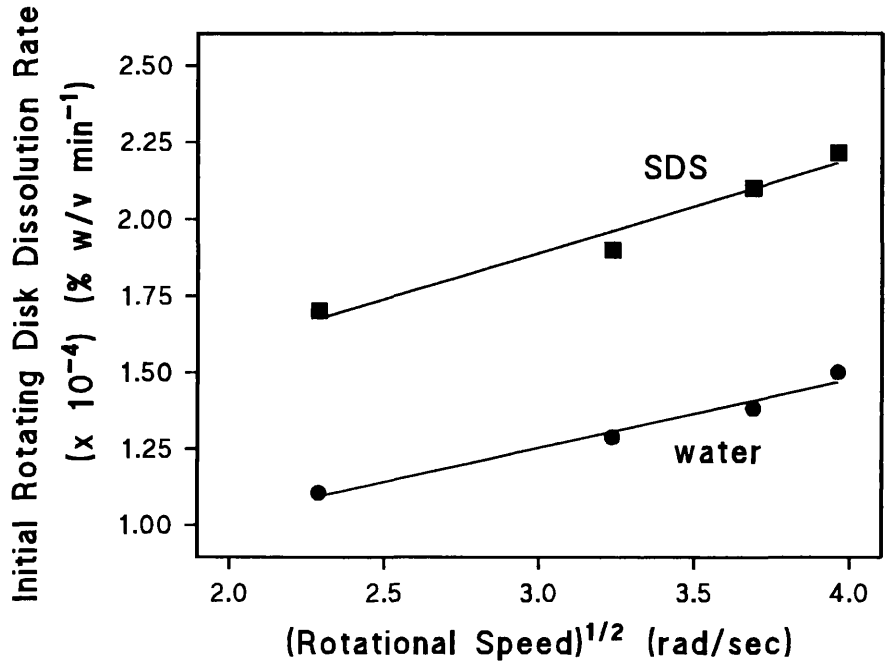

5.3.2.1. Relationship between initial rotating disk dissolution rates and varying stirring rates at 37°C in water and aqueous SDS solution.

Figures 5.3.4. to 5.3.7. show an increase in disssolution rate as the stirring speed increases from 50 rpm through to 150 rpm. Naylor *et al* (1993) observed similar findings with hydrocortisone incorporated in simple and mixed micelle systems.

Three of the sulphonamides studied (sulfadiazine, sulfamethazine and sulfanilamide) show a greater increase in dissolution rate in micellar solutions than in water alone as stirring rate increases. However in the case of sulfamerazine, although the dissolution rate increases with stirring speed, the dissolution rate is in fact slower in the aqueous SDS solution than in water. This is unusual as it can be seen in section 4.3.3. that the solubility of sulfamerazine is higher in a micellar solution than in water. Possible reasons for this behaviour are discussed later in Chapter 7.

5.3.3. Data obtained at various SDS concentrations.

The experiments performed here were at constant temperature (37°C) and stirring speed (100 rpm). The media used were various concentrations of SDS solutions, ranging below and above the CMC of SDS. See Table 5.3.6. for data ± standard deviations.

Table 5.3.6. Rotating disk dissolution rate data for compressed disks at 100 rpm and 37°C in solutions of various SDS concentration and water. All units for rate constants are % w/v min^{-1} for disks of 132.7 mm^2. Values are means ± standard deviations.

Concentration of SDS ($mol.dm^{-3}$)	Sulfamerazine	Sulfadiazine	Sulfamethazine	Sulfanilamide
water	5.7×10^{-6} $\pm 5.90 \times 10^{-3}$	1.5×10^{-6} $\pm 3.00 \times 10^{-4}$	6.8×10^{-6} $\pm 2.27 \times 10^{-3}$	1.29×10^{-4} ± 0.149
6.9×10^{-4}	5.3×10^{-6} $\pm 2.14 \times 10^{-3}$	1.7×10^{-6} $\pm 4.35 \times 10^{-4}$	7.4×10^{-6} $\pm 3.52 \times 10^{-3}$	1.49×10^{-4} ± 0.066
3.46×10^{-3}	4.8×10^{-6} $\pm 6.13 \times 10^{-3}$	2.0×10^{-6} $\pm 1.42 \times 10^{-3}$	8.5×10^{-6} $\pm 4.39 \times 10^{-4}$	1.59×10^{-4} ± 0.015
6.93×10^{-3}	4.2×10^{-6} $\pm 1.35 \times 10^{-3}$	2.9×10^{-6} $\pm 1.42 \times 10^{-3}$	9.1×10^{-6} $\pm 3.35 \times 10^{-3}$	1.65×10^{-4} ± 0.012
3.46×10^{-2}	3.0×10^{-6} $\pm 6.82 \times 10^{-4}$	4.4×10^{-6} $\pm 2.25 \times 10^{-3}$	1.17×10^{-5} ± 0.012	1.79×10^{-4} ± 0.013
6.93×10^{-2}	2.1×10^{-6} $\pm 4.02 \times 10^{-3}$	5.1×10^{-6} $\pm 1.42 \times 10^{-3}$	1.29×10^{-5} $\pm 1.05 \times 10^{-3}$	1.91×10^{-4} ± 0.019
0.1	2.0×10^{-6} $\pm 9.59 \times 10^{-3}$	5.2×10^{-6} ± 0.019	1.30×10^{-5} $\pm 7.23 \times 10^{-3}$	1.93×10^{-4} ± 0.173

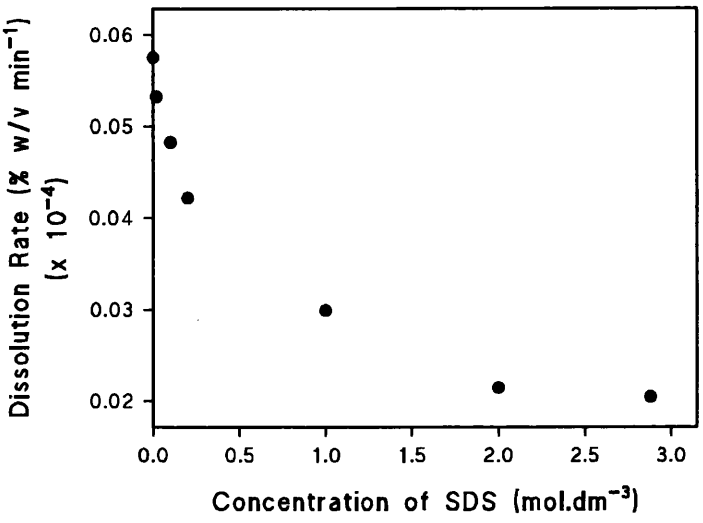

Figure 5.3.8. Initial rotating disk dissolution rate for Sulfamerazine at 37°C and 100 rpm as a function of aqueous SDS concentration.

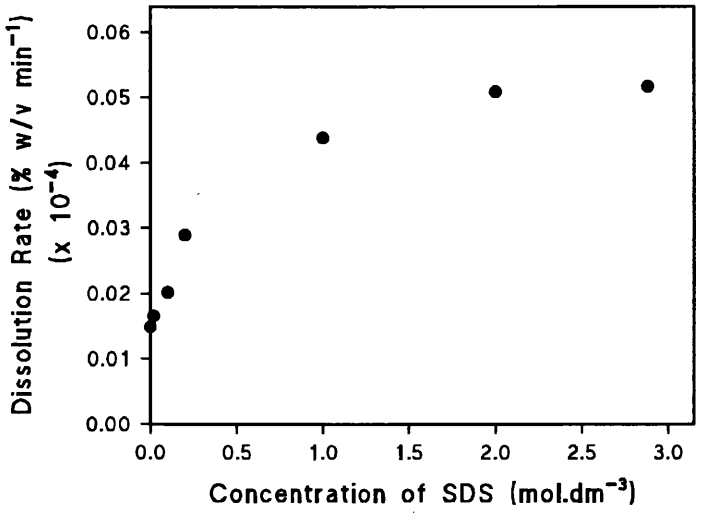

Figure 5.3.9. Initial rotating disk dissolution rate for Sulfadiazine at 37°C and 100 rpm as a function of aqueous SDS concentration.

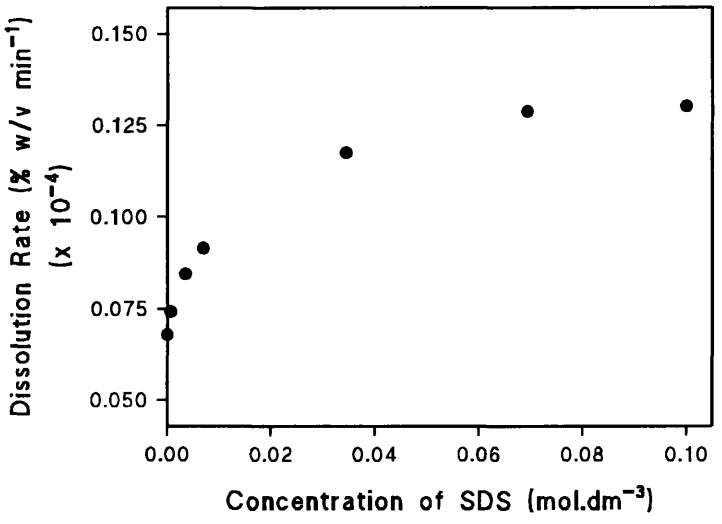

Figure 5.3.10. Initial rotating disk dissolution rate for Sulfamethazine at 37°C and 100 rpm as a function of aqueous SDS concentration.

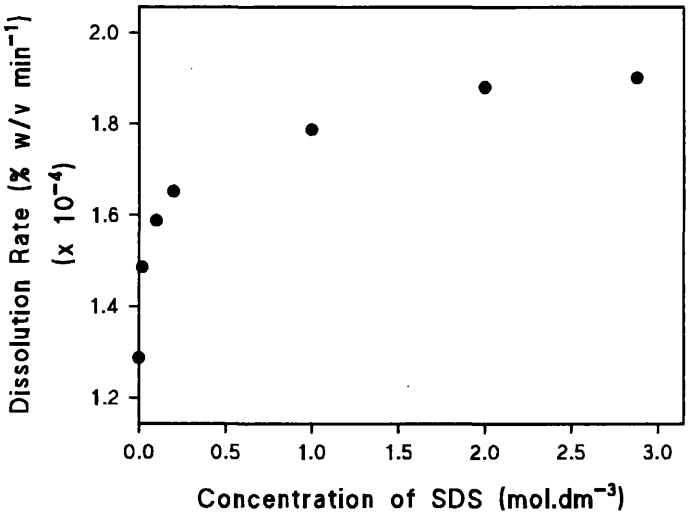

Figure 5.3.11. Initial rotating disk dissolution rate for Sulfanilamide at 37°C and 100 rpm as a function of aqueous SDS concentration.

5.3.3.1. Relationship between initial rotating disk dissolution rates at 37°C and 100 rpm and various concentrations of SDS solutions.

From Figures 5.3.8. to 5.3.11. an instant observation is that the dissolution rate increases with increasing aqueous SDS concentration for all the sulphonamides except sulfamerazine. This drug displays an exponential decrease in dissolution rate as the medium surfactant concentration increases. The reasons for this are discussed later in Chapter 7.

5.3.4. General discussion.

5.3.4.1. Thermodynamics of transfer from rotating disk dissolution experiments and relationships with the surface energy data.

The temperature dependence of the rate constants give a route by which it is possible to understand more about the mechanism of interaction between the drugs and the micelles. The data for the enthalpy of transfer between the water and the SDS micelles (Table 5.3.2.) can be seen to correlate well with the free energy of adhesion between the drugs and the SDS micelles in the presence of water (ΔG_{1w2}) (Figures 5.3.1 to 5.3.3.). It can be seen that the most negative enthalpy of transfer (most favoured interaction) correlates with the most negative ΔG_{1w2} (most favoured interaction) in each case, but the free energy of adhesion values (from surface energy data) show that the strongest attraction is between the drugs and the SDS tails, rather than between the drugs and the SDS head groups (as the values for ΔG_{1w2} are considerably more negative in each case for adhesion to the tails). Despite the fact that the interaction between the drugs and the SDS tails is

the most favoured, due to the relatively hydrophobic nature of the sulphonamides (Table 3.4.1.), the interaction between the SDS head groups and the drugs in all but one case (sulfanilamide) has a negative value for ΔG_{1w2} (with the value for sulfamethazine approaching zero). It follows that on surface energetic terms, sulfamerazine and sulfadiazine should have a favourable, sulfamethazine a relatively neutral, and sulfanilamide a disfavoured interaction with the SDS head groups. It is necessary to consider why it should be so that the drugs have different interactions with this polar region of the micelle. Instinctively one would feel that the interaction between the drug and the polar head of a micelle would be greatly influenced by the hydrophobicity of the drug, in that the more hydrophobic the more disfavoured would be the interaction with the micellar head group. In reality, however, from Table 3.4.1. it can be seen that values for γ^{LW} for each of the sulphonamides are quite similar in each case, thus they have roughly equal hydrophobic interactions. The difference is that the sulfanilamide and sulfamethazine have substantial polar interaction potential, both being monopoles of the γ^- type. As the major differences are in the values for the polar terms of the drugs, the value of ΔG_{1w2} will consequently be influenced by the polar interactions between the different drugs and water in comparison with the polar interactions between the drugs and the SDS head group. There will be minimal polar interaction between sulfadiazine and sulfamerazine and either the water or the SDS head groups, as both groups are comparatively apolar. However, for both sulfanilamide and sulfamethazine the polar interaction with water will be a composite of attraction between substantial γ^- values for the solid and γ^+ values for water and repulsion between the γ^- values for the solid and water. For the interaction between the drugs and the SDS head group there will however

only be repulsion between the γ^- monopoles.

In order for the favourable interaction between the drug and the hydrophobic tail of the micelle to be achieved it seems that the drug has to pass through water and be sufficiently close to the SDS head group so as to be influencial, as it is the interaction between the head group and the drug which appears to dominate the process. This transfer can be regarded as an activation step. For sulfamerazine and sulfadiazine the interaction with the SDS head groups (ΔG_{1w2}) is favoured, thus the activation step is also favoured and drug can be expected to interact with relative ease with the SDS micelle, a situation which is seen to correlate well with the data in Table 5.3.2. with a strongly favoured enthalpy of transfer. For sulfamethazine ΔG_{1w2} for the head groups approaches zero, as does the enthalpy of transfer (Table 5.3.2.), whilst for sulfanilamide ΔG_{1w2} is positive (disfavoured) as is the enthalpy of transfer. It follows that there is excellent correlation between the enthalpy of transfer data and the surface energy adhesion interactions, when the interaction with the SDS head group is taken as a model for the activation barrier.

This work gives a new insight into a possible mechanism of solubilisation into micellar structures and shows clearly that the repulsive polar interactions can cause drugs which exhibit mono-polarity to have a serious activation step prior to reaching a more stable equilibrium position.

The entropy of transfer data (Table 5.3.3.) also correlate with the ΔG_{1w2} data (for interaction with both the head groups and the SDS tails), however, the interaction is an inverse relationship, with favoured negative values for the free energy change correlating with the largest negative values for the entropy of transfer (*ie* the most disfavoured

response). For sulfamerazine and sulfadiazine the solubilisation into the SDS micelle would seem to be enthalpically driven, whilst the opposite may be true for sulfanilamide, with sulfamethazine being approximately neutral. There is no simple correlation between ΔG_{1w2} and the free energy of transfer data, due to compensating effects of the enthalpy and entropy changes.

5.3.5. Data obtained for initial powder dissolution rates (IPDR).

The data acquired was normalised (*ie* IPDR in SDS / IPDR in water) as shown in Table 5.3.8. The data studied here has been normalised to correct for differences in particle shape and size between the sulphonamides so that comparisons can be made. Mosharraf *et al* (1995) discusses how the dissolution rates of sparingly soluble drugs are related to the particle shape as well as to the particle size.

Table 5.3.7. Normalised Initial Powder Dissolution Rates in varying solutions of SDS concentrations for the sulphonamides at 37°C and 100 rpm.

SDS Conc. ($mol.dm^{-3}$)	sulfamerazine	sulfadiazine	sulfamethazine	sulfanilamide
6.9×10^{-4}	1.052	1.987	1.569	1.876
3.46×10^{-3}	1.141	1.999	1.695	2.077
6.93×10^{-3}	1.212	2.165	1.709	2.364
3.46×10^{-2}	8.869	5.547	2.659	4.322
6.93×10^{-2}	9.755	6.922	3.133	5.064

Figures 5.3.12. to 5.3.15. show plots of dimensionless IPDR of each of the sulphonamides against SDS concentration. However, by plotting dimensionless IPDR alongside dimensionless solubility data from Chapter 4 against SDS concentration, it is possible to determine how important the roles of wetting and solubilisation are for the individual drugs studied, which is discussed later in Chapter 7.

5.3.5.1. General discussion.

From Figures 5.3.12. to 5.3.15. it can be observed that for each of the sulphonamides, there is an increase in the IPDR with increasing SDS concentration. For sulfanilamide, there seems to be a gradual increase in IPDR whereas with sulfadiazine, sulfamerazine and sulfamethazine, the increase in IPDR is more apparent after the CMC of the SDS has been reached. This suggests that solubilisation does not seem to play an important role in the dissolution of sulfanilamide. However this will be discussed further in Chapter 7 alongside other factors which may be related to this.

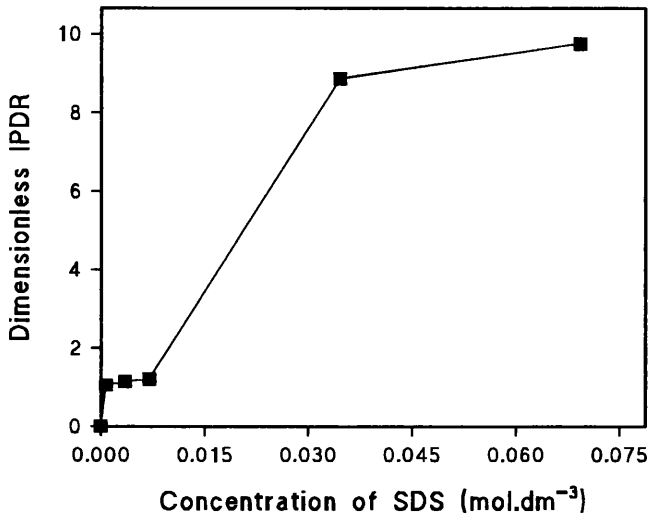

Figure 5.3.12. Plot of dimensionless IPDR of Sulfamerazine against SDS concentration.

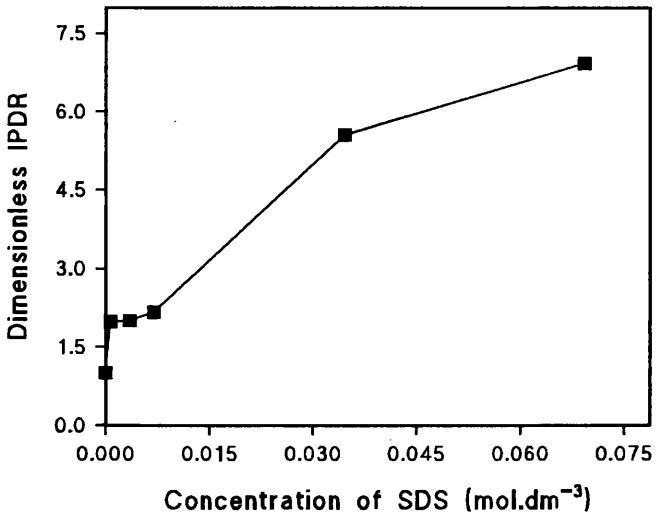

Figure 5.3.13. Plot of dimensionless IPDR of Sulfadiazine against SDS concentration.

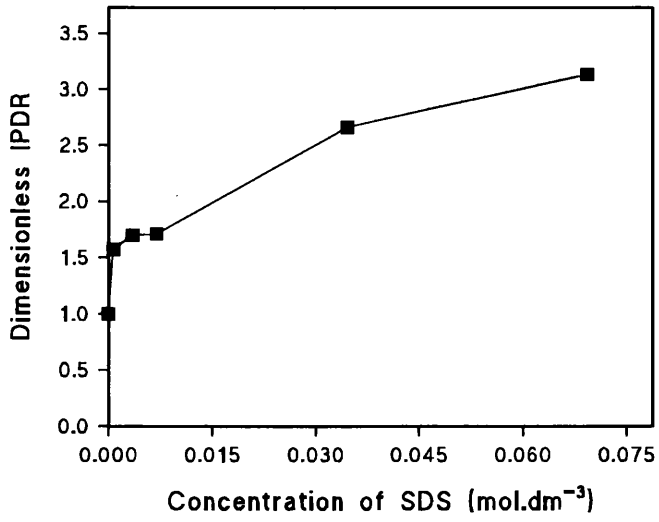

Figure 5.3.14. Plot of dimensionless IPDR of Sulfamethazine against SDS concentration.

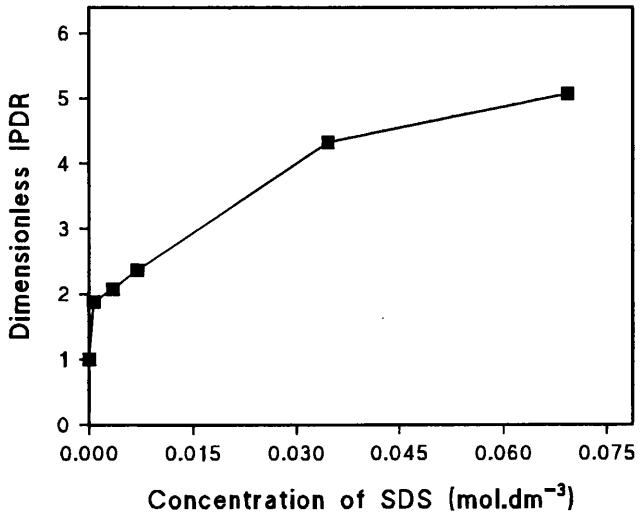

Figure 5.3.15. Plot of dimensionless IPDR of Sulfanilamide against SDS concentration.

5.4. CONCLUSIONS.

1. By performing experiments under various conditions, it was possible to determine which factors (*eg* temperature, stirring speed and medium concentration) were most influencial to the dissolution rates of the poorly soluble drugs studied.

2. It is generally true that increased solubility will result in increased dissolution rate, however, this is not always true. It was observed that one of the drugs, sulfamerazine, had a reduced dissolution rate in SDS than in water although solubilities were found to be higher in the surfactant solution than in an aqueous control.

3. The use of surface energy data obtained from contact angle studies allows a good understanding of drug solubilisation behaviour into SDS micelles. It can be seen that the solubilisation of the most polar drugs is restricted by the activation step of passage through the polar head groups, due to the repulsion which exists between the monopolar head group and the monopolar drugs.

This approach has given a valuable novel insight into the mechanisms of solubilisation which may have application to further studies directed towards understanding drug absorption.

CHAPTER 6

PARTITIONING STUDIES

6.1. INTRODUCTION

In medicinal chemistry it is common to equate the logarithm of the partition coefficient between octanol and water with the biological response of drug molecules as a basis of quantitative structure-activity relationships *eg* Leo and Hansch, 1971. The use of octanol for such experiments has been questioned (Beezer *et al*, 1987) in terms of the biological relevance of this solvent. It has been argued that better information may be obtained by studying partition into organic phases which contain more water than does octanol.

Examples of suitable partitioning systems would be micelles and liposomes. The partitioning behaviour of solutes between aqueous and non-aqueous phases is an indication of the hydrophilic-lipophilic balance of the molecules, although it has been argued that the affinity of water for the solute is important in partitioning, (Tsai *et al.*, 1993), due to water-dragging effects where the water is carried as a shell around the solute into the non-aqueous phase. It follows that the interactions between the solute and water, between the solute and the non-aqueous phase, and between water and the non-aqueous phase will all be important in the partitioning process.

Partition coefficients offer a rough prediction of the tendency for a drug to move from an aqueous environment into a membrane, and consequently have been found to correlate well with biological response *eg* Tomlinson *et al.*, (1983).

Yamagami *et al.*, (1993), found that the electron donor and electron acceptor roles of the solute and the solvents will determine partitioning. This would imply that partition

processes should be predictable by consideration of electron donor and electron receptor (Lewis acid-Lewis base) components to surface energy (see Chapter 3).

The aim of this work was to develop and evaluate similar techniques using aqueous and micellar phases of sodium dodecyl sulphate (SDS) solution. The values determined for the partition coefficients were then to be related to the surface energy data obtained previously from contact angle measurement in Chapter 3.

6.2. METHODS.

6.2.1. Log P values from a computer program.

Using a program designed by Dr.K. Valka, it was possible to calculate the values of log P in water/octanol systems from the structures of the sulphonamides studied. The values of these are presented in Table 6.2.1. and allow a comparison to be made between measured log P values in water/octanol systems and calculated values using this program.

6.2.2. Measurement of log P in water/octanol systems.

Standard solutions of drug dissolved in water were prepared. In each case, the aqueous solution was transferred to a perspex dish and an equal volume of octan-1-ol was added. The contained solution within the system was continuously stirred. (See Figure 6.2.1.). Ten minutes before sampling, the system was allowed to settle and a 2ml sample was extracted from the aqueous phase and analysed using UV spectroscopy with water as a standard. With time, more drug diffuses into the octan-1-ol phase and hence the absorbance readings from the aqueous phase decrease until equilibrium is reached.

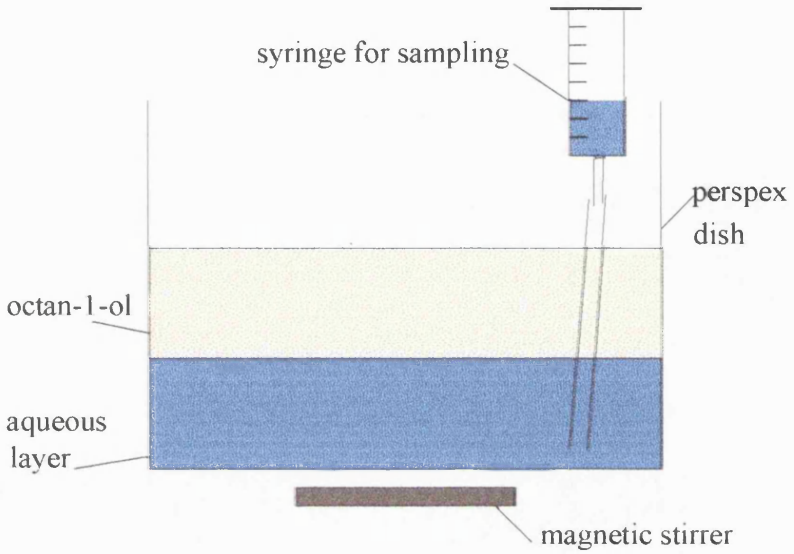

Figure 6.2.1. Apparatus used to measure log P values in an octan-1-ol / water system.

Previously constructed calibration curves (see Chapter 3), were used to determine the concentration of each drug in water from the absorbance values. By subtracting the concentration of drug in water from the total concentration of the standard solution, it was possible to calculate the concentration of drug in octan-1-ol. From Eq. 6.2.1. the partition coefficients in octan-1-ol /water systems were calculated and are presented in Table 6.3.2.

$$P = C_{oct} / C_{water} \qquad (6.2.1.)$$

where P = partition coefficient

C_{oct} = concentration of drug in octan-1-ol

C_{water} = concentration of drug in water

6.2.3. The Taylor-Aris diffusion technique.

This technique involves the measurement of diffusion coefficients, which are used to determine partition coefficients for the distribution of a variety of organic substrates between the micellar and aqueous phases of sodium dodecyl sulphate (SDS) solution, (Burkey *et al.*, 1984).

It is important to know the extent to which an organic molecule is partitioned between the aqueous and micellar phases. The principle of this method is quite simple. In a micellar solution containing an organic solute, the solute molecules in the water will diffuse with their normal diffusion coefficient, while those in the micelle will diffuse at the same rate as their host *ie* with the micellar diffusion coefficient. Thus, the observed diffusion coefficient for the organic solute will depend upon the fraction of organic molecules present in the micellar phase.

6.2.3.1. Experimental procedure.

The diffusion apparatus used in this work follows the design developed by Huggenberger *et al.*, (1980). Basically solvent was pumped at a steady flow (6ml/hour) through 10 metres of stainless steel tubing (0.03 inches in diameter) by using an infusion pump. The tubing was immersed in a thermostated water bath at a defined temperature. Samples (which had had hydrogen gas bubbled through them for ten minutes to eliminate air bubbles), were introduced at the beginning of the tubing by using a Rheodyne 7125 injector fitted with a 20μl loop. These conditions were chosen so as to establish a laminar flow in the apparatus. The dispersion of the sample which occurred during its passage

through the tubing was detected with a CE 2010 UV monitor. Signals were recorded on a Servogor 120 recorder. Samples were prepared by dissolving 0.016g of solute in 100ml of solvent and filtered through 0.45μm pore size filters. The solvents used were solutions of buffer (Svehla, 1979), at the pH equal to the pK_a (*ie* sulfamerazine, pK_a = 7.1; sulfamethazine, pK_a = 7.4; sulfadiazine, pK_a = 6.5; sulfanilamide, pK_a = 10.4), to ensure 50% ionisation in each case. Also solutions of 0.1M sodium dodecyl sulphate with the pH equal to the pK_a for each drug were used. See Figure 6.2.2. for the Taylor -Aris diffusion equipment employed.

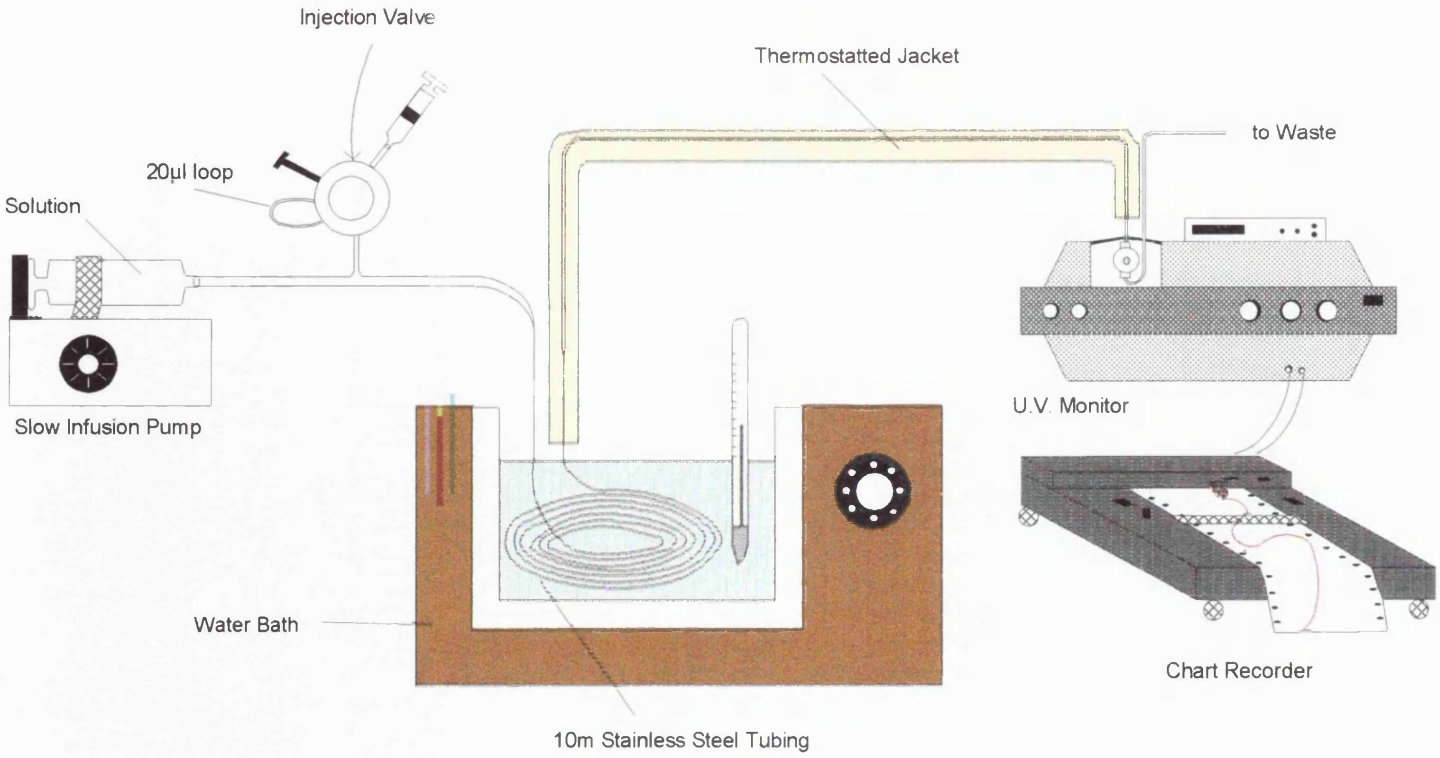

Figure 6.2.2. The Taylor-Aris diffusion apparatus.

6.2.3.2. Measurement of diffusion coefficient.

The Taylor-Aris method was used for the measurement of diffusion coefficients, as this has a number of advantages (Burkey *et al.*, 1984). The theory is well understood, analysis of the experimental data is straightforward, the apparatus is simple and inexpensive to build and operate and diffusion coefficients can routinely be measured to a precision of approximately ± 2%.

In this experiment a small sample of solute was introduced into a stream of solvent that was flowed slowly through a long capillary. The axial distribution of the solute at injection was essentially a 'Δ function spike', (Huggenberger *et al.*, 1980). That is, the time taken for the injection and the volume injected were very small when compared with the duration of the experiment and the volume of the capillary tube. This condition ensured that the dispersion of the sample when injected was negligible when compared with its dispersion at the detector.

The experimental conditions were such that laminar flow was established in the tube and therefore the solvent flow rate decreased as a function of the radial distance from the centre of the tube. As a result the solute near the centre of the tube flows faster than that near the walls causing a large axial dispersion of the solute. Axial diffusion of the solute does not contribute significantly to this effect. However, radial diffusion of the solute is quite significant when compared with the diameter of the tube and tends to counteract the effect of the solvent-induced axial dispersion. As a result, solutes that diffuse slowly adopt broad Gaussian distributions when detected a long distance from the injector, while the converse is true for solutes that diffuse rapidly.

Diffusion coefficient, **D**, was calculated by using Eq. 6.2.2:

$$D = r^2t / (24\sigma^2) \qquad (6.2.2.)$$

where r = radius of the tube

t = time elapsed between the injection of the sample and the appearance of the maximum of the dispersion curve of the solute.

σ = the variance of the dispersion curve.

The true (rather than nominal) radius (r) of the column was calculated by control experiments with materials of known partition behaviour (Burkey *et al.*, 1984). The method is based on the fact that the observed diffusion coefficient is based on a diffusion coefficient of the solute in water and a diffusion coefficient of the solute in micelles. See Eq. 6.2.3.

$$D = f D_m + (1\text{-}f)D_w \qquad (6.2.3.)$$

where D = observed diffusion coefficient

D_m = diffusion coefficient of the micelle in aqueous solution

D_w = solute diffusion in aqueous solution

f = fraction of solute in the micellar phase.

The diffusion of the micelles can be followed by injecting a material which will only be present in micelles (no free solute), thus $D = D_m$. Anthracene was used as such a marker solute, (Burkey, 1984 and Ajufo, 1991).

The partition coefficient was then obtained from Eq. 6.2.4:

$$P = f / (1-f) \qquad (6.2.4.)$$

where P = partition coefficient

f = fraction of solute present in the micellar phase

The flow was undertaken in a water bath at four different temperatures which were 25, 30, 37 and 42°C. The temperature was varied in order to calculate the thermodynamics of transfer from the van't Hoff isochore (Ajufo *et al.*, 1991).

Previously this method had been used for the evaluation of dye-micelle binding constants (Armstrong *et al.*, 1988) and also to obtain enthalpies of transfer of alkoxyphenols from water to sodium dodecyl sulphate micelles, (Beezer *et al.*, 1992).

6.3. RESULTS AND DISCUSSION.

6.3.1. Theoretical data obtained for log P.

Table 6.3.1. gives data obtained for log P for the four sulphonamides studied, calculated from a computer program designed by Dr. K. Valka. These are values for partitioning in an octan-1-ol / water system.

Table 6.3.1. Log P values for the sulphonamides in an octan-1-ol / water system.

Drug	log P
Sulfadiazine	-0.78
Sulfanilamide	-0.73
Sulfamerazine	-0.26
Sulfamethazine	0.25

6.3.2. Data obtained from measurements of log P in an octan-1-ol / water system.

Table 6.3.2. gives data obtained when the log P values were calculated from measurements of the partition coefficient.

Table 6.3.2. Measured log P values in an octan-1-ol / water system.

Drug	log P
Sulfadiazine	-0.25
Sulfanilamide	-0.59
Sulfamerazine	-0.17
Sulfamethazine	0.66

6.3.3. General discussion.

From the sets of data in sections 6.3.1. and 6.3.2. it can be seen that the measured log P values in an octan-1-ol system are fairly similar to the values obtained using the computer program, although the ranking order is not quite the same. For both computer obtained and measured methods, sulfadiazine, sulfanilamide and sulfamerazine log P values are negative, indicating disfavoured partitioning from the water to the octan-1-ol system. However the log P value for sulfamethazine is positive, with both methods suggesting that the partitioning here is more favourable and implying that this drug is more hydrophobic than the others. From Table 3.4.1. in Chapter 3, it can be seen that sulfamethazine has a larger γ^{LW} value than the other three drugs, once again suggesting that this is more hydrophobic.

The values for sulfadiazine and sulfanilamide are both fairly close with both methods, whilst sulfamerazine has a lower negative value implying that it is more hydrophobic than the other two. This data is discussed later in relation to data obtained from the Taylor-Aris diffusion technique.

6.3.4. Data obtained from the Taylor-Aris diffusion technique.

Table 6.3.3. shows data for log P values for the four sulphonamides studied in a buffer (at pH = pK_a of drug) and buffer with SDS micelles system.

Table 6.3.3. Partition coefficients (as log P) obtained from the Taylor-Aris diffusion technique at different temperatures for the drugs moving from buffer (at pH = pK_a of drug) to SDS micelles.

Drug	298 K	303 K	310 K	315 K	r[a]
sulfamerazine	-0.381	-0.419	-0.544	-0.618	0.989
sulfanilamide	-1.362	-1.868	-2.542	-3.280	0.996
sulfamethazine	1.531	0.945	0.555	0.074	0.991
sulfadiazine	-0.586	-0.786	-1.190	-1.373	0.996

[a] r is the correlation coefficient of a plot of log P as a function of 1/T.

6.3.4.1. Thermodynamics of transfer from Taylor-Aris diffusion experiments.

From equations 6.2.2. 6.2.3. and 6.2.4. it was possible to calculate log P values for each of the sulphonamides at temperatures of 25, 30, 37 and 42°C. By plotting log P against 1/T, in Kelvin, (*ie* van't Hoff isochore), the gradient of each plot could be used to obtain values for ΔH for both buffer and SDS systems. Hence, the thermodynamics of transfer from the buffered solution (at pH = drug pK_a) into the SDS micelles were determined, which is the difference between the values for the buffered and the micellar solutions and are presented in Table 6.3.4.

Table 6.3.4. Calculated thermodynamic parameters of transfer from buffer (at pH = pK_a of drug) to SDS micelles[a].

Drug	ΔH_{trans} ($kJ.mol^{-1}$)	ΔG_{trans} ($kJ.mol^{-1}$)	ΔS_{trans} ($J.mol^{-1}.K^{-1}$)
sulfamerazine	11.3	0.9	34.8
sulfanilamide	86.1	3.4	277.6
sulfamethazine	63.6	-3.8	255.9
sulfadiazine	37.4	1.5	120.6

[a] Free energy and entropy of transfer data calculated using 298 K data.

6.3.4.2. Comparison between the free energy of adhesion and the thermodynamics of transfer.

The relationships between the total free energy of adhesion (from surface energy considerations) and the enthalpy of transfer (from Taylor-Aris diffusion data) are shown in Figures 6.3.1., 6.3.2. and 6.3.3.

Figure 6.3.1. The relationship between the total free energy of adhesion (head and tail contribution) derived from surface energy data and the enthalpy of transfer into micelles by the Taylor-Aris diffusion technique at pH = pK_a of drug.

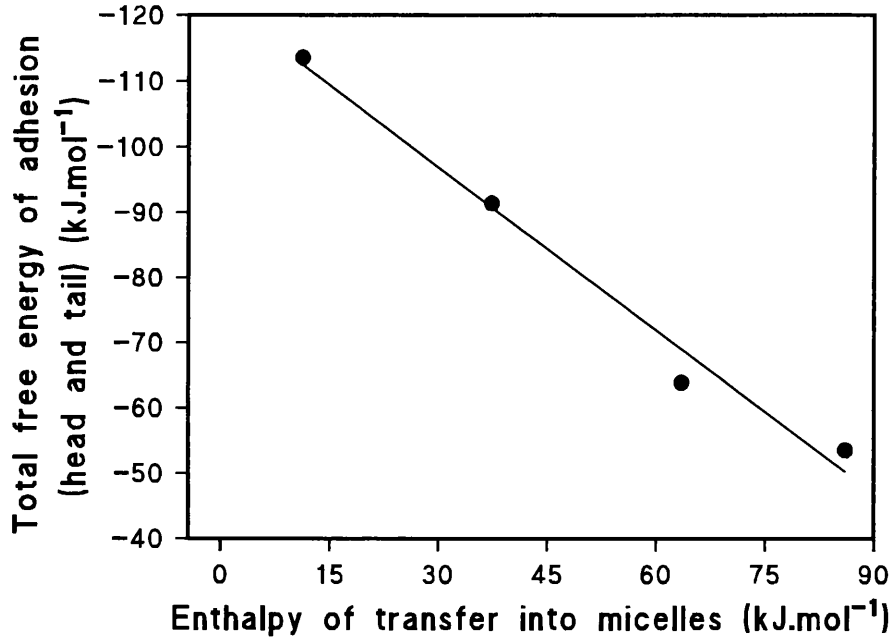

Figure 6.3.2. The relationship between the free energy of adhesion to the SDS head groups (derived from surface energy data) and the enthalpy of transfer obtained using the Taylor-Aris diffusion technique.

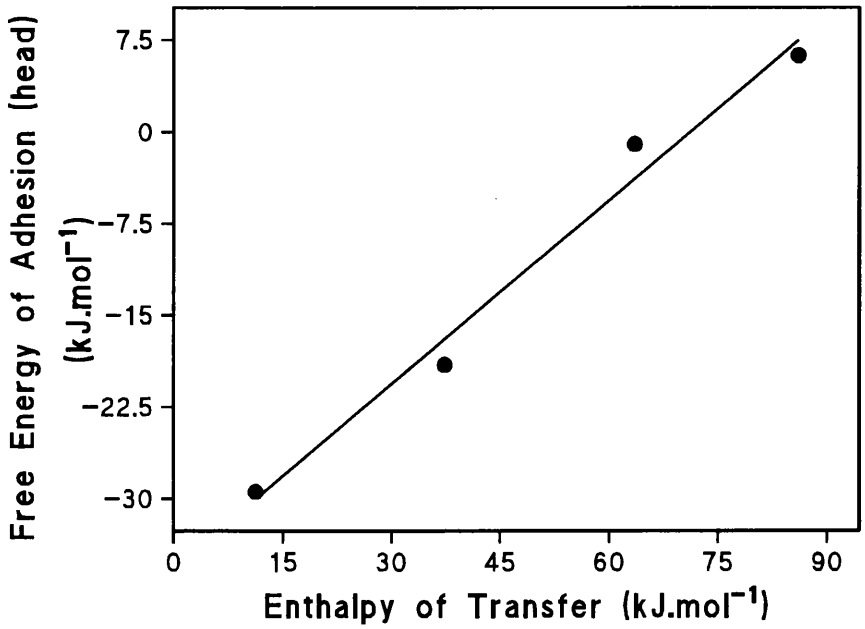

Figure 6.3.3. The relationship between the free energy of adhesion to the SDS tail groups (derived from surface energy data) and the enthalpy of transfer obtained using the Taylor-Aris diffusion technique.

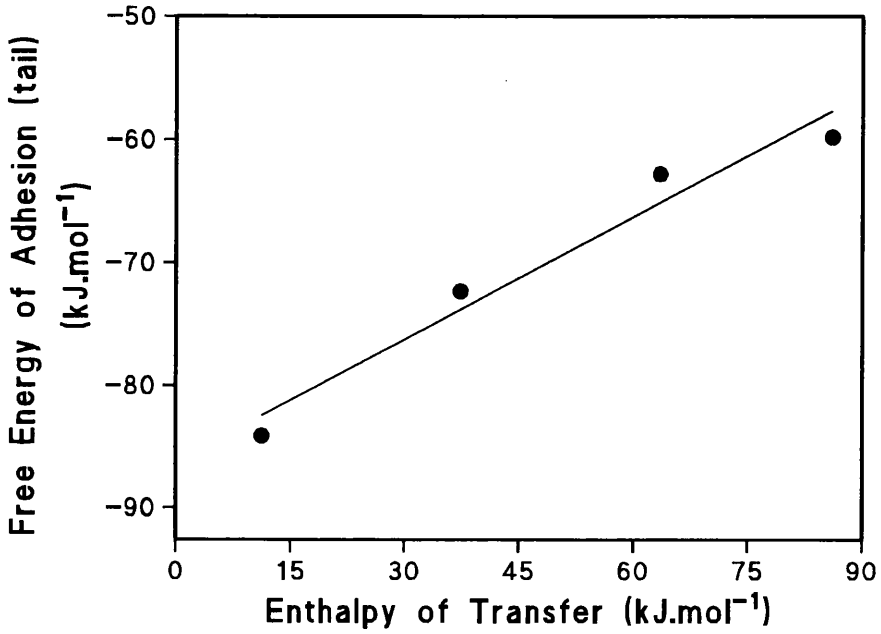

There is good agreement between the measured (from Taylor-Aris diffusion technique) and predicted (from surface energy values) partitioning behaviour as long as the ionization of the drug is not excessive. The relative contributions of the free energy of adhesion to the head group and the tail of the SDS can be considered in relation to the enthalpy of transfer. It can be seen from Figures 6.3.2. and 6.3.3. that there is a good linear correlation for both the interaction with the head ($r = 0.991$) and tail ($r = 0.979$) groups. In each case, for any one drug the free energy of adhesion to the surfactant tail is a significantly more favourable interaction than that with the head group, but the interaction with the head group is still very important. This provides an indication that the partition will not just be between the aqueous phase and the hydrophobic core of the micelle, but will also include an amount of material which will adhere to the surfactant head group. It is notable that the free energy of adhesion to the SDS head groups becomes positive for sulfanilamide. This is due to the repulsion between the monopolar drug and the monopolar head group (both being γ^-). In fact the values of the free energy of adhesion to the SDS head group correlates well with the magnitude of γ^- for the drugs, showing that this is a major contribution to the interaction.

The values for the entropy terms derived from the Taylor-Aris diffusion study are also seen to fit a linear correlation with the total free energy of adhesion ($r = 0.996$) and the free energy of adhesion to the SDS head groups ($r = 0.993$) and tails ($r = 0.989$). The largest entropy changes are for the drugs with the least negative free energy of adhesion, and this inverse relationship may possibly relate to the water-dragging effect which occurs during partitioning, (Tsai *et al.*, 1993).

Figure 6.3.4. The relationship between the entropy of transfer (from Taylor-Aris diffusion technique) and the γ^- contribution to the surface energy of the (largely monopolar) drugs.

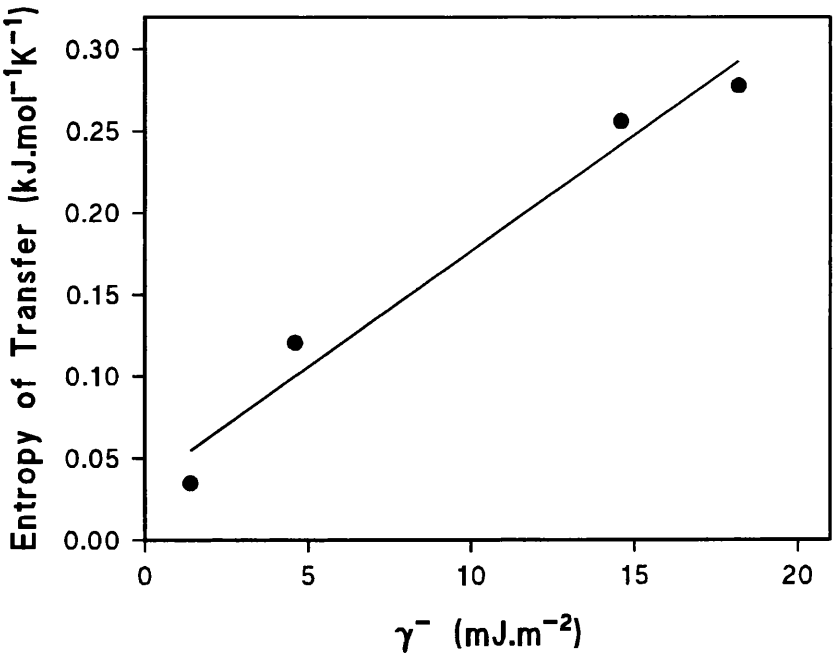

It has been shown that the water-dragging effect, (discussed in section 1.7.2.) is closely related to the solute nature in terms of the electron donor and electron acceptor capabilities and that the water content of relatively nonpolar organic phases increases in the presence of polar solutes, (Tsai *et al.*, 1993). The correlation between the γ^- contribution to the surface energy of each solute and the entropy of transfer to the non-aqueous tail region is shown in Figure 6.3.4. It must be assumed that the high entropic driving force for the transfer of the more polar materials relates to a significant disruption of structure in the micelle. These entropy changes may be due to the water-dragging effect or to the repulsion between the head groups and the drugs (which has been argued to be related to the dispersibility and solubility of monopolar solutes in water, (van Oss *et al.*, 1987).

6.3.4.3. General discussion.

The log P values obtained from the Taylor-Aris diffusion technique rank in the same order as the log P values measured in an octan-1-ol / water system. However, the ranking is different from log P values determined using the computer program and is discussed further in Chapter 7. It can be concluded that measuring is favourable to predicting log P.

The relationship between the free energy of adhesion and the thermodynamics of transfer ascertains that the polarity of the solute is vital in determining partition into SDS micelles and may prove to extend to many other partitioning systems. It has been noted, for example, that the partitioning behaviour of substituted diazines into a range of different

non-aqueous solvents correlated with the number of hydrogen bonding sites in the substituent, Yamagami *et al.*,(1993)

6.4. CONCLUSIONS.

1. It has been shown partition coefficient normally expressed as log P, correlates well with biological response and hence micelles were used as a suitable partitioning system. There has been little published evidence to suggest that the surface energies of drugs correlate with their log P values hence the Taylor-Aris diffusion technique was utilised to determine the partition coefficients of organic substrates between aqueous and micellar phases of sodium dodecyl sulphate (SDS). This technique proved to be simple, inexpensive to build and operate. Data is highly reproducible and diffusion coefficients could routinely be measured to a precision of ± 2%. Therefore this technique may provide more suitable data than previous methods used involving octan-1-ol / water systems.

2. Good correlations were found between the measured partitioning data and the free energy of adhesion obtained from surface energy data. It was concluded that the ionization of the drug was an important consideration if correlations were to be obtained between surface energy data and measured partition behaviour. It was shown that the partitioning process was strongly influenced by a polar repulsion energy between the monopolar drugs and the monopolar surfactant head group. This work has demonstrated that the novel approach of modelling partition from solid state measurements is practicable, and furthermore that the model provides useful information to assist in the understanding of different partitioning behaviour.

CHAPTER 7

INTER-RELATIONSHIPS

7.1. INTRODUCTION.

The purpose of this chapter is to relate the solubility, dissolution and partitioning data to surface energy parameters, exploring the presence and absence of any links between them. The inter-relationship between wettability, solubility, dissolution and partitioning remains an area of interest with respect to understanding drug absorption. It is generally accepted that both wettability and solubility in aqueous environments are influenced by the polarity of the solid (on the basis that "like dissolves like"). Lippold and Ohm, (1986) and Buckton and Beezer (1989) have shown that even though wettability and solubility can both be related to aspects of the molecular structure of the solid, it does not necessarily follow that they are related to each other.

The role of natural and synthetic surfactants in influencing the dissolution process is a subject of a great many publications *eg* Efentakis *et al.*, (1991), Wells *et al.*, (1992) and Bakatselou *et al.*, (1991). It has been shown that the dissolution of drugs in bile salt surfactants can be dominated by wetting, diffusivity or solubilisation effects (*eg* Naylor *et al.*, (1993) and Ten Hoor *et al.*, (1993).

In this chapter, the wettability, solubility and diffusivity will be considered with respect to the dissolution behaviour of the four sulphonamides studied in water and sodium dodecyl sulphate (SDS) solutions of various concentrations.

7.2. Slower dissolution rates of Sulfamerazine in an aqueous SDS solution than in water.

With respect to the Noyes-Whitney equation, it is quite usual for the dissolution rate to be influenced by solubility (see section 1.6.1.). This equation does not specifically deal with wettability, however this is partially covered by the surface area term, as poorly wetted surfaces will have a lower area of contact than those which are well wetted by the liquid. It would be expected, therefore, that materials with enhanced solubility and improved wettability would show an increase in dissolution rate.

7.2.1. Solubilities.

The normalised solubility of sulfamerazine (*ie* solubility in SDS / solubility in water), is shown in Figure 4.3.8. as a function of SDS concentration. In section 4.3.4. it can be seen that there is an exponential relationship, with the solubility of drug increasing 2.8 fold when the SDS concentration reaches 6.93×10^{-2} mol.dm^{-3}. This equates to a very significant increase in equilibrium solubility in the presence of SDS, and by the Noyes-Whitney equation (Eq. 1.6.1.) this would expect to be mirrored by a similar increase in dissolution rate.

The thermodynamic functions for the transfer between the water and the micelles, calculated from a van't Hoff relationship of measured solubility as a function of temperature are $\Delta H_{sol}^{trans} = -16.1$ kJ.mol^{-1}; $\Delta G_{sol}^{trans} = -3.1$ kJ.mol^{-1}; $\Delta S_{sol}^{trans} = -43.7$ J.mol^{-1}.K^{-1} (these three terms terms being the enthalpy, free energy and entropy of transfer from

the solubility data respectively as in Table 4.3.5.). The negative value for the free energy is indicative of a favoured overall process (*ie* thermodynamically spontaneous). The negative values for enthalpy and entropy change demonstrate that the driving force is enthalpic, this being dominant despite the disfavoured imposition of order.

7.2.2. Rotating disk initial dissolution rate studies (RDIDR).

As a function of SDS concentration.

The RDIDR as a function of SDS concentration (100 rpm and 37°C) in Figure 5.3.8. shows that the rate falls with increasing SDS concentration. A plateau is reached for the higher SDS concentrations, but the onset of this plateau is well above the CMC.

As a function of temperature.

The effect of temperature on RDIDR is shown in the Arrhenius relationship in Figure 7.2.2. where it can be seen that at each temperature, the RDIDR is lower in the presence of SDS than without, but in both cases the rate increases with increasing temperature.

Table 7.2.1. gives data for the thermodynamics of activation, calculated from the temperature dependence of the RDIDR. The data have been selected from Tables 5.3.2., 5.3.3. and 5.3.4. The data in Table 7.2.1. indicates a process with an enthalpic driving force, but a disfavoured entropy of transfer which combine to yield a small positive free energy of transfer. It is clear (from the equilibrium solubility data) that the transfer to the SDS micelle is indeed spontaneous, however, the rate data demonstrate an activation barrier which must be overcome prior to solubilisation.

Figure 7.2.1. Arrhenius relationship showing the effect of temperature on RDIDR of sulfamerazine in water and a SDS solution.

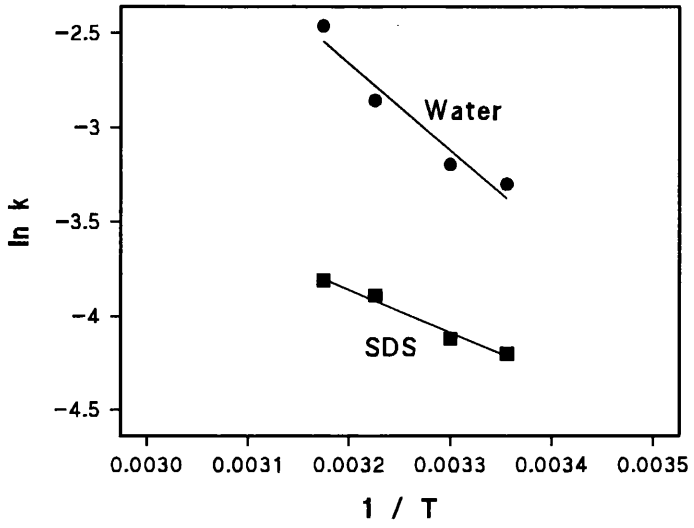

Table 7.2.1. The thermodynamics of activation calculated from the temperature dependence of the RDIDR.

	Water	SDS	Transfer
$\Delta G^{\ddagger}$ (kJ mol^{-1})	96.7	99.6	2.9
$\Delta H^{\ddagger}$ (kJ mol^{-1})	38.3	19.0	-19.2
$\Delta S^{\ddagger}$ (J mol^{-1} K^{-1})	-188.5	-260	-71.5

As a function of stirring speed.

The rate data as a function of stirring rate are given in Table 7.4.1. The RDIDR data, in the presence of SDS, show a reasonable linear correlation (r = 0.994) with an intercept of zero (within experimental error) and a gradient of 6.62×10^{-7}, after converting the rotational speed to radians$^{0.5}$. The data for dissolution in water shows a moderate correlation (r = 0.964) with an intercept at -0.117 on the y-axis and a gradient of 5.9×10^{-6}. For the SDS data it is reasonable to estimate a diffusion coefficient by use of the equation of Levitch (1962):

$$RDIDR = 0.62\ \phi^{0.5}\ D^{2/3}\ \nu^{-1/6} \qquad (7.2.1.)$$

where ϕ = the rotational speed

D = the apparent diffusion coefficient

ν = the kinematic viscosity

If the viscosity to the power of -1/6 is assumed to be approximately unity (which is reasonable given the change that is needed in ν is substantial if it is to seriously alter $\nu^{-1/6}$), then the value of D can be determined as 3.35×10^{-7} cm^2 s^{-1}. This is a low value for D compared to those which have been reported in the literature for other systems, for example, 3.05×10^{-6} and 3.44×10^{-6} for betamethasone in water and 30 mM sodium taurocholate respectively (Bakatselou *et al.*, 1991), 3.01×10^{-6} cm^2 s^{-1} for betamethasone in sodium taurocholate/lecithin mixed micelles (Naylor *et al.*, 1993). However, the value of D for Danazol in a sodium taurocholate/lecithin mixed micelle (Naylor *et al.*, 1993) fell to as low as 2×10^{-8} cm^2 s^{-1}, indicating extremely low diffusivity compared to danazol in

sodium taurocholate micelles which had a value of D similar to that which is reported here. The data in the presence of water do not allow the calculation of an accurate diffusion coefficient, as the intercept is not zero and linearity is comparitively poor, however, as a guide the value of D which would be obtained from the gradient is 8.93 x 10^{-6} cm^2 s^{-1}, which (despite the reservations expressed) shows that the diffusivity is much more rapid for the free than the solubilised drug.

7.2.3. General discussion.

Although it is generally assumed that the influence of solubility of a drug on dissolution will be very significant, it has been shown that the diffusivity may vary to a great extent between the water and the SDS systems. To reconsider the Noyes-Whitney equation in relation to the data for this system, it can be seen (Table 5.3.5.) that at 150 rpm the RDIDR with SDS present is a factor of 4.8 lower than that for water alone (the data at the highest rotational speed were selected so that the diffusion layer thickness term would be minimised). The diffusivity for the drug in SDS was determined as 3.35 x 10^{-7} cm^2 s^{-1} which was a factor of 26 lower than the rough estimate of diffusivity of the drug in water alone. The increase in solubility due to SDS was by a factor of 2.8, thus adding these factors to Equation 7.2.1:

$$(1/4.8)\ dm/dt = [\ (1/26)\ D\ (n)\ A_s / d_h\ ]((2.8)C_s - c) \qquad (7.2.2.)$$

(where n is an unknown factor for changes in A_s and d_h), by balancing these factors, n is equal to a little under 2. This factor can reasonably be explained by changes in contact angle affecting the apparent surface area (*ie* it is possible that only 50% of the compact

made true contact with the water due to the high contact angle, but spreading occurred with high SDS concentrations), together with some uncertainty about the exact changes in magnitude for D. It follows that the reduced dissolution rate of the drug in SDS is in keeping with the changes in the terms of the Noyes-Whitney equation, where in this case the diffusivity has the largest influence. For some reason this drug causes swelling of the micelle whilst others do not.

It remains necessary to consider the ease of access of the drug to the core of the micelle. Here it can be shown that the process of solubilisation is favoured thermodynamically (as indicated by the free energy of adhesion obtained from contact angle / surface energy data estimates, and from the thermodynamics of transfer obtained from van't Hoff analysis of solubility data). There is, however, indication of a disfavoured activation step from the Arrhenius treatment of the rate data.

7.2.4. Implications for dissolution testing.

The use of SDS as an additive to dissolution media is gaining in popularity in order to test poorly soluble drugs. It is generally true that increased solubility will result in increased dissolution rate, however, as shown above this is not always true. This situation is not limited to SDS systems, for example, Macheras and Reppas (1987) have shown slowing dissolution of dicumarol into solutions of proteins in which their solubilities were higher than for an aqueous control. It is, therefore, necessary to consider the data obtained from dissolution tests with great care when complex media are used in the test.

7.3. Relationship between dimensionless solubility and dimensionless initial powder dissolution rate (IPDR).

The results for dimensionless solubility are given in section 4.3.4. and those for dimensionless dissolution rate are given in section 5.3.5. However, by plotting these two dimensionless parameters together, against concentration of SDS solution, it is clearer to see whether wetting or solubilisation plays the more important role in the dissolution of each of the four sulphonamides. See Figures 7.3.1. to 7.3.4.

Figure 7.3.1. Plot of dimensionless IPDR and dimensionless solubility for sulfamerazine against SDS concentration.

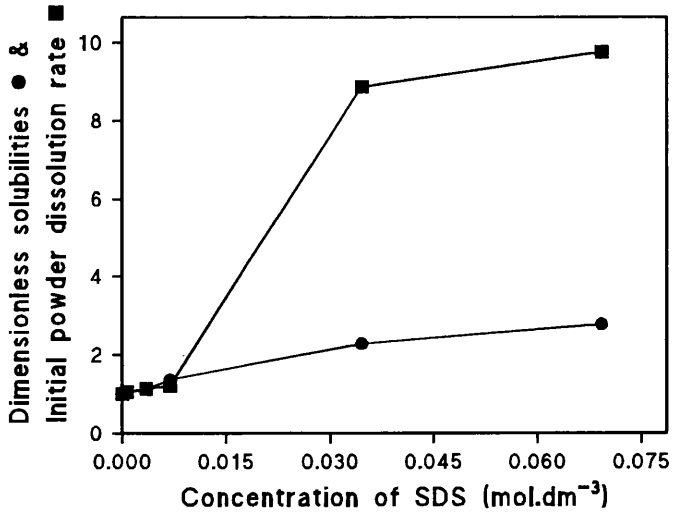

Figure 7.3.2. Plot of dimensionless IPDR and dimensionless solubility for sulfamethazine against SDS concentration.

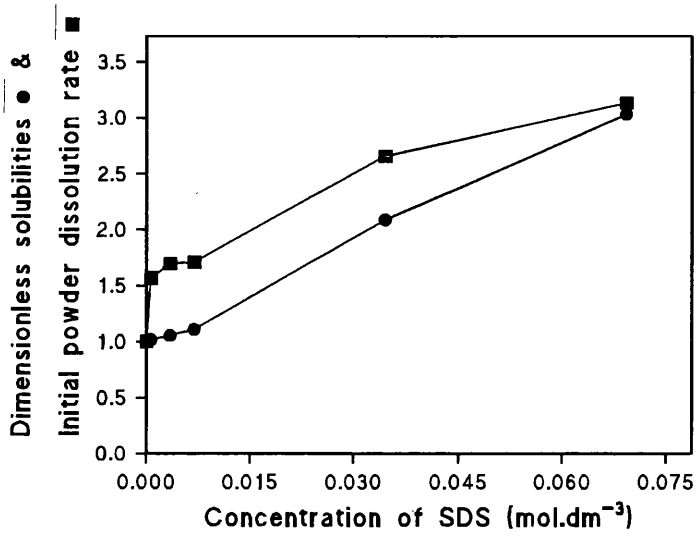

Figure 7.3.3. Plot of dimensionless IPDR and dimensionless solubility for sulfadiazine against SDS concentration.

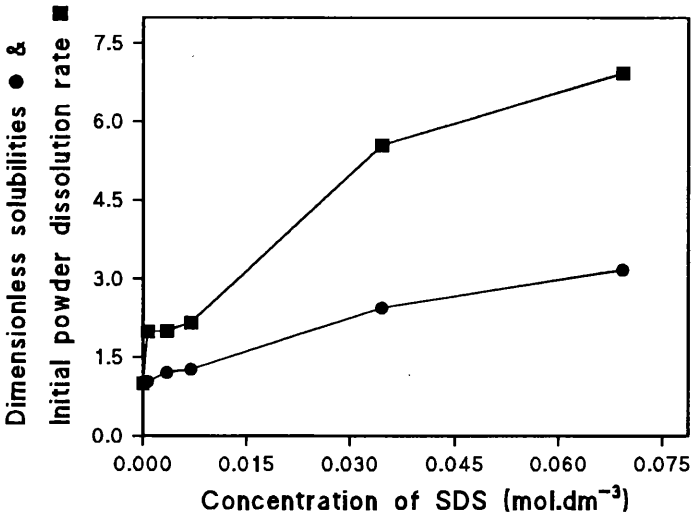

Figure 7.3.4. Plot of dimensionless IPDR and dimensionless solubility for sulfanilamide against SDS concentration.

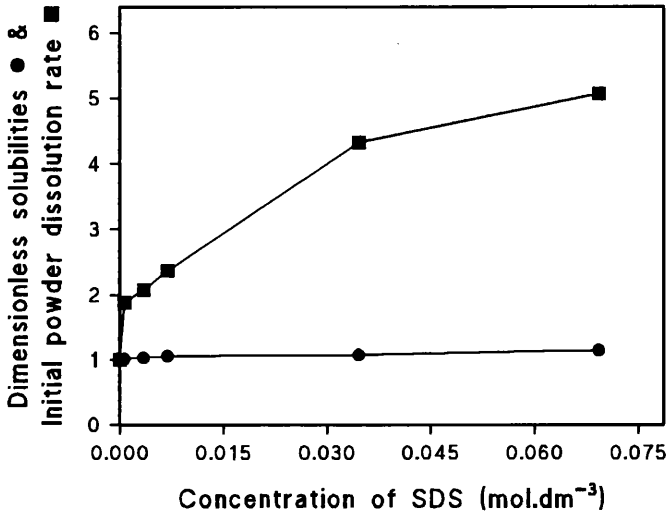

Table 7.3.1. gives contact angle values of the sulphonamides at selected SDS concentrations. It gives the same data as Table 3.3.6/7 in Chapter 3 and has been reproduced here to relate dimensionless solubilities and powder dissolution data to contact angle data *ie* wettability.

Table 7.3.1. Contact angles of the sulphonamides at selected SDS concentrations (in degrees).

SDS Conc. mol.dm^{-3}	sulfamerazine	sulfadiazine	sulfamethazine	sulfanilamide
6.9 x 10^{-4}	64.6	57.0	47.7	37.6
3.46 x 10^{-3}	52.4	49.5	31.8	28.6
6.93 x 10^{-3}	22.5	★	★	★
3.46 x 10^{-2}	★	★	★	★
6.93 x 10^{-2}	★	★	★	★
0.1	★	★	★	★

★ zero contact angle

7.3.1. General discussion.

The dimensionless IPDR and dimensionless solubility against SDS concentration data for sulfamerazine (Figure 7.3.1.) are notably different from the data for the other three sulphonamides (Figures 7.3.2. to 7.3.4.) in that the ratios are superimposed up to the CMC of the SDS, after which the powder dissolution data diverge: this is indicative of changes in wettability having no serious impact on the drug dissolution, but the influence of the micelle is significant. For sulfamerazine the contact angle gradually falls with increasing SDS concentrations (showing improved wettability, with zero contact angle, *ie* spreading, being obtained between 6.93 x 10^{-3} and 3.46 x 10^{-2} mol.dm^{-1}). See Table 7.3.1.

The dimensionless solubilities and powder dissolution data for sulfadiazine (Figure 7.3.2.) and sulfamethazine (Figure 7.3.3.) both show a jump in the dimensionless powder dissolution rate before the CMC of SDS, but a further jump at the CMC for both dimensionless solubility and powder dissolution. These data are indicative of a situation where the dissolution is influenced both by wetting and the presence of micelles. For both sulfadiazine and sulfamerazine the contact angle becomes zero before the CMC is reached, which means that any changes in dissolution for concentrations above 6.93×10^{-2} mol.dm^{-3} SDS are due to factors other than improved wettability.

Sulfanilamide forms the other extreme type of behaviour, whereby the dimensionless solubility is essentially unchanged throughout the range of SDS concentrations (Figure 7.3.4.), showing almost no tendency to solubilisation. The dimensionless powder dissolution rate for sulfanilamide shows continual increases with SDS concentration which implies that it is affected by improved wettability. There is no jump in the dimensionless solubility (Figure 7.3.4.) at the CMC, which fits with the fact that solubilisation is essentially absent for this drug. The contact angle data for sulfanilamide reach zero before the CMC (Table 7.3.1.) so the continued increase in dimensionless powder dissolution with increasing SDS concentration may be attributable to factors other than just wettability and solubilisation, such as improvements in diffusivity (see Table 7.3.2.).

Table 7.3.2. Diffusion coefficients for the sulphonamides in water and SDS, calculated using the equation of Levitch, (1962).

Drug In Medium		Diffusion coefficient ($cm^2.s^{-1}$)
Sulfamerazine	water	8.93×10^{-6}
	SDS	3.35×10^{-7}
Sulfadiazine	water	2.19×10^{-7}
	SDS	3.56×10^{-6}
Sulfanilamide	water	6.60×10^{-5}
	SDS	1.03×10^{-4}
Sulfamethazine	water	2.06×10^{-6}
	SDS	1.67×10^{-5}

It has been shown that there is a disfavoured activation barrier for the dissolution of sulfanilamide in SDS micelles. This is due to the fact that both the SDS head groups and the sulfanilamide are monopolar of the same sense (*ie* γ^-), producing a monopolar repulsion force. The apolar drugs such as sulfamerazine and sulfadiazine have no such repulsion.

7.4. Comparison of wettability, solubility and dissolution in water.

The complete set of data for contact angle, solubility, rotating disk, initial dissolution rate (RDIDR) and powder dissolution rate are presented in Table 7.4.1. This will enable a comparison to be made between the sulphonamides and these properties.

Table 7.4.1. Data shown for the sulphonamides for the values of a number of different parameters in water.

	sulfamerazine	sulfadiazine	sulfamethazine	sulfanilamide
θ	81.7	75.5	63.8	61.6
Solubility ($g.dm^{-3}$)	0.0340	0.0131	0.0667	1.818
RDIDR (% w/v min^{-1})				
50 rpm	2.55×10^{-6}	1.07×10^{-6}	4.79×10^{-6}	1.11×10^{-4}
100 rpm	5.75×10^{-6}	1.48×10^{-6}	6.79×10^{-6}	1.29×10^{-4}
150 rpm	1.27×10^{-5}	1.90×10^{-6}	8.62×10^{-6}	1.50×10^{-4}
IPDR (dimensionless)	4.7019	6.3219	25.95	560.4
$\Delta H^{\ddagger}$ ($kJ.mol^{-1}$)	38.3	47.5	42.2	30.4
$\Delta S^{\ddagger}$ ($J.mol^{-1}.K^{-1}$)	-188.5	-170.1	-175.2	-188.4
$\Delta G^{\ddagger}$ ($kJ.mol^{-1}$)	96.7	100.2	96.4	88.8
ΔH^{s} ($kJ.mol^{-1}$)	31.3	26.5	26.7	28.7

7.4.1. General discussion.

From the structures of the molecules (see Chapter 2), one would expect the ranking (of wettability, solubility and dissolution rate) to follow the order sulfanilamide (best wetting, highest solubility, fastest dissolution), followed by sulfadiazine, sulfamerazine and then sulfamethazine. This is on the basis that this is the ranking in terms of size and hydrophobicity of the added functional groups. From the data in Table 7.4.1. it can be seen that there are different rank orders, but none of the data sets rank as may be expected by looking at the structures.

It can be seen that the contact angle data do not rank in the same order as the equilibrium solubility values, and that the RDIDR data change rank order depending upon the rotating speed (at 50 rpm the ranking is the same as that for solubility, at 150 rpm it changes significantly). One can say little about the powder dissolution data as the effect of particle size will be significant here, however these data do rank in the order of the contact angle results, which may reflect the fact that the most hydrophobic drugs do not allow access to the powder system. This could be a significant difference between the compacts which are forced into the water (with a notional constant surface area) and the powder which can avoid interfacial contact with water by floating and aggregation. It would appear (from these rank orders) that the RDIDR data are influenced by solubility, diffusion coefficient and diffusion layer thickness, but do not seem to rank with wettability.

7.5. Thermodynamics of transfer from dissolution experiments and relationships with the surface energy data.

As discussed in section 5.3.4.1. there is an excellent correlation between the enthalpy of transfer data from dissolution experiments and the surface energy adhesion interactions, when the interaction with the SDS head group is taken as a model for the activation barrier.

This model may be expanded upon by investigating the process further. Whilst other workers have shown relationships between surface energy and dissolution rate (Chow *et al.*, 1994), previous studies have tended to argue a link between "improved wettability" and dissolution. In this study, such a simple link is *absent,* in that the rank order of contact angle values (using water as the liquid) is sulfamerazine (81.7°), sulfadiazine (75.5°), sulfanilamide (61.6°) and sulfamethazine (63.8°). See Table 7.4.1. The correlation is only seen when the components of surface energy are derived and the free energy of interaction between the different phases is considered. This extension to considering the interaction between three materials allows for modelling of competitive interactions, such that there is a strong argument that this work gives a new insight into the mechanism of solubilisation into micellar structures.

The correlations in the thermodynamic data, especially with respect to the change in sign at the same point for the surface energy and dissolution derived data, (see Figure 5.3.1.) present a compelling case for the interaction between the drugs and the SDS head group

being the dominant mechanism in the solubilisation process. The repulsion between the polar sulfanilamide and the SDS head group (as evidenced by the positive free energy of adhesion and positive enthalpy of transfer (Figure 5.3.1.)) may explain the limited solubilisation of this drug, (Table 7.5.1.), whilst the favourable free energy of adhesion and enthalpy of transfer should facilitate solubilisation of the other three sulphonamides. The equilibrium solubilities at 37°C for powdered drug are shown in Table 7.5.1.

Table 7.5.1. The solubility of each drug in water and a solution of 6.93 x 10^{-2} mol.dm^{-3} sodium dodecyl sulphate. Units of g.dm^{-3}.

	sulfamerazine	**sulfadiazine**	**sulfamethazine**	**sulfanilamide**
Water	0.0340	0.0131	0.0667	1.818
SDS	0.0943	0.0417	0.2024	2.076
	(x 2.8)	**(x 3.2)**	**(x 3.0)**	**(x 1.1)**

The number in brackets is the factor showing the increase in solubility in the presence of SDS.

It can be seen that the solubility for sulfamerazine, sulfadiazine and sulfamethazine each increase by a factor of three, whilst the solubility of sulfanilamide (despite the fact that it is already high) increases by a factor of just 1.1.

Micelles are relatively free structures for which there is frequent exchange of surfactant monomers. An important issue is whether solutes do diffuse across the polar region to the hydrophobe in order to reach the micellar core or whether the micelle forms around the drug during dissolution. Furthermore it is important to consider whether the solute is released from the micelle at regular intervals as surfactant monomers exchange with molecules in the micelle. The exchange of dynamic micelles, where surfactant molecules enter and leave does not mean that there has to be free exchange of the solute which is solubilised in the micellar structures. It is known that solubilised solutes are often more chemically stable than solutes in solution, thus it can be assumed that the solute is not regularly in contact with the aqueous phase and that it does stay solubilised even if the surfactant molecules exchange. The use of surface energy data obtained from contact angle studies allows a good understanding of drug interactions with SDS micelles. Assuming that drugs access through intact micellar structures, it can be assumed that the partitioning of the most polar drugs would be restricted by the activation step of passage through the polar head groups, due to the repulsion which exists between the monopolar head group and the monopolar drugs. If, however, the micelle forms around the drug during dissolution it may be argued that the drug is sufficiently close to the SDS head groups for the repulsion forces to be significant.

7.6. Partitioning behaviour in relation to surface energy data.

Direct numerical comparison is not possible between the thermodynamics of transfer obtained from solubility measurements (using a standard state of number of moles of solute dissolved in $1dm^3$ at the temperature of the experiment to define the equilibrium constant), and the Taylor-Aris diffusion data where the standard state refers to a dimensionless ratio of a fraction partitioned between the two phases (see Eq. 6.2.4.) Comparisons must be limited to trends and relationships between the partitioning data and the surface energy based predictions.

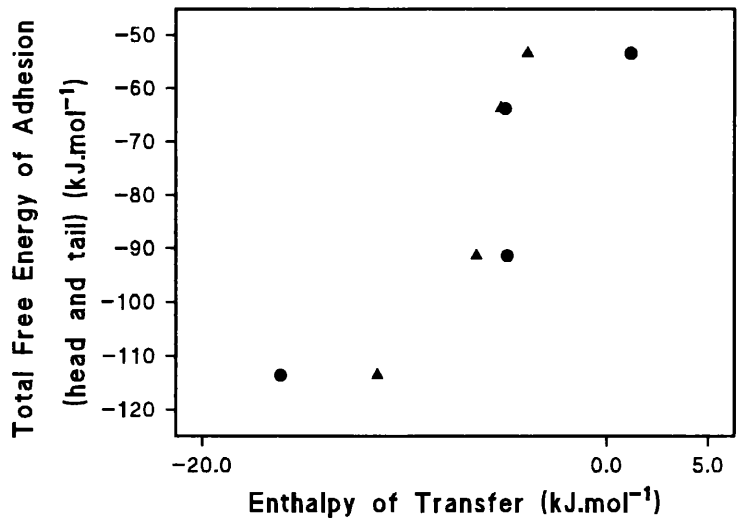

Figure 7.6.1. The relationship between the total free energy of adhesion (head and tail contribution) derived from surface energy data and the enthalpy of transfer into micelles from solubility experiments in water (●) and buffer at pH = pK_a of drug (▲).

It can be seen that there is a poor relationship (r = 0.889) between the total free energy of adhesion derived from surface energy data and the enthalpy of transfer into micelles from solubility experiments in water. The relationship is much better for the buffered solubility experiments (r = 0.945) as can be seen in Figure 7.6.1. There was a good correlation between the surface energy derived data and the enthalpy of transfer into micelles by the Taylor-Aris diffusion technique, also at pH = pK_a of drug (see Figure 6.3.1.). It appears that the diffusivity of the sulphonamides changes when in water to being in a buffered solution and as previously mentioned, the degree of ionisation is important.

The fact that the entropic and enthalpic contributions to the partition process (see Figures 6.3.1. to 6.3.4.) show opposite trends results in a free energy of transfer which does not correlate with the free energy of adhesion from surface energy data.

A comparison of the surface energy data (Table 3.4.1. in Chapter 3), with the relationships seen in Figures 6.3.1., 6.3.2. and 6.3.3. shows that the ranking of the partition behaviour is directly related to the magnitude of the γ^- term. The total surface energies and the Lifshitz-van der Waals contributions to the surface energy are rather similar for each material and are uncorrelated with the thermodynamics of transfer. It follows that it is not the extent of hydrophobicity (γ^{LW} similar in each case) which controls solubilisation to the non-aqueous phase, but rather the extent of hydrophilicity, due to a significant repulsive interaction. This statement is made on the basis that the measured data (from partition experiments) and the calculated free energy of adhesion between the drugs and the micelle

in the presence of water both show this ranking in relation to the value of γ^-, despite the fact that the hydrophobic core of the micelle is itself nonpolar. The polarity of the solute is vital in determining partition into SDS micelles.

7.7. Future work.

There are many areas still left uncovered, regarding this work, mainly due to lack of time. Further work to be carried out, which may be of interest is;

1. performing the dissolution work in buffer and buffer / SDS solutions as these solutions were used in the partitioning work and good correlations obtained.

2. the use of the acid/base theory can be applied to other drugs to see if similar relationships hold regarding enthalpy of transfer, enthalpy of activation and partitioning.

3. Other surfactants can be used in place of the SDS. Also liposomes may be utilised as a closer representation of biological membranes.

CHAPTER 8

WORK ON ANOTHER DRUG:

L-365-260

8.1. INTRODUCTION.

Work in previous chapters has been carried out on a series of related drugs *ie* the sulphonamides and relationships have been explored. However, it was necessary to find out if the correlations obtained, extended further to other types of drugs. One particular drug selected was L-365-260, a compound developed by M.S.D. which has the formula $C_{24}H_{22}N_4O_2$. The structure of this drug can be seen in Figure 8.1.1. This drug is also poorly soluble, as are the sulphonamides. See Table 8.1.1. for solubility data available from M.S.D. on this drug.

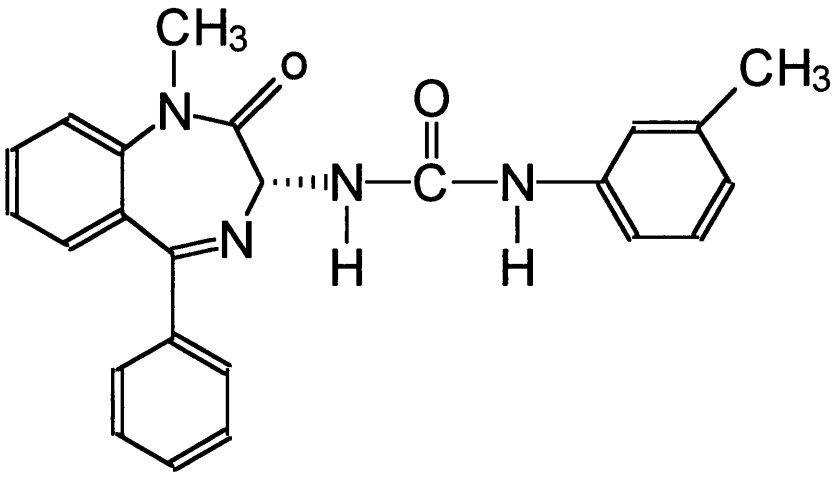

Figure 8.1.1. The structure of L-365-260.

Table 8.1.1. Solubility data in various solvents for L-365-260.

Solvent	Solubility
water	≤ 0.0001 mg/ml
ethanol	11 mg/ml
methanol	10 mg/ml
DMF	≥150 mg/ml
PEG 400	22 mg/ml

This drug is a clean, white crystalline powder, present as anisotropic, irregular needles. It melts in the range 162 - 167°C and has a molecular weight of 398.5.

This drug, L-365-260, was selected by M.S.D. on which to carry out some absorption studies (see Appendix). Therefore it seemed necessary to carry out some preliminary tests on this drug to obtain a better understanding of its behaviour and also to see if it showed similar trends to the sulphonamides.

8.2. METHODS.

Basically all the different methods carried out are the same as those performed in previous chapters for the sulphonamides. However, due to a lack of time, only a few tests were selected and will be discussed further.

8.2.1. λ_{max} value and calibration curve.

The maximum absorbance value for L-365-260 was obtained as described previously in section 4.2.1. The value was then used in further analytical work. The calibration curve for this drug was constructed in the same manner as described in section 4.2.2. from which an equation of best fit was found.

8.2.2. Contact angle measurement.

See Chapter 3 for details on how this was carried out. Regarding the powder plate preparation for L-365-260, it was necessary to use a lower compaction force than with the sulphonamides because lamination of the powder plates occurred at higher compression forces. See Table 8.2.1. for compaction pressure and dwell time used.

Table 8.2.1. The compaction pressure and dwell time employed for L-365-260 powder.

Material	Compaction force ($kNm^{-2} \times 10^5$)	Dwell time (mins)
L-365-260	2	1

The compaction force and dwell time ensured the smoothest surface possible for the powder compacts.

8.2.2.1. Assessment of surface energy.

In order to determine the surface energy parameters of the L-365-260, contact angle measurements were carried on powder compacts of the drug, using various probe liquids. The liquids used were water, formamide, bromonaphthalene and di-iodomethane.

8.2.2.2. Contact angle measurement in solutions of various SDS concentration.

Again, the method for this can be found in section 3.3.3. whereby powder compacts of the drug substance were used. The various concentrations of the SDS employed were 6.9 x 10^{-4}, 3.46 x 10^{-3}, 6.93 x 10^{-3}, 3.46 x 10^{-2}, 6.93 x 10^{-2} and 0.1 mol.dm^{-3}. This gives information about the wetting properties of the L-365-260.

8.2.3. Solubility studies.

8.2.3.1. Equilibrium solubilities.

As described in section 4.2.3.1. the solubility of this drug was obtained in:

i) water and

ii) 0.1M SDS solution.

This was carried out at temperatures of 25, 30, 37 and 42°C. However, as in section 4.2.3.1. these experiments were not carried out in buffered solutions.

8.2.3.2. Dimensionless solubilities.

Details of this method are descibed in section 4.2.4. where the solubility of L-365-260 was determined in solutions of SDS below and above its CMC. This was carried out at one temperature of 37°C. The concentrations of the SDS solutions were 0, 6.9×10^{-4}, 3.46×10^{-3}, 6.93×10^{-3}, 3.46×10^{-2}, 6.93×10^{-2} and 0.1 $mol.dm^{-3}$.

8.2.4. Initial powder dissolution rates.

The experimental procedure is as described in section 5.2.5. In each case, 100mg of powdered drug was added to 400ml of dissolution media at 37°C. The dissolution media used were water, 6.9×10^{-4}, 3.46×10^{-3}, 6.93×10^{-3}, 3.46×10^{-2}, 6.93×10^{-2} and 0.1 $mol.dm^{-3}$ solutions of SDS.

These experiments were performed to identify whether wettability or solubilisation had the greatest effect on the dissolution of L-365-260.

8.3. RESULTS AND DISCUSSION.

8.3.1. λ_{max} value and calibration curve obtained.

From the UV scan carried out on a standard solution of L-365-260, the λ_{max} was found to be 232 nm. This λ_{max} value remained unchanged for a UV scan on a micellar solution of L-365-260, thus the addition of the surfactant did not cause a shift in the λ_{max} value. Figure 8.3.1. shows the calibration curve constructed for this drug from the standard solutions prepared.

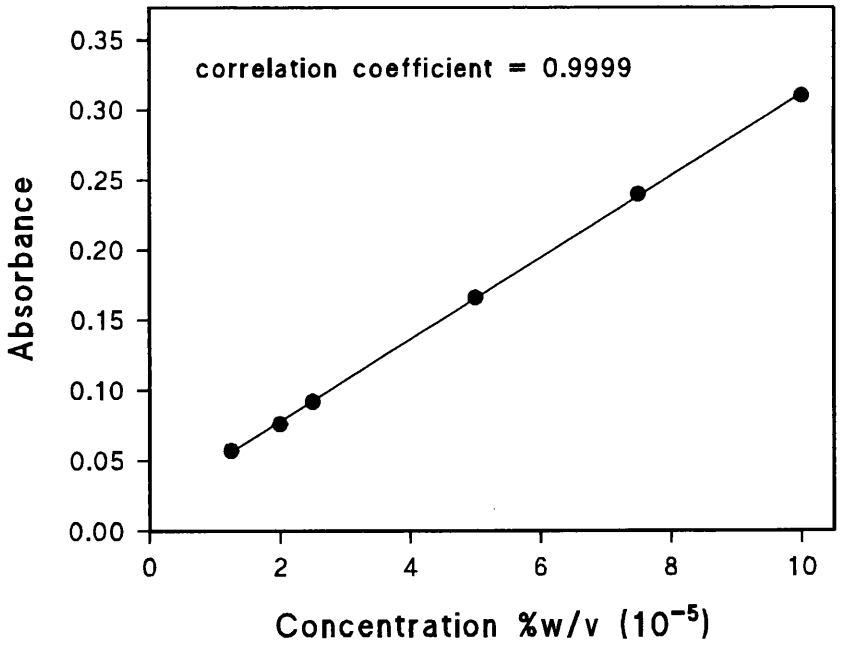

Figure 8.3.1. Calibration curve for L-365-260.

The equation of best fit for this calibration curve is:

$$y = 0.029186x + 0.019414$$

with a correlation coefficient of 0.9999.

8.3.2. Contact angle data.

8.3.2.1. Data for surface energy analysis.

As with the sulphonamides, the advancing contact angle data was utilised and the results can be seen in Table 8.3.1.

Table 8.3.1. Advancing contact angle data for L-365-260 against water and formamide ± the standard deviation. Values are means ± the standard deviation.

θ (water)	cos θ (water)	θ (formamide)	cos θ (formamide)
71.67 ± 2.55	0.314 ± 0.042	48.3 ± 2.46	0.665 ± 0.032

One of the aims of this study was to obtain contact angle data measurements using three liquids; two of which must be polar and one non-polar. However, with the L-365-260, it was only possible to acquire data with two polar liquids *ie* water and formamide. Both non-polar liquids (di-iodomethane and bromonaphthalene) gave a cos θ of 1, indicating that they perfectly wetted the L-365-260 powder. There are other non-polar liquids

available (*eg* the alkanes), however, they all have a lower surface tension than di-iodomethane and bromonaphthalene. Therefore, these liquids would also spread over the powder surface, giving a cos θ of 1. This illustrates the difficulty of selecting a suitable probe liquid when attempting to obtain contact angle data for a broad range of materials.

8.3.2.2. Data against solutions of various SDS concentrations.

Table 8.3.2. Advancing contact angle data for L-365-260 against solutions of various SDS concentrations in water ± the standard deviation. Values are means ± the standard deviation.

Concentration of SDS ($mol.dm^{-3}$)	θ	cos θ
6.9×10^{-4}	71.67 ± 0.897	0.314 ± 0.015
3.46×10^{-3}	62.41 ± 1.043	0.463 ± 0.016
6.93×10^{-3}	★	★
3.46×10^{-2}	★	★
6.93×10^{-2}	★	★
0.1	★	★

★ zero contact angle

From the data in Table 8.3.2. it can be seen that solutions of 6.93×10^{-3} $mol.dm^{-3}$ SDS and higher were all found to spread (*ie* had zero contact angle) on the drug. This indicates that the drug seems to be fairly well wetted by the surfactant solutions.

8.3.3. Solubility data.

8.3.3.1. Data for equilibrium solubilities.

Table 8.3.3. Solubility of L-365-260 in water and 0.1M SDS solution ($mol.dm^{-3}$) at four different temperatures. Values are means ± the standard deviation.

Medium	Temperature (°C)			
	25	30	37	42
Water	1.019×10^{-3} ± 1.9×10^{-5}	1.124×10^{-3} ± 2.1×10^{-5}	1.225×10^{-3} ± 1.1×10^{-5}	1.335×10^{-3} ± 8×10^{-5}
0.1M SDS	6.130×10^{-3} ± 5.3×10^{-5}	6.216×10^{-3} ± 6.1×10^{-5}	6.299×10^{-3} ± 4.2×10^{-5}	6.499×10^{-3} ± 4.8×10^{-5}

See Figures 8.3.2. and 8.3.3. for the solubility for L-365-260 in water and 0.1M SDS solution respectively.

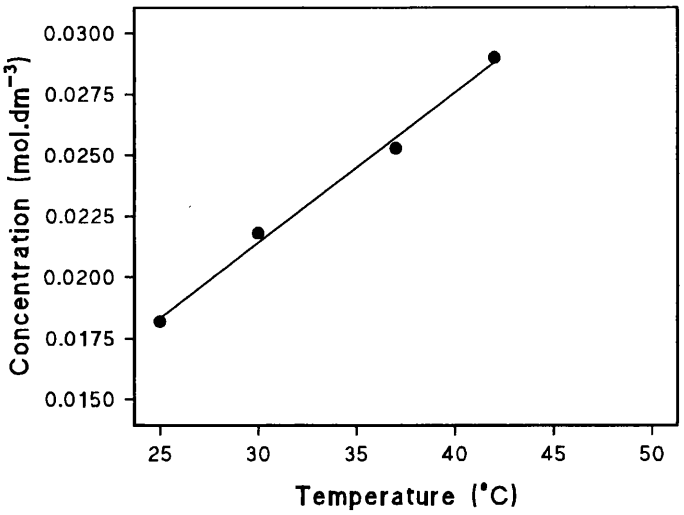

Figure 8.3.2. Solubility of L-365-260 in water (mol.dm^{-3}) at four different temperatures.

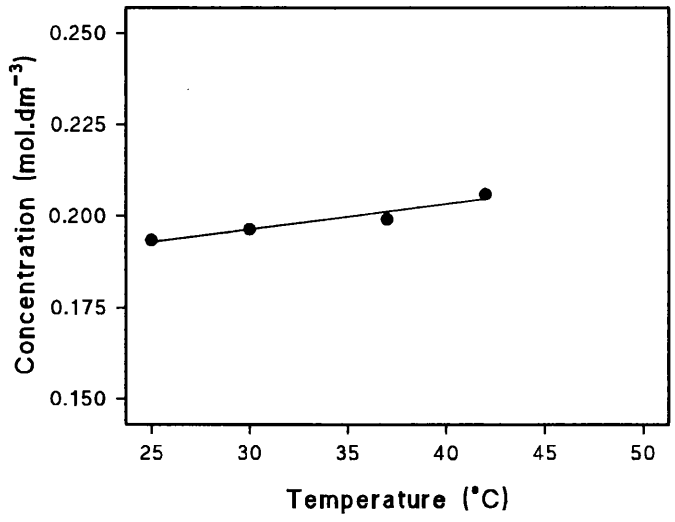

Figure 8.3.3. Solubility of L-365-260 in 0.1M SDS solution (mol.dm^{-3}) at four different temperatures.

From Figures 8.3.2. and 8.3.3. it can be seen that with increasing temperature the solubility of L-365-260 also increased. There is a great improvement in solubility in the micellar solutions thus indicating that this drug is affected by wetting and/or solubilisation.

8.3.3.2. Dimensionless solubilities.

Table 8.3.4. Dimensionless solubilities of L-365-260 in various solutions of SDS concentrations at 37°C.

Concentration of SDS ($mol.dm^{-3}$)	Dimensionless solubility
6.9×10^{-4}	1.0136
3.46×10^{-4}	1.0647
6.93×10^{-3}	3.0144
3.46×10^{-2}	6.8630
6.93×10^{-2}	7.6967

See Figure 8.3.4. for plot of dimensionless solubility against surfactant concentration.

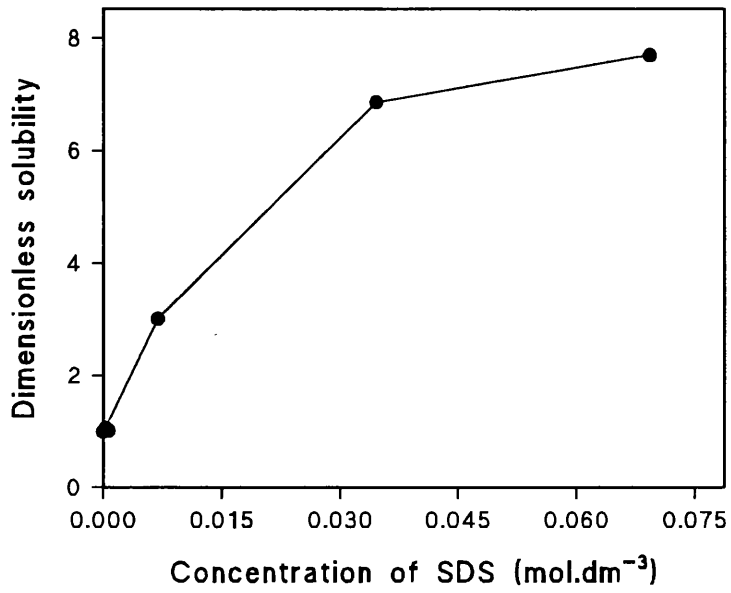

Figure 8.3.4. Plot of dimensionless solubility against surfactant concentration for L-365-260.

This data is discussed later in the chapter alongside dissolution data.

8.3.4. Initial powder dissolution rates.

Table 8.3.5. shows the normalised values of initial powder dissolution rate of L-365-260. The values have been normalised (*ie* IPDR in SDS / IPDR in water) to correct for differences in particle shape and size so that comparisons can be made between this drug and the sulphonamides.

Table 8.3.5. Normalised initial powder dissolution rates (IPDR) in varying solutions of SDS concentrations for L-365-260 at 37°C and 100 rpm.

Concentration of SDS ($mol.dm^{-3}$)	Normalised IPDR
6.9×10^{-4}	6.5766
3.46×10^{-3}	21.375
6.93×10^{-3}	119.02
3.46×10^{-2}	1346.3
6.93×10^{-2}	1357.8

To determine how important the roles of wetting and solubilisation are to the dissolution of L-365-260, the normalised IPDR data has been plotted against the dimensionless solubilities of this drug and can be seen in Figure 8.3.5.

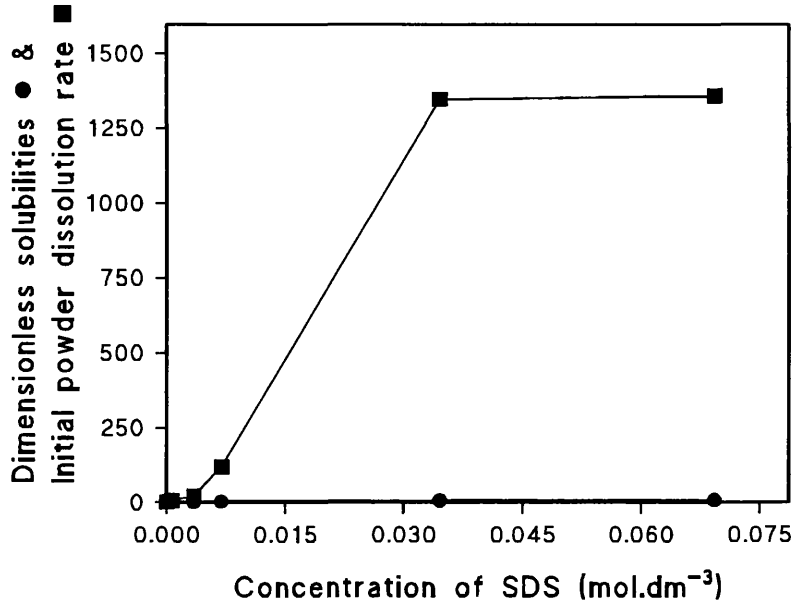

Figure 8.3.5. Plot of dimensionless IPDR and dimensionless solubility for L-365-260 against SDS concentration.

8.3.5. General discussion.

With the L-365-260, the dimensionless solubility shows little variation throughout the range of SDS concentrations, which, indicates that there is almost no tendency to solubilisation. As the SDS concentration increases, the dimensionless powder dissolution rate for L-365-260 also increases, suggesting improved wettability.

At the CMC there is no immediate rise in the dimensionless solubility and this again confirms that solubilisation is extremely limited for this drug. However, from Table 8.3.2.

it is noted that with increasing SDS concentration, the contact angle of L-365-260 falls quickly to zero showing improved wetting. Therefore the wetting process plays an important role in the dissolution of L-365-260.

An animal study on the bioavailability of L-365-260 was undertaken at M.S.D. (see Appendix). The levels of SDS used in the bio-study were both sub CMC in order to overcome complications due to uncertain levels of dilution when the product reached the stomach of the dog. In retrospect, having obtained the data described in this chapter, it is not surprising that two sub CMC concentrations yielded identical bioavailability as the major changes in drug dissolution and solubility are seen above CMC.

8.4. CONCLUSIONS.

1. Due to the fact that contact angle data for L-365-260 could only be obtained for two polar liquids, as the non-polar liquids perfectly wetted the powder (*ie* cos $\theta = 1$), the surface energy parameters of this drug were not able to be assessed in the same way as the sulphonamides. Therefore the free energy of adhesion between this drug and the SDS head and tail groups was not calculated from the equation by van Oss and Costanzo (1992). This meant that no direct comparison could be made between the L-365-260 and the sulphonamides.

2. The solubility of L-365-260 was found to improve with increasing concentrations of SDS, as did the initial powder dissolution rate. However, the wetting appears to play a more important role in the dissolution of L-365-260 than the solubilisation effect.

3. The work carried out on L-365-260 allows a basic understanding of this drug's behaviour in water and micellar solutions. Therefore we have more knowledge of this drug when considering its absorption behaviour which is discussed in the Appendix.

CHAPTER 9

CONCLUSIONS

9.1. CONCLUSIONS.

The conclusions are divided into two different areas;

1. Consideration of each of the techniques for the assessment of the surface properties of pharmaceutical powders, investigated in this study,
    a. Contact angle measurement, using the Wilhelmy plate technique and also the calculation of surface energies from contact angles,
    b. Solubilities of the powdered drugs in water and micellar solutions,
    c. Dissolution properties under various conditions,
    d. Partitioning behaviour in solutions buffered to the pK_a of the drug, with and without micelles.
2. Overall conclusions, addressing the relationships between the above methods and how they affect interfacial interactions.

9.1.1. Contact angle measurement and calculation of surface energies.

It has been shown that the reproducibility of contact angle data obtained for these pharmaceutical powders, was rather better than data published previously using a non automated Wilhelmy plate method. Presumably, this is because the automated technique is less operator dependent.

The critical micelle concentration of sodium dodecyl sulphate (obtained using the Wilhelmy plate technique again), was found to vary with temperature *ie* an increase in temperature led to an increase in the CMC of SDS. However, pH seemed to have little effect on the CMC of SDS over the range studied.

The van Oss acid/base theory has been used to model interfacial interactions and has been shown to be a more appropriate theory than previous ones, which do not split the polar component into electron donor and electron receptor parameters.

9.1.2. Solubilities of the powdered drugs in water and micellar solutions.

The solubility of each of the sulphonamides was found to be an important factor, which also governs many other processes. The solubility studies carried out under various conditions showed that the incorporation of the surfactant, sodium dodecyl sulphate, increased the solubility in each case in water and in buffered solutions. However, use of buffers can also present difficulties in terms of ionic strength. Solubility improved for each drug following an increase in temperature. This was also found to be the case with increased surfactant concentration, particularly above CMC levels, indicating a solubilisation process.

A relationship exists between the enthalpy of transfer between water and micelles (from solubility experiments) and the free energy of adhesion between head and tail groups of SDS. This indicates that the surface energy approach gives a good prediction of the interaction between drugs and micellar structures.

9.1.3. Dissolution properties under various conditions.

From dissolution experiments carried out under various conditions, it was possible to determine which factors (*eg* temperature, stirring speed and medium concentration) were most influential on the dissolution rates of the poorly soluble drugs studied.

Generally, an increased solubility will result in an increased dissolution rate. However, with this particular series of drugs, it was found that one of the drugs, sulfamerazine, had a reduced dissolution rate in SDS than in water, although solubilities were found to be higher in the surfactant solution than in an aqueous control. This was due to a reduced diffusion rate of the swollen micelle.

The use of surface energy data from contact angle studies allowed a good understanding of drug solubilisation behaviour into SDS micelles. It could be seen that the solubilisation of the most polar drugs was restricted by the repulsive interaction with the polar head groups, due to the repulsion which exists between the monopolar head group and the monopolar drugs.

9.1.4. Partitioning behaviour in solutions buffered to the pK_a of the drug, with and without micelles.

As partition coefficient, normally expressed as log P, has been shown in the past (Leo and Hansch, 1971), to correlate well with biological response, micelles were used in this study as a suitable partitioning system. A Taylor-Aris diffusion technique was utilised to determine the partition coefficients of organic substrates between aqueous and micellar phases of sodium dodecyl sulphate.

Good correlations were found between the measured partitioning data and the free energy of adhesion obtained from surface energy data. It was concluded that the drug's ionization was an important consideration when correlating surface energy data and measured

partition behaviour. It was shown that the partitioning process was strongly influenced by a polar repulsion energy between the monopolar drugs and the monopolar surfactant head group.

9.1.5. Overall conclusions.

The physical characteristics of the interaction between some drugs and sodium dodecyl sulphate have been investigated. Each method probes different aspects of the behaviour of the powders.

Contact angles offer a relatively fast and simple method of probing the surfaces of pharmaceutical powders during reformulation studies. It was shown that the solubilisation of the sulphonamides was closely linked to the surface energy values obtained from the contact angle experiments. The discovery of the importance of the monopolar repulsion between the drug and the SDS head group as a dominant factor in solubilisation is, I believe, novel. The use of the surface energy data to give the free energy of adhesion between drugs and SDS (head and tails) in the presence of water has given a valuable insight into the mechanisms of solubilisation and partitioning. This application may be developed in future studies on other drugs, other surfactants or even biological membranes.

The dominant process for the dissolution of the four sulphonamides was seen to vary, with some being heavily influenced by wettability (sulfanilamide and sulfamethazine), one by the extent of solubilisation (sulfadiazine) and another by the rate of diffusion of the

swollen micelle from the dissolution surface (sulfamerazine). There is no obvious link between the structure of the molecules and their dominant mechanism of dissolution, thus there may be advantages in considering molecular modelling and / or NMR studies of the drug surfactant interaction, to further understand the positioning of the drugs in the micelles.

APPENDIX

Exploratory Study of Bioavailability Following a Single Oral Administration of L-365-260 to Female Dogs.

TT # 94-69-13

SUMMARY

An exploratory study was conducted in female dogs to assess the bioavailability after a single oral administration of three different formulations of L-365-260. The L-365-260 in 0.5% methylcellulose (formulation A) was used as reference, in comparison with L-365-260 in 0.5% methylcellulose + sodium lauryl sulphate (SLS) at 0.02% (formulation B) and L-365-260 in 0.5% methylcellulose + 0.2% SLS (formulation C) to improve the bioavailability by addition of a detergent (SLS).

A total of six beagle dogs, 12-14 months old and weighing 9.1-11.9 kg, at experimental start, were housed in individual stainless steel cages in an environmentally controlled room with a 12-hour light cycle. Approximately 350 grams of UAR 125 Cl Certified Lab Chow in pelletized form was usually provided once daily. The food was withdrawn overnight prior dosing and provided 6 hours after drug administration. Drinking water was available ad libitum. Three groups of 2 female dogs were given 5 mg/kg of L-365-260 suspended in three different formulations A, B and C, three times, in a cross-over design such that each group received each formulation once. An interval of one week between each administration was selected to ensure elimination of the drug at a dosing volume of 5 ml/kg. A factor of 1.0 was used for L-365-260 dose calculation. There were no control animals.

The animals were observed on the dosing day for mortality and clinical signs of drug effect. Body weights were measured prior to each dosing day. Bleeding were conducted on Drug Days 1, 8 and 15 at 0, 0.5, 1, 2, 3, 4, 6 and 8 hours at each administration for drug level analysis from all animals.

There were no deaths during the study.

There were no drug-related clinical signs and no drug-related body weight changes.

Mean C_{max} values for formulations A, B and C were 0.38, 0.25 and 0.35 μg/ml, respectively. The corresponding T_{max} values were 0.6, 0.7 and 0.8 h.

Plasma drug half-lives for formulation A, B and C were 1.7, 1.8 and 1.6 h, respectively.

The $AUC_{(0 - 8 h)}$ values for formulation A, B and C were 0.96, 0.67 and 0.92 μg.h/ml respectively. The systemic exposure of L-365-260 following administration of formulation B was generally lower than that from formulation A. Similar systemic exposures were obtained with formulations A and C. The addition of SLS at concentrations of 0.02% and 0.2% therefore did not increase bioavailability of L-365-260.

TABLE OF CONTENTS

L-365-260

Exploratory Study of Bioavailability Following a Single Oral Administration to Female Dogs

TT # 94-69-13

Section A. Antemortem Report

Objective of the study:

Assessment of the bioavailability of L-365-260 in female dogs after a single oral administration of three different formulations.

Period during which study was conducted:

Study initiation date: March 21, 1994.

Experimental start date: March 22, 1994.

Study termination date: April 5, 1994.

Experimental termination date: July 21, 1994.

A. Antemortem Report:

1. Methods:

a) Test system:

1) Species:

- Beagle dogs, six females.

2) Age at experimental start:

- approximately 12-14 months old.

3) Weight at experimental start:

- Females: 9.1 to 11.9 kg.

4) Source:

- Marshall Farms, North Rose, NY.

5) Identification method:

- tattoos.

6) Assignment to dosage groups:

- dogs were assigned to dosage groups without prior knowledge of treatment regimen.

b) Environmental conditions:

1) Housing:

- dogs were housed in individual stainless steel pens, in an environmentally controlled room with a 12-hour light cycle.

2) Diet:

- approximately 350g of UAR A04C Certified Dogs Chow in pelletized form was provided once daily. Animals were fed once daily, and food withdrawn overnight before dosing and provided 6 hours after dosing on dosing days.

c) Drug administration:

1) Compound Identification:

- L-365-260, batch number 017, was used throughout the study. The purity was of 98.0 per cent.

2) Vehicle:

Methylcellulose, Methocel® A4C premium, batch MM91032602A, from Colorcon, Bougival, France.

Sodium Lauryl Sulphate, batch DN93003, from Devlab, Hoddesdon, U.K.

3) Drug Preparation and Assay Sampling:

Formulation A: L-365-260 in 0.5% methylcellulose:

The appropriate amount of L-365-260 (factor = 1.0) was pulverized by mortar and pestle before suspending in 0.5% methylcellulose. The suspension was then sonicated for two minutes and stirred until the administration. The concentration of the suspension was 1 mg/ml in order to administer the desired dosage at a dosing volume of 5 ml/kg. The particle size was 2.5 - 5 μm when measured by microscopy.

Formulation B: L-365-260 in 0.5% methylcellulose + 0.02% SLS (Sodium Lauryl Sulphate) below its critical micelle concentration (CMC):

The appropriate amount of L-365-260 was ground by mortar and pestle before suspending in 0.5% methylcellulose + 0.02% SLS (previously added in methylcellulose). The suspension was then sonicated for two minutes and stirred until the dministration. The concentration of the suspension was 1 mg/ml in order to administer the desired dosage at a dosing volume of 5 ml/kg. The particle size was 2.5 - 5 μm when measured by microscopy.

Formulation C: L-365-260 in 0.5% methylcellulose + 0.2% SLS; near its CMC:

The appropriate amount of L-365-260 was ground by mortar and pestle before suspending in 0.5% methylcellulose + 0.2% SLS (previously added in methylcellulose). The suspension was then sonicated for two minutes and stirred until the administration. The concentration of the suspension was 1 mg/ml to

administer the desired dosage at a dosing volume of 5 ml/kg. The particle size was 10 - 12 μm in Week 1, 7 - 12 μm in Week 2 and 2.5 - 5 μm in Week 3.

4) Treatment groups:

L-365-260 at 5mg/kg in formulation A, B or C was used in 3 groups of two females in a cross-over design as follows:

	DW1	DW2	DW3
group 1	A	B	C
group 2	B	C	A
group 3	C	A	B

5) Route of administration:

Oral, by gavage using a rubber catheter.

6) Dosing volume:

5ml/kg.

7) Frequency of dosing:

Once daily.

8) Total number of doses received:

One single dose in 3 repetitive periods. An interval of one week between each administration was selected to ensure elimination of the drug.

d) Physical examination:

Dogs were observed on the dosing day for mortality and for clinical signs of drug effect.

e) Body weights:

Dogs were weighed prior each dosing day of the study.

f) Biochemical toxicology (See Section B. Bioanalytical Report):

Blood samples were taken for drug level analysis from all animals, on drug days 1, 8 and 15, at 0, 0.5, 1, 2, 3, 4, 6 and 8 hours after each administration. The blood samples were collected in heparinized tubes and centrifuged at about 4°C and the plasma separated and stored at approximately -20°C until they were assayed for their drug content.

2. RESULTS (Table A.A.1.):

a Clinical Signs:

There were no drug-related clinical signs.

b Mortality:

There were no deaths during the study.

c Body Weights

There were no drug-related changes.

3. CONCLUSION:

The oral administration of the L-365-260 at 5 mg/kg in three different formulations produced no clinical signs and no change in body weight gain.

Table A.A.1. Individual body weight (kg) for females before and after a single oral administration of L-365-260.

Treatment group & animal number	Pretest peroid	Drug day		Total weight change*
		8	15	
GROUP 1**				
93-0275F	10.3	10.2	10.2	-0.1
93-0277F	10.6	10.5	10.5	-0.1
GROUP 2**				
93-0279F	9.8	10.1	10.2	0.4
93-0281F	9.1	9.5	9.3	0.2
GROUP 3**				
93-0139F	9.5	9.8	9.7	0.2
93-0283F	11.9	11.8	11.7	-0.2

* Difference in body weight (kg) between pretest period and weight obtained on drug day 15.
** Received successively each formulation (A), (B) or (C).

L-365-260

Exploratory Study of Bioavailability Following a Single Oral Administration to Female Dogs.

TT # 94-69-13

Section B. Bioanalytical Report

Objective of the Study:

Assessment of the bioavailability of L-365-260 in female dogs after a single oral administration of three different formulations

Period during which the study was conducted:

Study Initiation Date: March 21, 1994.

Experimental Start Date: March 22, 1994.

Study Termination Date: April 5, 1994.

Experimental Termination Date: July 21, 1994.

B. Bioanalytical Report

1. METHODS:

a) Antemortem Methods:

The methods used during the antemortem phase of the study are reported in Section A (Antemortem Report).

b) Dosing and Blood Sampling:

Six female beagle dogs were given , on three different occasions, single oral doses of 5 mg/ml of L-365-260 in either (A) 0.5% methylcellulose, (B) 0.5% methylcellulose +

0.02% SLS (Sodium Lauryl Sulphate), or (C) 0.5% methylcellulose + 0.2% SLS. Formulation A served as a reference, formulation B was a suspension with SLS below its critical micelle concentration (CMC), and formulation C was a suspension with SLS near its CMC. The animals were fasted overnight and given food after blood sampling at 6 hours.

The study was a cross-over design such that each formulation was given to two of the animals on three occasions. An interval of one week between each administration was selected to ensure elimination of the drug.

In Drug Week 1 (Day 1), Week 2 (Day 8), Week 3 (Day 15) all drug-treated animals had blood sampled at 0. 0.5, 1, 2, 3, 4, 6 and 8 hours after each administration. The blood samples were collected in heparinized tubes and centrifuged at about 4°C and the plasma separated and stored at approximately -20°C until they were assayed for their drug content.

c) Dosage Form Preparation:

150 ml each of the following solutions were prepared:

Formulation (A): 1 mg/ml of L-365-260 (factor 1.0) in 0.5% methylcellulose (Methocel A4C).

A previously prepared 0.5% methylcellulose solution was added dropwise to 150mg of L-365-260, mixing continually with the aid of a pestle and mortar. The volume was then made up to 150ml and sonicated for 2 minutes. The particle size was 2.5 - 5 μm when measured by microscopy.

Formulation (B): 1mg/ml of L-365-260 in 0.5% methylcellulose + 0.02% SLS.

50mg of SLS was dissolved in 250ml of a previously prepared 0.5% methylcellulose solution. This vehicle was then added dropwise to 150mg of L-365-260, mixing continually with the aid of a pestle and mortar. The volume was then made up to 150ml and sonicated for 2 minutes. The particle size was 2.5 - 5 μm when measured by microscopy.

Formulation (C): 1mg/ml of L-365-260 in 0.5% methylcellulose + 0.2% SLS.

500mg of SLS was dissolved in 250ml of a previously prepared 0.5% methylcellulose solution. This vehicle was then added dropwise to 150mg of L-365-260, mixing continually with the aid of a pestle and mortar. The solution was then made up to 150ml and sonicated for 2 minutes. The particle size was 10 - 12 μm in Week 1, 7 - 12 μm in Week 2 and 2.5 - 5 μm in Week 3 .

d) Bioanalytical Method:

L-365-260 was assayed in the plasma of dogs using a modification of SABAM-25. The method involves the addition of a constant known quantity of the internal standard (MK-0329) to the sample, followed by extraction of the compounds into methyl-t-butyl ether under basic conditions. The organic phase was evaporated and the residue was dissolved in the mobile phase. An isocratic reversed-phase HPLC method was used to elute the compounds and the detection was made using UV detection at 239nm.

The limit of quantification was 10 ηg/ml in the sample. Known amounts (10 - 1000 ηg) of L-365-260 were added to 1 ml of plasma untreated animals and carried through the procedure to validate the assay. The recovery of L-365-260 from dog plasma was 102.2

± 2.1 % (n = 6). Quantification of L-365-260 in samples was determined using the equations generated from a linear regression analysis of the standard curves, using the Nelson Analytical System. A standard curve was constructed for each analytical run.

e) Pharmacokinetic parameters:

The area under the curve (AUC) of plasma concentration versus time was calculated by the trapezoidal rule using the L-365-260 concentrations fron 0 to 8 hours, post-dating. The half-life of elimination of L-365-260 from plasma was calculated from regression analysis of the log concentration vs. time plot.

2. RESULTS

(Tables A.B.1. to A.B.4. and Figures A.1. to A.7.):

Table A.B.1. contains the pharmacokinetic parameters obtained with the different formulations. Tables A.B.2. to A.B.4. summarize the concentrations of L-365-260 found in the plasma of the individual dogs following oral administration of 5 mg/kg of formulations A, B and C respectively. Figures A.1. to A.6. show the plasma drug concentration profile of the individual dogs following oral administration of 5 mg/kg of formulations A, B and C.

Mean C_{max} values for formulations A, B and C were 0.38, 0.25 and 0.35 µg/ml, respectively. The corresponding T_{max} values were at 0.6, 0.7 and 0.8 hours. Plasma drug half-lives for formulation A, B and C were 1.7, 1.8 and 1.6 hours respectively. The mean $AUC_{(0\ -8\ h)}$ values for formulation A, B and C were 0.96, 0.67 and 0.92 µg.h/ml respectively. Figure A.7. presents the AUC values of individual dog following oral

administration of 5 mg/kg of formulations A, B and C. For formulation C there were no obvious differences in systemic exposure with the slight variation in particle size.

The systemic exposure of L-365-260, following administration of formulation B was generally lower than that from formulation A (methylcellulose alone). In contrast similar systemic exposures were obtained with formulations A and C (methylcellulose + SLS at the CMC). In conclusion, the addition of SLS at concentrations of 0.02% and 0.2% to methylcellulose did not increase the bioavailability of L-365-260.

Table A.B.1. Mean pharmacokinetic parameters (n = 6) following a single oral adminstration of L-365-260 to female dogs.

Formulation	A	B	C
C_{max} (µg/ml)	0.38	0.25	0.35
T_{max} (h)	0.6	0.7	0.8
$T_{1/2}$ (h)	1.7	1.8	1.6
K_{el} (h^{-1})	0.416	0.412	0.429
$AUC_{(0-8)}$ (µg.h/ml)	0.96	0.67	0.92

Table A.B.2. Plasma concentrations of L-365-260 (µg/ml) after a single oral dose administration of 5mg/kg of formulation A.

	Dog Number					
Hours	**930275**	**930277**	**930139**	**930283**	**930279**	**930281**
0	0	0	0	0	0	0
0.5	0.64	0.44	0.39	0.33	0.29	0.13
1	0.7	0.37	0.37	0.21	0.25	0.1
2	0.3	0.18	0.2	0.11	0.21	0.05
3	0.16	0.1	0.12	0.08	0.14	0.03
4	0.12	0.1	0.11	0.07	0.09	0.02
6	0.08	0.05	0.05	0.06	0.04	0.01
8	0.02	0.01	0.02	0.03	0.01	0
AUC (0-8h) (µg.h/ml)	1.67	1.04	1.08	0.75	0.91	0.28
C max (µg/ml)	0.70	0.44	0.39	0.33	0.29	0.13
T max (h)	1	0.5	0.5	0.5	0.5	0.5
$T_{1/2}$ (h)	1.5	1.6	1.8	NC	1.7	1.7
K el (1/h)	0.449	0.434	0.389	NC	0.407	0.4

Half-life was calculated over the range T max to 8 hours.
NC: not calculated because plot was non-linear.

Table A.B.3. Plasma concentrations of L-365-260 (μg/ml) after a single oral administration of 5mg/kg of formulation B.

	Dog Number					
Hours	**930275**	**930277**	**930139**	**930283**	**930279**	**930281**
0	0	0	0	0	0	0
0.5	0.32	0.16	0.37	0.2	0.23	0.22
1	0.27	0.17	0.28	0.22	0.23	0.11
2	0.14	0.1	0.18	0.12	0.18	0.06
3	0.08	0.07	0.13	0.08	0.11	0.04
4	0.05	0.05	0.1	0.06	0.06	0.03
6	0.04	0.03	0.07	0.05	0.02	0
8	0.01	0.02	0.03	0.03	0	0
AUC (0 -8h) (μg.h/ml)	0.74	0.54	1.03	0.67	0.71	0.34
C max (μg/ml)	0.32	0.17	0.37	0.22	0.23	0.22
T max (h)	0.5	1	1	1	0.5	0.5
$T_{1/2}$ (h)	1.7	2.2	2.2	NC	1.6	1.2
K el (1/h)	0.412	0.321	0.310	NC	0.444	0.575

Half-life was calculated over the range T max to 8 hours.
NC: Not calculated because plot was non-linear.

Table A.B.4. Plasma concentrations of L-365-260 (µg/ml) after a single oral administration of 5 mg/kg of formulation C.

	Dog Number					
Hours	**930275**	**930277**	**930139**	**930283**	**930279**	**930281**
0	0	0	0	0	0	0
0.5	0.43	0.45	0.41	0.26	0.19	0.15
1	0.46	0.35	0.35	0.31	0.31	0.13
2	0.21	0.19	0.22	0.14	0.23	0.06
3	0.12	0.12	0.15	0.09	0.16	0.04
4	0.09	0.09	0.11	0.09	0.09	0.02
6	0.05	0.05	0.07	0.07	0.04	0.01
8	0.02	0.02	0.02	0.03	0.01	0
AUC (0 - 8h) (µg.h/ml)	1.14	1.06	1.14	0.89	0.95	0.34
C max (µg/ml)	0.46	0.45	0.41	0.31	0.31	0.15
T max (h)	1	0.5	0.5	1	1	0.5
$T_{1/2}$ (h)	1.6	1.7	1.8	NC	1.5	1.5
K el (1/h)	0.427	0.396	0.387	NC	0.464	0.742

Half-life was calculated over the range T max to 8 hours.
NC: Not calculated because plot was non-linear.

Figure A.1. Concentration of L-365-260 in the plasma of dog (N° 930275) following an oral dose of 5mg/kg.

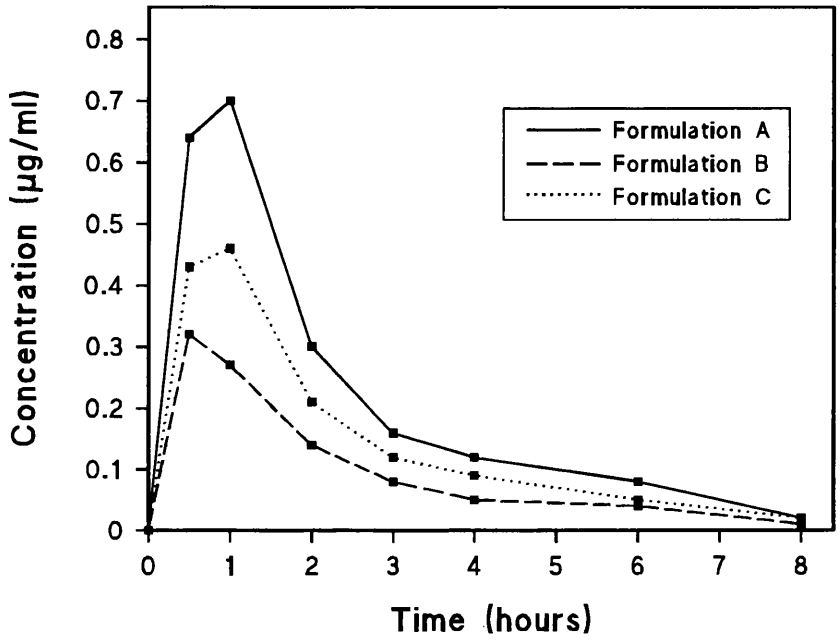

Figure A.2. Concentration of L-365-260 in the plasma of dog (N° 930277) following an oral dose of 5mg/kg.

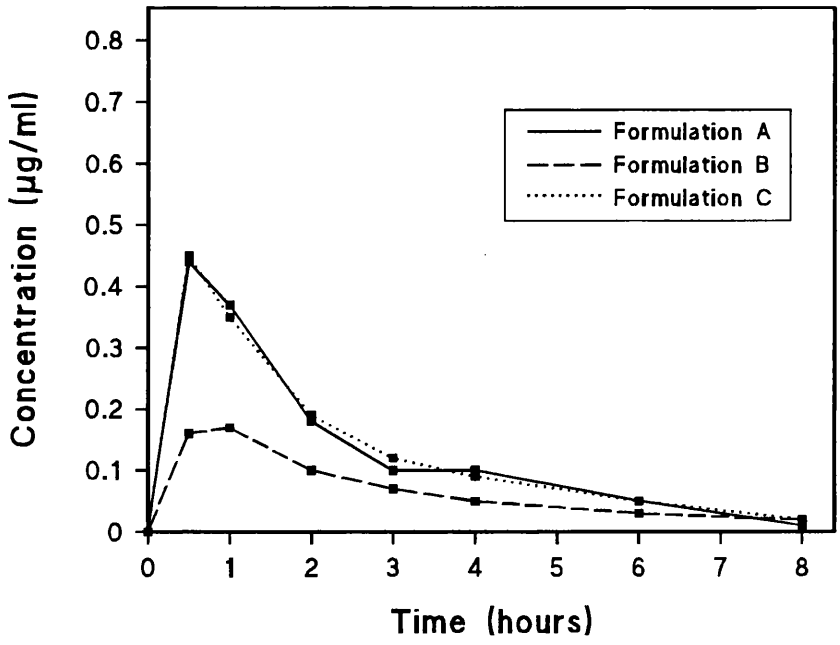

Figure A.3. Concentration of L-365-260 in the plasma of dog (N° 930139) following an oral dose of 5mg/kg.

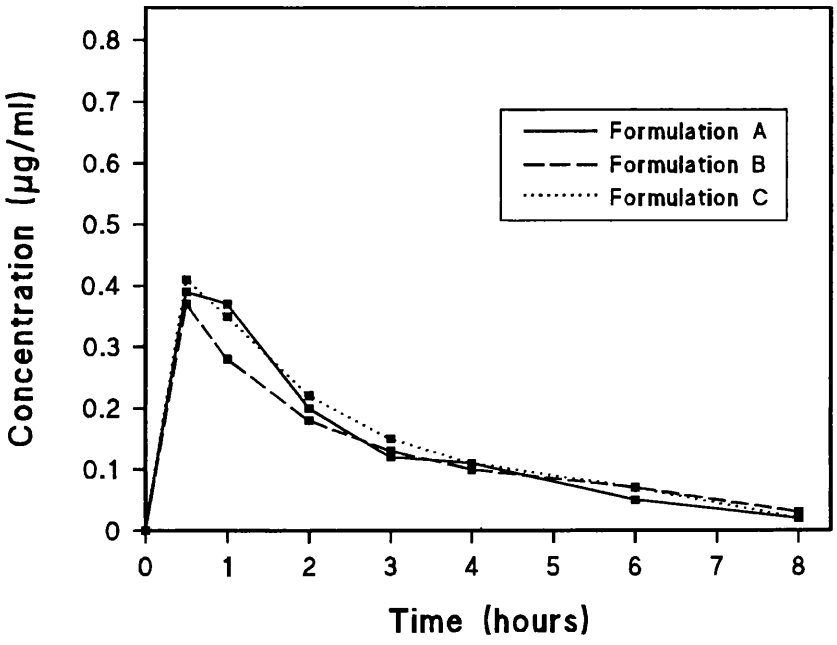

Figure A.4. Concentration of L-365-260 in the plasma of dog (N° 930283) following an oral dose of 5mg/kg.

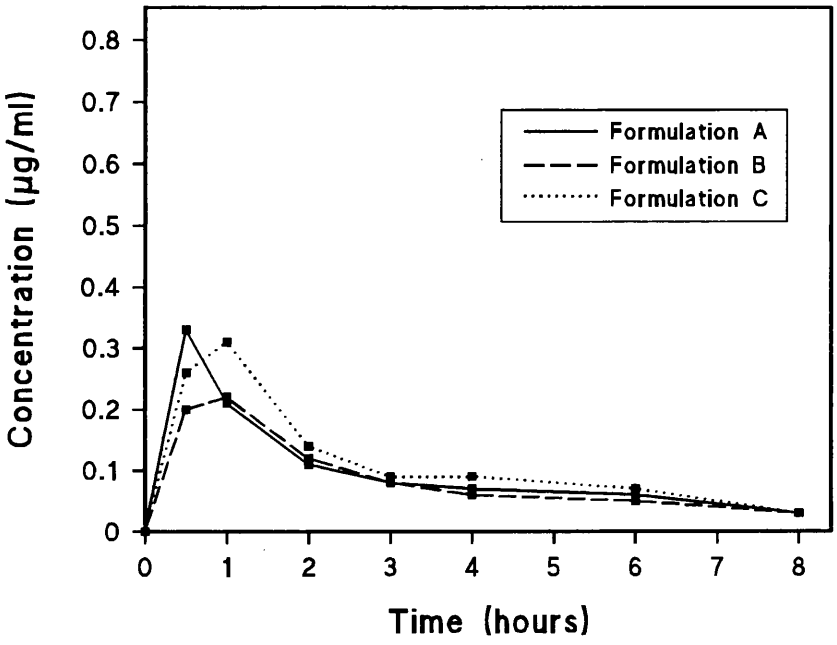

Figure A.5. Concentration of L-365-260 in the plasma of dog (N° 930279) following an oral dose of 5mg/kg.

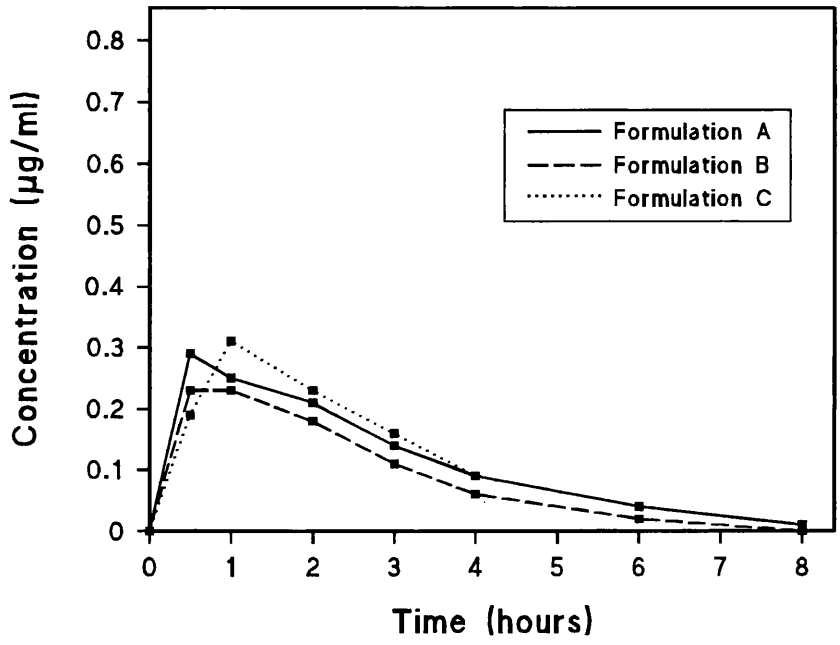

Figure A.6. Concentration of L-365-260 in the plasma of dog (N° 930281) following an oral dose of 5mg/kg.

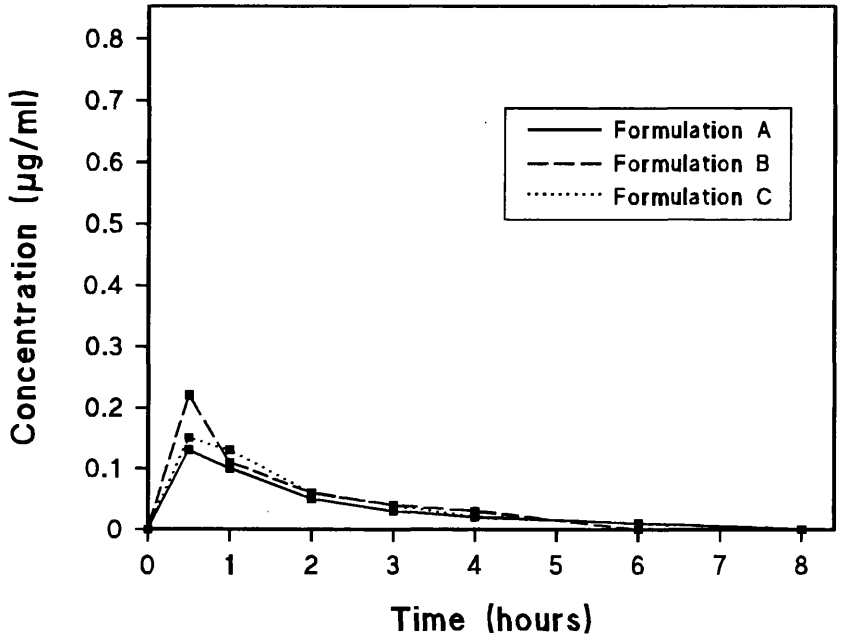

Figure A.7. Comparison of AUC in the plasma of dogs following an oral dose of L-365-260 at 5mg/kg.

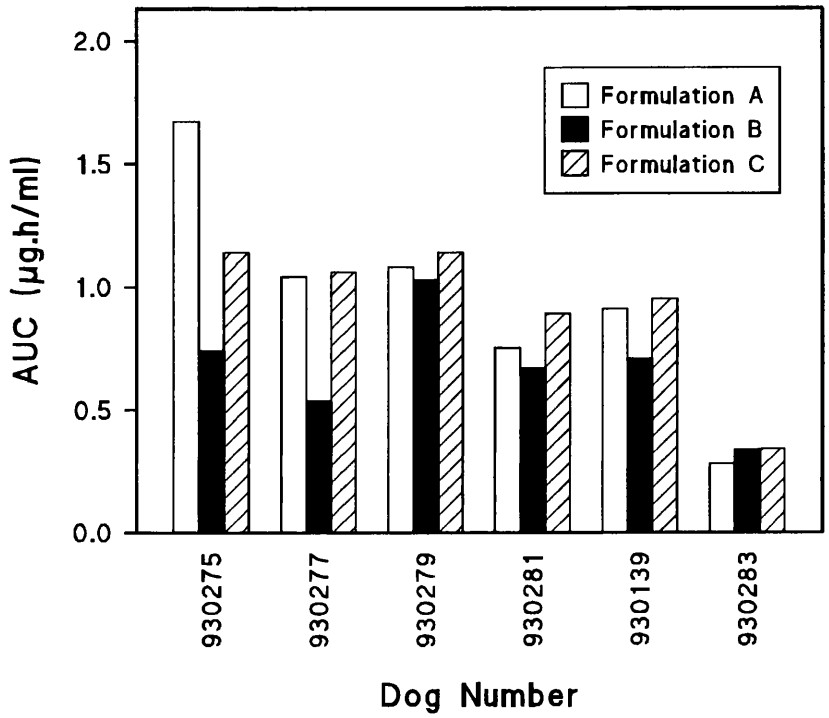

Formulation A: L-365-260 in 0.5% methylcellulose.

Formulation B: L-365-260 in 0.5% methylcellulose + 0.02% SLS.

Formulation C: L-365-260 in 0.5% methylcellulose + 0.2% SLS.

REFERENCES

Ajufo, M.A., Burke, A., Perkins, M.J., Beezer, A.E., Mitchell, J.C. and Volpe, P.L.O. (1991) Determination of the thermodynamic parameters for transfer of alkoxyphenols from aqueous solution to SDS micelles by a Taylor-Aris diffusion technique. *J. Chem. Soc., Faraday Trans.*, **87**, 2741-2744.

Anderberg, E.K., Nyström, C. and Artursson, P. (1992) Epithelial transport of drugs in cell culture. VII Effects of pharmaceutical surfactant excipients and bile acids on transepithelial permeability in monolayers of human intestinal epithelial (Caco-2) cells. *J. Pharm. Sci.*, **81**, 879-887.

Anderberg, E.K. and Artursson, P. (1993) Epithelial transport of drugs in cell culture. VIII Effects of sodium dodecyl sulfate on cell membrane and tight junction permeability in human intestinal epithelial (Caco-2) cells. *J. Pharm. Sci.*, **82**, 392-398.

Armstrong, D.W., Menges, R.A. and Han, S.M. (1988) Evaluation of dye-micelle binding constants using diffusion sensitive band broadening effects. *J. Coll. Interface Sci.*, **126**, 239-242.

Attwood, D. and Florence, A.T. (1983) *Surfactant Systems. Their chemistry, pharmacy and biology.* Chapman and Hall, London.

Aulton, M. (1988) *Pharmaceutics: The Science of Dosage Form Design*, Churchill Livingstone, Edinburgh.

Bakatselou, V., Oppenheim, R.C. and Dressman, J.B. (1991) Solubilization and wetting effects of bile salts on the dissolution of steroids. *Pharm. Res.*, **8**, 1461-1469.

Beezer, A.E., Forster, S., Park, W-B., Rimmer, G.J. and Buckton, G. (1991) Solution thermodynamics of 4-hydroxybenzoates in water, 95% ethanol-water, 1-octanol and hexane. *Thermochim. Acta.*, **178**, 59-65.

Beezer, A.E., Gooch, C.A., Hunter, W.H. and Volpe, P.L.O. (1987) A thermodynamic analysis of the Collander equation and establishment of a reference solvent for use in drug partitioning studies. *J. Pharm. Pharmacol.*, **39**, 774-779.

Beezer, A.E., Mitchell, J.C. and Andrews, D.J. (1992) Microcalorimetry and the Taylor-Aris method in the study of partition processes. *Pestic. Sci.*, **35**, 375-379.

Buckton, G. (1990a) The role of compensation analysis in the study of wettability, solubility, disintegration and dissolution. *Int. J. Pharm.*, **66**, 175-182.

Buckton, G. (1990b) Contact angle, adsorption and wettability - a review with respect to powders. *Powder Technol.*, **61**, 237-249.

Buckton, G. (1992) The estimation and application of surface energy data for powdered systems. *Drug Dev. Ind. Pharm.*, **18**, 1149-1167.

Buckton, G. (1995) *Interfacial Phenomena in Drug Delivery and Targeting.* Harwood Academic Publishers, Switzerland.

Buckton, G. and Beezer, A.E. (1989) Structure-activity relationships for solubility and wettability of a number of substituted barbituric acids. *Thermochim. Acta.*, **138**, 319-326.

Buckton, G. and Chandaria, B. (1993) Consideration of adhesion to modified container walls, by use of surface energy and polarity data, and Lewis acid-Lewis base interactions. *Int. J. Pharm.*, **94**, 223-229.

Buckton, G. and Newton, J.M. (1986) Assessment of the wettability of powders by use of compressed powder discs. *Powder Technol.*, **46**, 201-208.

Burkey, T.J., Griller, D., Lindsay, D.A., Scaiano, J.C. (1984) Simple method for quantifying the distribution of organic substrates between the micellar and aqueous phases of sodium dodecyl sulfate solution. *J. Am. Chem. Soc.*, **106**, 1983-1985.

Burns, S.J., Corness, D., Hay, G., Higginbottom, S., Whelan, I., Attwood, D. and Barnwell, S.G. (1995) Development and validation of an in vitro dissolution method for a floating dosage form with biphasic release characteristics. *Int. J. Pharm.*, **121**, 37-44.

Burton, P.S., Conradi, R.A., Hilgers, A.R., Ho, N.F.H. and Maggiora, L.L. (1992) The relationship between peptide structure and transport across epithelial cell monolayers. *J. Cont. Rel.*, **19**, 87-98.

Cammarata, A., Collett, J.H. and Tobia, E, (1980) Simultaneous determination of the solubility parameter and molar volume for some para-substituted acetanilides in water. In S.H. Yalkowsky, A.A. Sinkula, and S.C. Valvani, (eds) *Physical Chemical Properties of Drugs.* Marcel Dekker, New York, pp. 267-276.

Chawla, A., Buckton, G., Taylor, K.M.G., Newton, J.M. and Johnson, M.C.R. (1994) Wilhelmy plate contact angle data on powder compacts: considerations of plate perimeter. *Eur. J. Pharm. Sci.*, **2**, 253-258.

Chow, S-L. and Nagwekar, J.B. (1994) Possible changes in luminal surface charge densities of small intestine membrane in the 4 - 7.4 pH range exhibit varied influence on the absorption rate constants of the ionized and un-ionized species of sulfadiazine in rats. *J. Pharm. Sci.*, **83**, 152-155.

Coles, C.L.J. and Thomas, D.F.W. (1952) The stability of vitamin A alcohol in aqueous and oily media. *J. Pharm. Pharmacol.*, **4**, 898-903.

de Smidt, J.H., Grit, M. and Crommelin, D.J.A. (1994) Dissolution kinetics of griseofulvin in mixed micellar solutions. *J. Pharm. Sci.*, **83**, 1209-1212.

Dettre, R.H. and Johnson, Jr. R.E. (1965) Contact angle hysteresis. IV Contact angle measurements on heterogeneous surfaces. *J. Phys. Chem.*, **69**, 1507-1515.

Efentakis, M., Al-Hmoud, H., Buckton, G. and Rajan, Z. (1991) The influence of surfactants on drug release from a hydrophobic matrix. *Int. J. Pharm.*, **70**, 153-158.

Elworthy, P.H., Florence, A.T. and Macfarlane, C.B. (1968) *Solubilization by surface-active agents.* Chapman and Hall, London.

Fell, J.T. (1988) Surface and interfacial phenomena. In M.E. Aulton (ed.) *Pharmaceutics: The Science of Dosage Form Design,* Churchill Livingstone, Edinburgh, pp. 50-61.

Fincher, J.H. (1968) Particle size of drugs and its relationship to absorption and activity. *J. Pharm. Sci.*, **57**, 1825-1835.

Florence, A.T. and Attwood, D. (1988) *Physicochemical Principles of Pharmacy*, 2nd edn., Macmillan, London.

Forster, S., Buckton, G. and Beezer, A.E. (1991) The importance of chain length on the wettability and solubility of organic homologs. *Int. J. Pharm.*, **72**, 29-34.

Fowkes, F.M. (1964) Dispersion force contributions to surface and interfacial tensions, contact angles and heats of immersion. *Adv. Chem. Ser.*, **43**, 99-111.

Fowkes, F.M., Riddle, Jr. F.L., Pastore, W.E. and Weber, A.A. (1990) Interfacial interactions between self-associated polar liquids and squalene used to test equations for solid-liquid interfacial interactions. *Colloids and Surfaces,* **43**, 367-387.

Fox, H.W. and Zisman, W.A. (1950) The spreading of liquids on low energy surfaces. I. Polytetrafluoroethylene. *J. Colloid Sci.*, **5**, 514-531.

Good, R.J. (1977) Surface free energy of solids and liquids: Thermodynamics, molecular forces, and structure. *J. Colloid Interface Sci.*, **59**, 398-419.

Hansch, C., Quinlan, J.E. and Lawrence, G.L. (1968) The linear free-energy relationship between partition coefficients and the aqueous solubility of organic liquids. *J. Organic Chem.*, **33**, 347-350.

Heertjes, P.M. and Kossen, N.W.F. (1967) Measuring the contact angles of powder-liquid systems. *Powder Technol.*, **1**, 33-42.

Holder, L.B. and Hayes, S.L. (1965) Diffusion of sulfonamides in aqueous buffers and into red cells. *Mol. Pharmacol.*, **1**, 266-279.

Huggenberger, C., Lipscher, J. and Fischer, H. (1980) Self-termination of benzoyl radicals to ground and excited state benzil. Symmetry control of a radical combination. *J. Phys. Chem.*, **84**, 3467-3474.

Jashnani, R.N., Dalby, R.N. and Byron, P.R. (1993) Preparation, characterization, and dissolution kinetics of two novel albuterol salts. *J. Pharm. Sci.*, **82**, 613-616.

Katz, Y. and Diamond, J.M. (1974a) Non-solvent water in liposomes. *J. Membrane Biol.*, **17**, 87-100.

Katz, Y. and Diamond, J.M. (1974b) Thermodynamic constants for nonelectrolyte partition between dimyristoyl lecithin and water. *J. Membrane Biol.*, **17**, 101-120.

Kayes, J.B. (1988) Disperse Systems. In M.E. Aulton (ed.) *Pharmaceutics: The Science of Dosage Form Design,* Churchill Livingstone, Edinburgh, pp. 81-118.

Leeson, L. and Carstensen, J.T. (1974) *Dissolution Technology.* I.P.T. Academy of Pharmaceutical Sciences, Washington DC.

Leo, A. and Hansch, C. (1971) Linear free energy relationships between partitioning solvent systems. *J. Organic. Chem.*, **36**, 1539-1544.

Lerk, C.F., Schoonen, A.J.M. and Fell, J.T. (1976) Contact angles and wetting of pharmaceutical powders. *J. Pharm. Sci.*, **65**, 843-847.

Levitch, V. (1962) *Physicochemical Hydrodynamics.* Prentice-Hall. Englewood Cliffs, N.J.

Lippold, B.C. and Ohm, A. (1986) Correlation between wettability and dissolution rate of pharmaceutical powders. *Int. J. Pharm.*, **28**, 67-74.

Macheras, P. and Reppas, C. (1987) Dissolution and in vitro permeation behaviours of dicumarol, nitrofurantoin and sulfamethizole in the presence of protein. *Int. J. Pharm.*, **37**, 103-112.

Moffat, A.C. (1986) Ed. *Clarke's Isolation and Identification of Crude Drugs,* 2nd ed. Pharmaceutical Press, London.

Mosharraf, M. and Nyström, C. (1995) The effect of particle size and shape on the surface specific dissolution rate of microsized practically insoluble drugs. *Int. J. Pharm.*, **122**, 35-47.

Naylor, L.J., Bakatselou, V. and Dressman, J.B. (1993) Comparison of the mechanism of dissolution of hydrocortisone in simple and mixed micelle systems. *Pharm. Res.*, **10**, 865-870.

Neumann, A.W. and Good, R.J. (1979) Techniques of measuring contact angles. In R.J. Good, and R.R. Stromberg, (eds.) *Surface and Colloid Science, Volume 2,* Plenum, New York, pp. 31-91.

Onori, G. and Santucci, A. (1992) Effect of temperature and solvent on the critical micelle concentration of sodium dodecyl sulfate. *Chem. Phys. Letters,* **189**, 598-602.

Otsuka, M., Teraoka, R. and Matsuda, Y. (1992) Rotating disk dissolution kinetics of nitrofurantoin anhydrate and monohydrate at various temperatures. *Pharm. Res.*, **9**, 307-311.

Ozturk, S.S., Palsson, B.O. and Dressman, J.B. (1988) Dissolution of ionizable drugs in buffered and unbuffered solutions. *Pharm. Res.*, **5**, 272-282.

Parfitt, G.D. (1973) *Dispersion of Powders in Liquids,* 2nd edn, Applied Science, London, pp 3-6.

Parsons, G.E., Buckton, G. and Chatham, S.M. (1992a) The extent of the errors associated with contact angles obtained using liquid penetration experiments. *Int. J. Pharm.*, **82**, 145-150.

Parsons, G.E., Buckton, G. and Chatham, S.M. (1992b) The use of surface energy and polarity determinations to predict physical stability of non-polar, non-aqueous suspensions. *Int. J. Pharm.*, **83**, 163-170.

Pinto, J.F., Buckton, G. and Newton, J.M. (1995) A relationship between surface free energy and polarity data and some physical properties of spheroids. *Int. J. Pharm.*, **118**, 95-101.

Poelma, F.G. J., Tukker, J.J. and Crommelin, D.J.A. (1990) The role of bile salts in the intestinal absorption of drugs. *Acta. Pharm. Technol.*, **36**, 43-52.

Rahman, A. and Brown, C.W. (1983) Effect of pH on the critical micelle concentration of sodium dodecyl sulphate. *J. Appl. Polym. Sci.*, **28**, 1331-1334.

Reddy, R.K., Khalil, S.A. and Gouda, M.W. (1976) Effect of dioctyl sodium sulfosuccinate and poloxamer 188 on dissolution and intestinal absorption of sulfadiazine and sulfisoxazole in rats. *J. Pharm. Sci.*, **65**, 115-117.

Rowe, R.C. (1989) Binder-substrate interactions in granulation: A theoretical approach based on surface free energy and polarity. *Int. J. Pharm.*, **52**, 149-154.

Shaw, D.J. (1992) *Introduction to Colloid and Surface Chemistry,* 4th Edn, Butterworth-Heinemann, Oxford.

Sheridan, P.L., Ph D Thesis (1994a) University of London, U.K.

Sheridan, P.L., Buckton, G. and Storey, D.E. (1994b) The extent of errors associated with contact angles. II Factors affecting data obtained using a Wilhelmy plate technique for powders. *Int. J. Pharm.*, **109**, 155-171.

Sjöström, B., Kronberg, B. and Carlfors, J. (1993) A method for the preparation of submicron particles of sparingly water-soluble drugs by precipitation in oil-in-water emulsions. I: Influence of emulsification and surfactant concentration. *J. Pharm. Sci.*, **82**, 579-583.

Svehla, G. (1979) *Vogel's Textbook of Macro and Semimicro Qualitative Inorganic Analysis,* 5th edn, Longman, London, pp. 52-53.

TenHoor, C.N., Bakatselou, V. and Dressman, J.B. (1993) Prediction of solubility and wetting effects in the presence of bile salts for poorly soluble drugs. *Pharm. Res.*, **10**, S-183.

The Merck Index, 9th edn, (1979) Merck,

Tomlinson, E. (1983) Enthalpy-entropy compensation analysis of pharmaceutical, biochemical and biological systems. *Int. J. Pharm.*, **13**, 115-144.

Tsai, R-S., Fan, W., Tayar, N.E., Carrupt, P-A., Testa, B. and Kier, L.B. (1993) Solute-water interactions in the organic phase of a biphasic system. I. Structural influence of organic solutes on the 'water-dragging' effect. *J. Am. Chem. Soc.*, **115**, 9632-9639.

Uchegbu, I.F., Double, J.A., Turton, J.A. and Florence, A.T. (1995) Distribution, metabolism and tumoricidal activity of doxorubicin administered in sorbitan monostearate (Span 60) niosomes in the mouse. *Pharm. Res.*, **12**, 1019-1024.

United States Pharmacopoeia XX and National Formulary XV (1980) The United States Pharmacopoeial Convention Inc., Rockville, Md.

van Oss, C.J., Chaudhury, M.K. and Good, R.J. (1987) Monopolar surfaces. *Adv. Colloid Interface Sci.*, **28**, 35-64.

van Oss, C.J. and Costanzo, P.M. (1992) Adhesion of anionic surfactants to polymer surfaces and low-energy materials. *J. Adhesion Sci. Technol.*, **6**, 477-487.

van Oss, C.J., Giese, R.F., Li, Z., Murphy, K., Norris, J., Chaudhury, M.K. and Good, R.J. (1992) Determination of contact angles and pore sizes of porous media by column and thin layer wicking. *J. Adhesion Sci. Technol.*, **6**, 413-428.

Ward, C.A. and Neumann, A.W. (1974) On the surface thermodynamics of a two-component liquid-vapour-ideal solid system. *J. Colloid Interface Sci.*, **49**, 286-290.

Warren, S.J. and Farr, S.J. (1995) Formulation of solution metered dose inhalers and comparison with aerosols emitted from conventional suspension systems. *Int. J. Pharm.*, **124**, 195-203.

Wells, M.L. and Parrott, E.L. (1992) Effect of surfactants on release of a highly water-soluble medicinal compound from an inert, heterogeneous matrix. *J. Pharm. Sci.*, **81**, 453-457.

Wu, S. (1971) Calculation of interfacial tension in polymer systems. *J. Polymer Sci.*, Part C, **34**, 19-30.

Wu, S. (1979) Surface tension of solids: An equation of state analysis. *J. Colloid Interface Sci.*, **71**, 605-609.

Wu, W., Giese, Jr. R.F. and van Oss, C.J. (1995) Evaluation of the Lifshitz van der Waals / acid-base approach to determine surface tension components. *Langmuir*, **11**, 379-382.

Yalkowsky, S.H., Flynn, G.L. and Slunick, T.G. (1972) Importance of chain length on physicochemical and crystalline properties of organic homologs. *J. Pharm. Sci.*, **61**, 852-857.

Yalkowsky, S.H., Sinkula, A.A. and Valvani, S.C. (eds) (1980) *Physical Chemical Properties of Drugs.* Marcel Dekker, New York.

Yamagami, C., Takao, N. and Fujita, T. (1993) Hydrophobicity parameter of diazines. III Relationship of partition coefficients of monosubstituted diazines and pyridines in different partitioning systems. *J. Pharm. Sci.*, **82**, 155-161.

York, P. (1983) Solid-state properties of powders in the formulation and processing of solid dosage forms. *Int. J. Pharm.*, **14**, 1-28.

Young, S.A. and Buckton, G. (1990) Particle growth in aqueous suspensions: the influence of surface energy and polarity. *Int. J. Pharm.*, **60**, 235-241.

Zajik, L. and Buckton, G. (1990) The use of surface energy values to predict optimum binder selection for granulations. *Int. J. Pharm.*, **59**, 155-164.

Zografi, G. and Tam, S.S. (1976) Wettability of pharmaceutical solids: Estimates of solid surface polarity. *J. Pharm. Sci.*, **65**, 1145-1149.